Kumamoto Journal of Science

Series A (Mathematics, Physics and Chemistry)

Vol. 1, No. 3, March 1954

Published by the
Faculty of Science, Kumamoto University
Kumamoto, Japan

熊本大學理學部紀要　第一部　第一卷　第三號　昭和二十九年三月
熊　本　大　學　理　學　部

ON RELATIONS AMONG VARIOUS CONNECTIONS IN FINSLERIAN SPACE

Takeo OHKUBO

(Received Oct. 1. 1953)

1. Introduction.

In Finslerian space F_n Berwald's[1] and Cartan's[2] connections are most famous. Recently. H. Rund[3] determined another linear connection in Finslerian space F_n introbucing four convensions, as is shown below.

Cartan's and Rund's connections are metric, but Berwald's is not. Cartan gave the relation between the coefficients of his and Berwald's connections. The connection determined by Rund's convensions A, B, C and D is not unique but its coefficients are of the form (11').

We shall show that if Berwald's connection is metrised, it is coincident with Cartan's, during a supporting element is displaced parallelly to itself.

In Finslerian space F_n two metric connections being introduced, we shall also show that there are some relations among their coefficients. Now we adjoint a tangential Minkowskian space $T_n(P)$ to every point $P(x^i)$ in Finslerian space F_n. Rund observed two points $A(x^i)$, $B(x^i+dx^i)$ and a vector field $X^i(x)$ in F_n. These points A, B decide an unique geodesic E, which passes the both points. He seeked such a vector $X^i+d^*X^i$ in $T^n(B)$ that would satisfy the following conditions and defined a covariant differentiation by $D=d-d^*$:

A. *The scalar products of the vectors* X^i *and* $X^i+d^*X^i$ *with respect to the tangent vectors in A and B on E are identical.*

B. $dX^i - dX^i \equiv 0$, *when* $X^i = x'^i$

C. d^*X^i *are linear in* X^k.

D. $Dg_{ij}(x, x') = 0$, *where* $x'^i ds = dx^i$ *express the direction of displacement* AB *along the geodesic* E.

We shall also determine a metric connection with some uncertainties introducing three convensions analogous to those introduced by Rund. In our case the convension which corresponds to the convension C in Rund's connection is needles, because it is reduced from

1) See [1]. Numbers in brackets refer to the bibliography at the end of the paper.
2) See [2].
3) See [3], [4].
4) See [2]. VIII.

the convensions I and II. His results are different from ours.

2. **Metrisation of Berwald's connection.**

As is well known, we have the following relations between the coefficients G^i_{jk} of Berwald's connection and those of Cartan's connection which enter in the expressions of the absolute differential of a vector when its supporting element displaces parallelly to itself:

$$G_{ihj} = \Gamma^*_{ihj} + A_{ihj|o} \,. \tag{1}$$

Berwald's connection being not metric, if we metrise it we obtain the corresponding coefficients as follows:

$$\begin{aligned}
\hat{\omega}^i_j &= \omega^i_j + \tfrac{1}{2}\,\delta g_{jr}\, g^{ir} \\
&= G^i_{jk}\, dx^k + \tfrac{1}{2}\,(dg_{jr} - G^l_{jk}\, g_{lr}\, dx^k - G^l_{rk}\, g_{jl}\, dx^k)\, g^{ir} \\
&= \tfrac{1}{2}\,(\Gamma^{*i}_{jk} + A^i_{jk\,|o})\, dx^k + \tfrac{1}{2}\,\frac{\partial g_{jr}}{\partial x'^k}\, g^{ir}\, dx'^k + \tfrac{1}{2}\,\frac{\partial g_{jr}}{\partial x^k}\, g^{ir}\, dx^k \\
&\qquad - \tfrac{1}{2}\, g^{ir}\,(\Gamma^*_{rjk} + A_{rjk\,|o})\, dx^k \\
&= C^i_{jk}\, dx'^k + \Gamma^i_{jk}\, dx^k \,,
\end{aligned}$$

on account of $\Gamma^{*i}_{jk} = \Gamma^i_{jk} - C^i_{jr}\, G^r_k$, where we put $\omega^i_j = G^i_{jk}\, dx^k$ and denote an absolute differentiation in Berwald's sense by δ.

Thus we see that the coefficients $\hat{\omega}^i_j$ coincide with those of Cartan's connection.

3. **Relations between two metric connections.**

Suppose that in Finslerian space F_n two kinds of metric connections are defined in the following forms:

$$DX^i = dx + \omega^i_j\, X^j = dX^i + (C^i_{jk}\, dx'^k + \Gamma^i_{jk}\, dx^k)\, X^j \tag{2}$$

and

$$\hat{D}X^i = dx^i + \hat{\omega}^i_j\, X^j = dx^i + (\hat{C}^i_{jk}\, dx'^k + \hat{\Gamma}^i_{jk}\, dx^k)\, X^j \tag{3}$$

The differences

$$DX^i - \hat{D}X^i = X^j\left[(C^i_{jk} - \hat{C}^i_{jk})\, dx'^k + (\Gamma^i_{jk} - \hat{\Gamma}^i_{jk})\, dx^k\right]$$

are the components of a vector and so under a transformation of the coordinates the relations

$$(4) \qquad (C^i_{jk} - \hat{C}^i_{jk}) \frac{\partial x^k}{\partial \overline{x}^\alpha} \frac{\partial^2 \overline{x}^\alpha}{\partial x^l \partial x'^m} x'^l + \frac{\partial x^i}{\partial \overline{x}^\alpha} (\overline{\Gamma}^\alpha_{\beta\gamma} - \hat{\overline{\Gamma}}^\alpha_{\beta\gamma}) \frac{\partial \overline{x}^\beta}{\partial x^j} \frac{\partial \overline{x}^\gamma}{\partial x'^m} = \Gamma^i_{jm} - \hat{\Gamma}^i_{jm}$$

hold. By hypofhesis, as the both connections are metric, the relations

$$(5) \qquad C_{ijk} + C_{jik} = \frac{\partial g_{ij}}{\partial x'^k}, \quad \hat{C}_{ijk} + \hat{C}_{jik} = \frac{\partial g_{ij}}{\partial x^k}$$

hold, therefore C_{ijk} and $\hat{C}_{ijk}$ have the same symmetric parts with respect to the first two indices. Accordingly the differences $C_{ijk} - \hat{C}_{ijk}$ are the components of a skew symmetric tensor, which we denote by b_{ijk}, i. e.

$$(6) \qquad C_{ijk} - \hat{C}_{ijk} = b_{ijk} \text{ or } \hat{C}_{ijk} = C_{ijk} - b_{ijk}, \; b_{(ij)k} = 0.$$

1°. when $C_{ijk} = C_{jik}$ and $\hat{C}_{jik} = \hat{C}_{ijk}$, we have $C_{ijk} = \hat{C}_{ijk}$. In this case the expressions $\Gamma^i_{jk} - \hat{\Gamma}^i_{jk}$ are the components of a tensor, as is seen from (4). Now we put

$$(7) \qquad \Gamma_{ijk} - \hat{\Gamma}_{ijk} = a_{ijk},$$

then the relations

$$(8) \qquad a_{ijk} = - a_{jik}$$

hold, because the both connections are metric by hypothesis.

2°. Suppose that one of the connections (2) and (3), say (2), is Cartan's and the other is general metric one. According to Cartan's symbols[5] we have the following transformation law:

$$(9) \qquad x'^m \frac{\partial^2 \overline{x}^\alpha}{\partial x^k \partial x'^m} + G^\alpha_\beta \frac{\partial \overline{x}^\beta}{\partial x^k} = G^i_k \frac{\partial \overline{x}^\alpha}{\partial x^i}.$$

If we put the above relations (9) into (4), we get

$$\left(\Gamma^\alpha_{\beta\gamma} - \hat{\Gamma}^\alpha_{\beta\gamma} - b^\alpha_{\beta\tau} G^\tau_\gamma\right) \frac{\partial x^i}{\partial \overline{x}^\alpha} \frac{\partial \overline{x}^\beta}{\partial x^j} \frac{\partial \overline{x}^\gamma}{\partial x^k} = \Gamma^i_{jk} - \hat{\Gamma}^i_{jk} - b^i_{jl} G^l_k .$$

Putting

$$(10) \qquad T^i_{jk} = \Gamma^i_{jk} - \hat{\Gamma}^i_{jk} - b^i_{jl} G^l_k ,$$

we see that the expressions T^i_{jk} are the compressions of a tensor. Moreover the relations $T_{(ij)k} = 0$ hold. More generally we may use in place of G^i_j in (9) any expressions which are transformed by the transformation law as (9).

5) See [2].

From (10) and (4) we obtain the following:

$$(11)\qquad \begin{cases} \hat{\Gamma}_{ijk} = \Gamma_{ijk} - b_{ijl} G^l_k - T_{ijk}\ , \quad T_{(ij)k} = 0, \\ \hat{C}_{ijk} = C_{ijk} - b_{ijk}\ , \quad b_{(ij)k} = 0, \end{cases}$$

which are the relations among the coefficients of the two metric connections.

4. **Another metric connection.**

Now we consider a vector field $X^i\ (x,\ x')$ and two points $A\ (x^i)$ and $B\ (x^i + dx^i)$ in F_n, which an unique geodesic passes. We search for the vector $X^i + d^* X^i$ which satisfies the following convensions:

I. *The scalar products of the vectors* X^i *and* $X^i + d^* X^i$ *with respect to the tangent vectors in* A *and* B *on* E *are identical.*

II. $d^* X^i$ *are Paffian forms of* dx^k *and* dx'^k *linear in* X^k.

III. $Dg_{ij}\ (x,\ x') = 0$, *where we put* $DX^i = dX^i - d^* X^i$,

We define the absolute differential of X^i by DX^i. From I we have

$$g_{ij}\,(x,\ x')\,x'^i\,X^j = g_{ij}\,(x + dx,\ x' + dx')\,(x'^i + dx'^i)\,(X^j + d^* X_j)$$

or

$$(12)\qquad \frac{\partial g_{ij}}{\partial x^k}\,x'^i\,X^j\,dx^k + g_{ij}\,(x,\ x')\,x'^i\,d^* X^j + g_{ij}\,X^j\,dx'^i = 0.$$

By II for any vector X^i, $d^* X^i$ are expressed in the forms:

$$(13)\qquad d^* X^i = -\,P^i_{jk}\ (x,\ x')\,dx'^k\ X^j - Q^i_{jk}\ (x,\ x')X^j\,dx^k\ ,$$

so that we have

$$(14)\qquad DX^i = dX^i - d^* X^i = dx^i + (P^i_{jk}\ dx'^k + Q^i_{jk}\ dx^k)\,X^j.$$

Considering that our connection is metric from III, if we put (13) into (12) we obtain:

$$Q_{ilk}\ x'^i\,X^l\,dx^k - g_{ij}\,x'^i\,P^j_{lk}\ dx'^k\ X^l + g_{il}\,dx'^i\,X^l = 0,$$

where $Q_{ilk} = g_{lh}\,Q^h_{ik}$. As the vector X^i is arbitrary we get

$$(15)\qquad g_{il}\,dx'^i - P_{lik}\ dx'^k\ x'^i + Q_{ilk}\ x'^i\,dx^k = 0.$$

On the other hand from III we have

$$x'^i\ P_{ilk} + x'^i\ P_{lik} = 0$$

or

$$(16)\qquad -\,P_{lik}\ x'^i = P_{ilk}\ x'_i\ ,$$

where $P_{ilk} = g_{hl} P^h_{ik}$. When we put (16) into (15) and multiply the resulting equation by g^{mj} and contract with respect to the indices l and m, we have

$$dx'^j + P^j_{ik}\ x'^i\ dx'^k + Q^j_{ik}\ x'^i\ dx^k = 0. \tag{17}$$

The left side of the above equation (17) is coincident with

$$dx'^j - d^* x'^j \equiv Dx'^j ,$$

therefore the equation (17) is nothing but the convension B in Rund's case, that is to say, the convension B in Rund's case follows from our three convensions I, II, and III.

In particular when the relation $dx'^i + G^i_j dx^j = 0$ holds, we get from (15)

$$-G^i_j + g^{li} P_{lmk} G^k_j\ x'^m + Q^i_{mj} x'^m = 0. \tag{18}$$

When the equations (11) or

$$Q_{ijk} = \Gamma_{ijk} - b_{ijl}\ G^l_k - T_{ijk} , \qquad P_{ijk} = C_{ijk} - b_{ijk} \tag{11'}$$

are subsfituted in (18), we get

$$T_{ilj}\ x'^i = 0, \tag{19}$$

owing to the relations $b_{lik} + b_{ilk} = 0$ and $\Gamma_{ilj}\ x'^i = G^r_j\ g_{rl}$. From (19) and the skew symmetricity of T_{ilj} with respect to first two indices, we get immediately

$$T_{lij}\ x'^l = 0. \tag{20}$$

Therefore we have:

Given two arbitrary tensors b_{ijk} *and* T_{ijk} *satisfying the relations* $b_{(ij)k} = 0$, $T_{(ij)k} = 0$ *and* $T_{ijk}\ x^i = 0$, *a metric connection in* F_n *is determined by* (11').

The coefficients Q^{*i}_{jk} which enter in the expressions of the absolute differential of a vector, when its supporting element is displaced parallelly to itself, are as follow

$$\begin{aligned} Q^{*j}_{ik} &= -P^j_{il} G^l_k + Q^j_{ik} \\ &= -(C^j_{il} - b^j_{il}) G^l_k + \Gamma^j_{ik} - b^j_{il} G^l_k - T^j_{ik} \\ &= -C^j_{il} G_k + \Gamma^j_{ik} - T^j_{ik} = \Gamma^{*j}_{ik} - T^j_{ik} , \end{aligned}$$

where C^j_{il}, Γ^j_{ik} and Γ^{*j}_{ik} are Cartan's symbols.

Thus we see that Q^*_{ijk} are only different from Cartan's symbols Γ^*_{ijk} by a skew symmetric tensor T_{ijk} ,

Bibliography

1. L. Berwald, Untersuchung der Krümmung allgemeiner metrischer Räume auf Grund des in ihnen herrschenden Parallelismus. Math. Zeitschr. 25 (1929), 40-73.
2. E. Cartan, Les espaces de Finsler. Paris 1934.
3. H. Rund, Über die Parallelverschiebung in Finslerschen Räumen. Math. Zeitschr. 54 (1651), 115-128.
4. 〃 , Theory of Subspaces of a Finsler space. I and II. Math. Zeitschr. 56 (1952), 363-375; 57 (1953), 191-210.

ON THE ELECTRICAL CHARACTERISTICS OF CONCRETE AND OTHERS (III)

Shigeichi FUJITA

(Received July 27, 1953)

Abstract

As reported in parts (I) [1] and (II) [2], the resistances of concrete and others are different when the electric current flows in one direction and in the reverse direction and the difference depends on the composition of concrete and on the bodies cemented in one end or both ends. On investigating the cause of the difference of the resistances, we discovered the fact that the specimen itself has an E. M. F., and the E. M. F. has an intimate relation to the asymmetry of resistance. So we measured the E. M. F. of each specimen and investigated the relation between the E. M. F. and the asymmetry of the electric resistance.

1. Asymmetry of Electric Resistances

We have reported many examples on the asymmetry of electric resistance in (I) and (II). We give some more examples of experiments on concrete, each of which has a stone in one end, in Table I.

Table 1.

Resistances of Concrete Cubes (length of a side is 6 cm) having a piece of stone cemented in one end.

Specimens	Stones cemented	Resistances	
		Stone→Concrete	Concrete→Stone
(93)	Greywacke	$8.1\times10^4\Omega$	$2.0\times10^4\Omega$
(96)	Limestone	58.0	46.0
(97)	Limestone	58.6	47.6
(102)	Brick	2.8	5.6
(125)	Tuff	21.0	14.6
(127)	Greywacke	24.6	17.2
(128)	Quartz-porphyry	45.2	33.1
(131)	Quartz veins	12.1	9.1
(132)	Greywacke	11.2	7.2
(133)	Hornstone	42.4	28.4

As seen in the Table, in many of cases, the resistance when the electric current flows from stone to concrete is greater than that when the electric current flows in the reverse direction, that is, the direction of easy flow is the direction from concrete to stone. But in a few cases it is found, when we use natural stones, that the diretion of easy flow is the direction from stone to concrete as in the case of brick in the Table. Perhaps the impurity contained in or attached to the surface of the stone may be the cause to this phenomenon. In these cases, also, the difference of resistances in both directions, $\alpha \rightarrow \beta$ and $\beta \rightarrow \alpha$, depends on the kind and quality of stone, the character of concrete, the applied voltage, the time after the application of voltage, temperature and humidity. Also, we examined the asymmetry of resistance of the concrete which is made under the application of electric field, but we noticed no asymmetry of resistance.

If a small quantity of moisture is given to one end of a timber or stone which has no asymmetry of resistance, they acquire the asymmetry of resistance, the direction of easy flow is always in the direction from wet end to dry end.

2. Asymmetry of Electric Resistances and the E.M.Fs. of the specimens.

From the fact that the difference of moisture in both ends of timber or stone give rise to an asymmetry of resistance, we supposed that the ions in the specimen would probably strongly affect the asymmetry. If we assume the existence of ions in the specimen, it is natural to suppose that it would have some E. M. F. which has the intimate relation to the asymmetry of the resistance.

We, therefore, examined the E. M. Fs. of the specimens which have been proved to have asymmetry of resistances, and ascertained that all of them have some E. M. Fs. Some examples of the results of the measurement are given in Table 2. (1)...(8) are the concrete columns which contain gravel, the direction of gravity at the time of making them are not known. The direction of easy flow is the direction $\alpha \rightarrow \beta$ in (1), (3), (5) and (8), and $\beta \rightarrow \alpha$ in (2). The E. M. Fs. are of the order of 0.1 volt and the (+) ends are β ends in (1), (3), (5) and (8), and α end in (2).

In these and other specimens which have been studied so far, the directions of easy flow of the electric current is the directions from (−) ends to (+) ends on the whole.

In the concrete columns (33), (34), (36) and (37) which contain gravel, the direction of gravity at the time of making is $\alpha \rightarrow \beta$, that is, the upper and the lower ends of them are α and β respectively, and the direction of easy flow is $\alpha \rightarrow \beta$. All of them also have some E. M, Fs., the (−) ends are α.

In the concrete column which has a metal at one end or two different metals at both ends cemented, the asymmetry of resistance and E. M. F. always appear and the direction of easy flow is always the direction from (−) and to (+) end. (90), (99), (108), (113) and

Table 2
E. M. Fs. of Various Specimens

Specimens	E. M. F.	Specimens	E. M. F.
I. Concrete circular columns (containiug gravel)		II. Concrete cubes having a piece of metal or stone in one end or both ends	
(1) (β+α−)	10.2×10^{-2}V	(90) (C+Pb−)	17.9×10^{-2}V
(2) (α+β−)	18.8	(93) (Sandstone+C−)	10.9
(3) (β+α−)	11.5	(96) (C−Limestone+)	4.6
(5) (β+α−)	10.6	(97) (C−Limestone+)	6.2
(8) (β+α−)	2.0	(99) (C+Cu−)	13.1
⋮	⋮	(108) (Cu+Zn−)	10.5
(33) (β+α−)	15.2	(113) (C+Zn−)	23.0
(34) (β+α−)	14.5	(121) (Ni+Cu−)	5.4
(36) (β+α−)	7.0	(125) (Tuff+C−)	4.0
(37) (β+α−)	5.6	(127) (Greywacke+C−)	6.4
⋮	⋮	(128) (Quartz-porphyry+C−)	8.2
⋮	⋮	(131) (Quartz-veins+C−)	7.1
⋮	⋮	(132) (Greywacke+C−)	6.9
⋮	⋮	(133) (Hornstone+C−)	8.3

(121) in Table 2 are the examples of this case.

In each of the concrete columns which has a piece of stone cemented in one end, the direction of easy flow is almost always the direction from concrete to stone. On measuring the E. M. F., we notice that the stone is (+) end and concrete is (−). (93), (96), (127), (128), (132) and (133) in Table 2 are the examples of this case.

From these facts it is considered that these specimens have some character like galvanic cells.

3. Relation between the Electric Current and the Applied Voltage

As it is found that specimens themselves have E. M. Fs. in them, and these E. M. Fs. may be the principal causes of the asymmetry of resistances, we have studied the relation between the currents and the applied voltages, the values of which are varied successively in the neighbourhood of the E. M. Fs. of the specimens.

Examples of the measurement are shown in Fig. 1, Fig. 2, Fig. 3, Fig. 4 and Fig. 5.

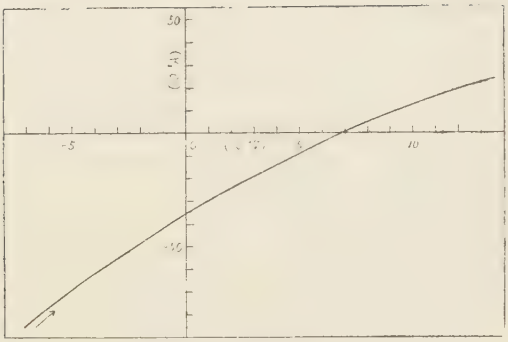

Fig. 1. Concrete column. (1) (β_+, α_-)

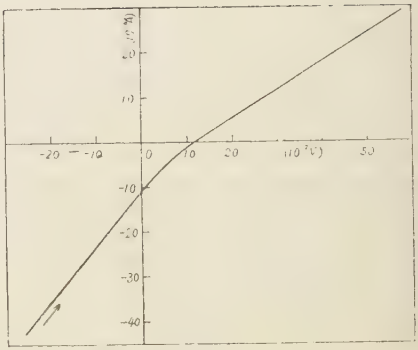

Fig. 2. Concrete cube. (90) (C_+, Pb_-)

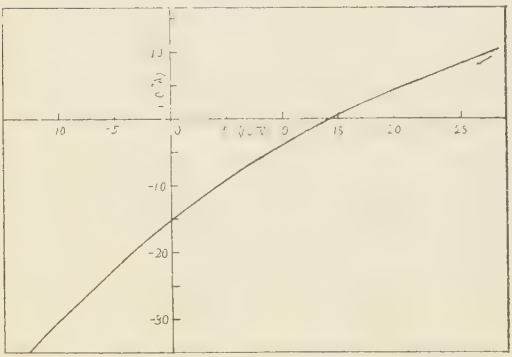

Fig. 3. Concrete cube (107) (C_+, Cu_-)

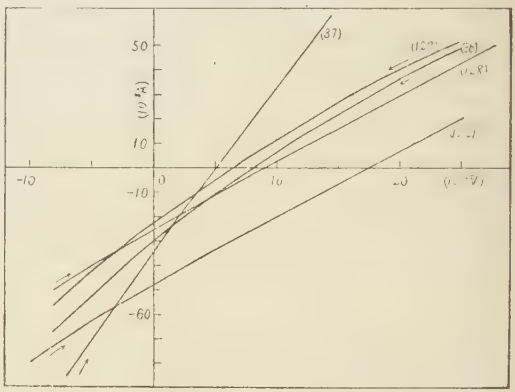

Fig. 4. Concrete columns and cubes.
(36) (β_+, α_-)
(37) (β_+, α_-)
(120) (Cu_+, Zn_-)
(127) ($Greywacke_+, C_-$)
(128) ($Quartz\text{-}porphyry_+, C_-$)

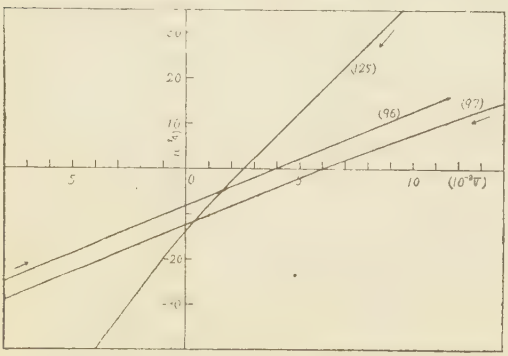

Fig. 5. Concrete cubes.
(96) ($Limestone_+, C_-$)
(97) ($Limestone_+, C_-$)
(125) ($Tuff_-, C_-$)

If electric current flow in a specimen like these, the quality of the specimen is changed and a counter E. M. F. is caused in it. The curve showing the relation between the current and the applied voltage changes a little by reversing the direction of current at the beginning. In the graphs arrows (→)

show the direction of changes in the measurement. Fig. 1 and Fig. 2 show the variation of current in the cases, at the beginning the voltage is applied in the same direction as the E. M. F. of the specimen, and it is gradually diminished until it becomes 0 and is gradually increased from 0 in the reverse direction. Fig. 3 shows the variation of current in the case, at the beginning the voltage is applied in the reverse direction to the E. M. F. of the specimen and a little greater than it, and is gradually diminished until it becomes 0, and is gradually increased from 0 in the reverse direction. In Fig. 4, (36) and (127) show the variation of currents as in the case of Fig. 3, and (37), (120) and (128) show the variation of currents as in the case of Fig. 1 and Fig. 2. The arrow (→) in Fig. 5 has similar meaning as before.

In these graphs the curves showing the relation between the currents and the applied voltages are almost straight lines. This fact shows that the Ohmic resistances of the specimens have no asymmetry and almost independent of the applied voltages in the small range as shown in the graphs.

4. Rectifying Action and E.M.F.

As it was ascertained that in each of all the specimens used, the asymmetry of electric resistance is caused principally from the existence of E. M. F. in the specimen, we considered that some of other rectifiers would have some E. M. Fs. and these would have intimate relations to the rectifying action. Accordingly we studied the E. M. Fs. and the relations between currents and applied voltages for various crystal detectors, a photo-cell and a photoelectric tube. Crystal detectors are composed of the crystals (pyrite, chalco-phrite and bornite) and brass needle contacting on them. As the rectifying action of tbe crystal detectors are greatly changed with the place of the contacting point, and affected by the electric current flowing through the contacting point, it was difficult to study precisely the relation of rectifying action and the E. M. F. We could, however, recognize that these rectifiers have minute E. M. Fs., and the rectifier which has greater E. M. F. has the greater rectifying action.

In Fig. 6, (3) shows the case where the rectifier, excellent in rectifying action, has comparatively great E. M. F. (9) shows no rectifying action and has no E. M. F. (8) show a minute E. M. F. and a small rectifying action. But these states are unstable so that even in the case (3), if the contacting point is displaced a little, the E. M. F. and the rectifying action would suddenly disappear.

In Fig. 7, the E. M. F. and the relation between the electric currents and the applied voltages for a Mazda photo-cell when day light of various intensities fall on it, are shown. The E. M. F. is affected by the intensity of illumination and the relations between the electric currents and the applied voltages are shown by nearly straight lines as in the case

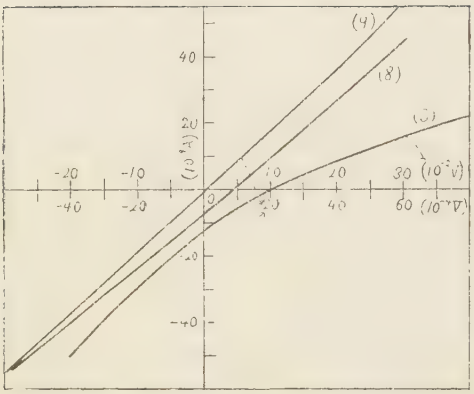

Fig. 6. Crystal detectors.
A brass needle contacts on crystals.
[pyrite (3), chalco-pyrite (8), bornite (9)]

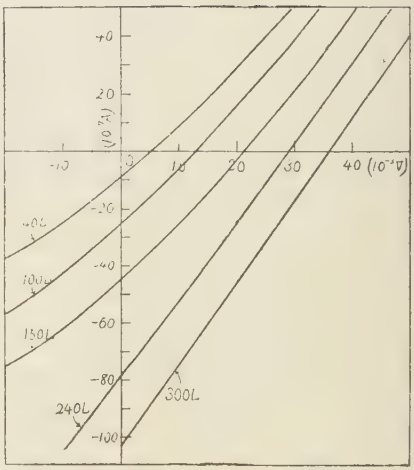

Fig. 7. Mazda Photo-cell.

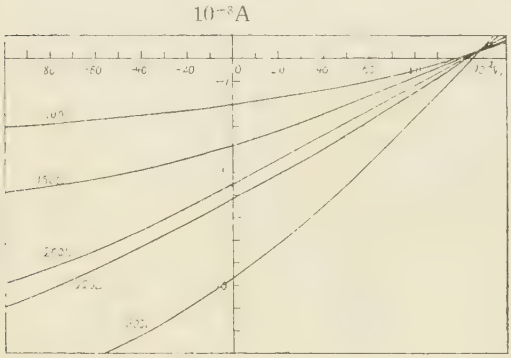

Fig. 8. Photo-electric tube (K).

of the concrete columns.

In Fig. 8, the E.M.F. and the relation between the electric currents to the applied voltages of a K-photo-electric tube when day light of various intensities fall on it, are shown. The E.M.F. is affected slightly by the intensity of light, but the strength of electric current is greatly affected by it. The electric current is rapidly increased by a small increase of the applied voltage in the direction of the E.M.F. of the tube, and then attains a saturation current, the strength of which depends on the intensity of light. When a voltage in the inverse direction, greater than the E.M.F. of the tube, is applied, a small (perhaps leakage) current is observed.

5. Conclusion

It was found that the asymmetries of the electric resistances of concrete and others have intimate relations to the E.M.Fs. of the specimens, that the direction of easy flow of the specimens is always in the direction from (−) ends to (+) ends of the specimens, that is, they are considered as some kinds of galvanic cells.

The relation between the electric currents and the applied voltages was studied, and

it was found that the curves explaining the relation are almost straight lines.

Crystal detectors, a photo-cell and a photoelectric tube was studied by a similar manner, and it was found that crystal detectors have minute E. M. Fs. and these E. M. Fs. have intimate relations to their rectifying actions, that the E. M. Fs. of the photo-cell and the photoelectric tube depend on the intensity of light falling on them, the dependence are very different in the case of the photo-cell from the case of the photoelectric tube.

In conclusion, I wish to express sincere gratitude to Prof. Nakamura and to Prof. Namba for their kind guidance and encouragement and to Mr. Chikazawa for his co-operation in measurement.

This report was read Dec. 1952 at the regular meeting of Kyushu Branch of the Physical Society of Japan.

References

1. Kumamoto J. Sci. A. Vol. I, No. 1, (Oct. 1952) 74.
2. Kumamoto J. Sci. A. Vol. I, No. 2, (March 1953) 17.

ON THE NUMERICAL SOLUTION OF THE SECOND ORDER DIFFERENTIAL EQUATION UNDER SOME CONDITIONS.

Ryuzo ADACHI

(Received Sept. 1, 1953)

Abstract

We have treated of the numerical solution of the second order differential equation $\frac{d^2y}{dx^2} = f\left(x, y, \frac{dy}{dx}\right)$ under the following conditions

"the solution curve $y = y(x)$ intersects with two given curves $\Psi_1(x, y) = 0$ and $\Psi_2(x, y) = 0$, and at the intersections (X_1, Y_1) and (X_2, Y_2), given relations $g_1(X_1, Y_1, P_1) = 0$, $g_2(X_2, Y_2, P_2) = 0$ must be satisfied,

where P_1 and P_2 are the values of $\frac{dy}{dx}$ when $x = X_1$ and $x = X_2$ respectively, and $g_1(x, y, p)$, $g_2(x, y, p)$ are given functions of x, y, p, ."

1. Introduction

Let a given differential equation be

$$\frac{d^2y}{dx^2} = f\left(x, y, \frac{dy}{dx}\right)$$

and as usual, put $\frac{dy}{dx} = p$, then

$$\frac{dy}{dx} = p, \quad \frac{dp}{dx} = f(x, y, p) \quad \cdots\cdots (1).$$

When we calculate the numerical solution of these equations, it is obvious that we must give two conditions, and as these, we consider followimg conditions

(a) $g_1(X_1, Y_1, P_1) = 0$ ····· at the intersection (X_1, Y_1) of the solution curve $y = y(x)$ and a giyen curve $\Psi_1(x, y) = 0$

(b) $g_2(X_2, Y_2, P_2) = 0$ ····· at the intersection (X_2, Y_2) of the solution curve $y = y(x)$ and a given curve $\Psi_2(x, y) = 0$

where P_1 and P_2 are the values of P when $x = X_1$ and $x = X_2$ respectively and $g_1(x, y, p)$, $g_2(x, y, p)$ are given functions of x, y, p and involve at least one of y, p actually.

At first, we take any approximate function $y_1(x)$ (actually, we divide the interval of x into small intervals and the numerical values of $y_1(x)$ at each dividing point of x are given), and by successive approximation of the iterative method, we calculate the numerical values of $y(x)$. Namely starting from the first approximation $y_1(x)$, $P_1(x)$ we calculate the second approximation $y_2(x)$, $p_2(x)$, the third approximation $y_3(x)$. $p_3(x)$, ····· successively, and when $y_{n-1}(x) \equiv y_n(x)$ is reached within the required accuracy, stop this procedure.

Generally we put

$$\left.\begin{aligned} &f(x, y_{n-1}(x), p_{n-1}(x)) = F_{n-1}(x) \\ &q_n(x) = \int_0^x F_{n-1}(x)\,dx, \quad r_n(x) = \int_0^x q_n(x)\,dx \end{aligned}\right\} \cdots\cdots (2)$$

here $q_n(o) = 0$, $r_n(o) = 0$

and if the values of $y_{n-1}(x)$, $p_{n-1}(x)$ at each value of x are known, we can calculate the values of $q_n(x)$, $r_n(x)$ at each value of x by ordinary numerical integration. Putting

$$\frac{dy_n}{dx} = p_n, \quad \frac{dp_n}{dx} = F_{n-1}(x)$$

we have

$$p_n(x) = q_n(x) + c_n, \quad y_n(x) = r_n(x) + c_n x + d_n \cdots\cdots (3)$$

where c_n, d_n are some indeterminate constants, and in the following section we consider how to determine c_n, d_n. It is obvious that c_n, d_n are the values of $p_n(o)$, $y_n(o)$ respectively.

Let $({}_nX_1, {}_nY_1)$, $({}_nX_2, {}_nY_2)$ be the intersections of $y = y_n(x)$ with $\Psi_1(x, y) = 0$ and $\Psi_2(x, y) = 0$ respectively, then from the given condtions we have

$$\Psi_1({}_nX_1, r_n({}_nX_1) + c_n\,{}_nX_1 + d_n) = 0,$$

$$g_1({}_nX_1, r_n({}_nX_1) + c_n\,{}_nX_1 + d_n, q_n({}_nX_1) + c_n) = 0$$

$$\Psi_2({}_nX_2, r_n({}_nX_2) + c_n\,{}_nX_2 + d_n) = 0,$$

$$g_2({}_nX_2, r_n({}_nX_2) + c_n\,{}_nX_2 + d_n, q_n({}_nX_2) + c_n) = 0$$

and solving these equations simultaneously with respect to ${}_nX_1$, ${}_nX_2$, c_n, d_n, we get the values of c_n, d_n. But generally, it is very difficult that we solve these simultaneous

equations and it is rather convenient that we consider the given conditions (a) and (b) by dividing into following elementary cases.

At the beginning, in the condition (a), if $\Psi_1(x, y)$ involves y actually, solving $\Psi_1(x, y) = 0$ with respect to y we have $y = \varphi_1(x)$, and if $\Psi_1(x, y)$ does not involve y, by solving $\Psi_1(x, y) = 0$ with respect to x we have $x = \text{const}$.

Next, if $g_1(x, y, p)$ involves p actually, solving $g_1(x, y, p) = 0$ with respect to p we have $p = h_1(x, y)$ and at (X_1, Y_1), we get $Y_1 = \varphi_1(X_1)$ or $X_1 = \text{const} = a_1$, therefore

$P_1 = h_1(X_1, Y_1) = h_1(X_1, \varphi_1(X_1)) = k_1(X_1)$ or $P_1 = h_1(a_1, Y_1) = l_1(Y_1)$. And if $l_1(Y_1)$ involves Y_1 actually, $P_1 = l_1(Y_1)$ can be transformed to a form $Y_1 = m_1(P_1)$, or if $l_1(Y_1)$ does not involve Y_1, we have $P_1 = l_1(Y_1) = \text{const}$. If $g_1(x, y, p)$ does not involve p, it must involve y actually and $g_1(x, y, p) = 0$ can be deformed to a form $y = g(x)$, therefore we get $Y_1 = g(X_1)$ and $\Psi_1(X_1, Y_1) = 0$ and from these relations, we have $X_1 = \text{constant}$, $Y_1 = \text{constant}$.

Consequently the condition (a) becomes one of the forms

$y = m_1(p)$ ····· when $x = a_1$

$p = \alpha_1$ ····· when $x = a_1$

$p = k_1(x)$ ····· at the intersection of the solution curve $y = y(x)$ and a given curve $y = \varphi_1(x)$

where a_1, α_1 are given constants and $m_1(p)$, $k_1(x)$ are given functions and can take a constant as a special case.

Similarly the condition (b) becomes one of the forms

$y = m_2(p)$ ····· when $x = a_2$

$p = \alpha_2$ ····· when $x = a_2$

$p = k_2(x)$ ····· at the intersection of the solution curve $y = y(x)$ and a given curve $y = \varphi_2(x)$

where a_2, α_2 are given constants and $m_2(p)$, $k_2(x)$ are given functions.

We can put "one of a_1, $a_2 = 0$; and one of α_1, $\alpha_2 = 0$" for the sake of simplicity

but it is obvious that there is no loss of generality. Accordingly two conditions (a) and (b) together become one of the forms

(i) $y = m_1(p)$ when $x = 0$ and $y = m_2(p)$ when $x = a_2$

(ii) $p = 0$ when $x = 0$ and $y = m_2(p)$ when $x = a_2$

(iii) $p = 0$ when $x = 0$ and $p = \alpha_2$ when $x = a_2$

(iv) $y = m_1(p)$ when $x = 0$ and $p = k_2(x)$ at the intersection of the solution curve $y = y(x)$ and a given curve $y = \varphi_2(x)$

(v) $p = 0$ when $x = 0$ and $p = k_2(x)$ at the intersection of the solution curve $y = y(x)$ and a given curve $y = \varphi_2(x)$

(vi) $p = k_1(x)$ at the intersection of the solution curve $y = y(x)$ and a given curve $y = \varphi_1(x)$

$p = k_2(x)$ at the intersection of the solution curve $y = y(x)$ and a given curve $y = \varphi_2(x)$

where a_2, α_2 are given constants and $m_1(p)$, $m_2(p)$, $k_1(x)$, $k_2(x)$ are given functions. Therefore in the following sections we consider these six cases.

The condition "$g(x, y, p,) = 0$ when $x = a$" can be transformed to a form "$g(x, y, p) = 0$ at the intersection of the solution curve and a given curve $y = \varphi(x)$" by turnning the coordinate axis. Therefore in above discussion we can put $y = \varphi(x)$ in place of $\Psi(x, y) = 0$ with no loss of generality. But in practice, frequently the given condition takes such form ($g(x, y, p) = 0$ when $x = a$), therefore we treated of such cases.

2. Case (i), (ii) and (iii).

Case (i)

Conditions ····· $y = m_1(p)$ when $x = 0$ and $y = m_2(p)$ when $x = a_2$.

From (3)

$$d_n = m_1(c_n),\ r_n(a_2) + c_n a_2 + d_n = m_2(q_n(a_2) + c_n)$$

solving these simultaneous equations with respect to c_n, d_n numerically, we have the values of c_n, d_n.

Case (ii)

Conditions ····· $p = 0$ when $x = 0$ and $y = m_2(p)$ when $x = a_2$.

From (3)

$$c_n = 0,\ r_n(a_2) + d_n = m_2(q_n(a_2))$$

that is

$$c_n = 0,\ d_n = m_2(q_n(a_2)) - r_n(a_2).$$

Case (iii)

Conditions ····· $p = 0$ when $x = 0$ and $p = \alpha_2$ when $x = a_2$.

From (3) $c_n = 0$, $y_n(x) = r_n(x) + d_n$

and d_n is determined from the relation

$$p_{n+1}(a_2) = \int_0^{a_2} f(x,\ r_n(x) + d_n,\ q_n(x))\,dx = \alpha_2$$

that is, we solve above equation with respect to d_n numerically.

3. Case (iv) and (v).

Case (iv)

Conditions ····· $y = m_1(p)$ when $x = 0$ and $p = k_2(x)$ at the intersection of the solution curve $y = y(x)$ and a given curve $y = \varphi_2(x)$.

From (3)

$$d_n = m_1(c_n) \quad \cdots\cdots (\mathrm{I})$$

and let $({}_nX_2,\ {}_nY_2)$ be the intersection of $y = y_n(x)$ and $y = \varphi_2(x)$, then

$$r_n({}_nX_2) + c_n\,{}_nX_2 + d_n = \varphi_2({}_nX_2) \quad \cdots\cdots (\mathrm{II})$$

$$q_n({}_nX_2) + c_n = k_2({}_nX_2) \quad \cdots\cdots (\mathrm{III})$$

from these 3 relations we have

$$r_n({}_nX_2) + [k_2({}_nX_2) - q_n({}_nX_2)]\,{}_nX_2 + m_1(k_2({}_nX_2) - q_n({}_nX_2)) = \varphi_2({}_nX_2)$$

therefore putting

$$s_n(x) \equiv r_n(x) + [k_2(x) - q_n(x)]x + m_1(k_2(x) - q_n(x)) - \varphi_2(x),$$

${}_nX_2$ is determined as a root of $s_n(x) = 0$, then c_n, d_n are determined from (II) and (III).

Case (v)

Conditions ····· $p = 0$ when $x = 0$ and $p = k_2(x)$ at the intersection of the solution curve $y = y(x)$ and a given curve $y = \varphi_2(x)$.

Similarly

$$c_n = 0,\ r_n\ (\ {}_nX_2\ ) + d_n = \varphi_2\ (\ {}_nX_2\ ),\ q_n\ (\ {}_nX_2\ ) = k_2\ (\ {}_nX_2\ ),$$

therefore ${}_nX_2$ is determined as a root of $s_n\ (\ x\ ) \equiv q_n\ (\ x\ ) - k_2\ (\ x\ ) = 0$, then the value of d_n obtained from $d_n = \varphi_2\ (\ {}_nX_2\ ) - r_n\ (\ {}_nX_2\ )$.

4. Case (vi).

Conditions ····· $p = k_1\ (\ x\ )$ at the intersection of the solution curve $y = y\ (\ x\ )$ and a given curve $y = \varphi_1\ (\ x\ )$,

$p = k_2\ (\ x\ )$ at the intersection of the solution curve $y = y\ (\ x\ )$ and a given curve $y = \varphi_2\ (\ x\ )$.

Let $(\ {}_nX_1,\ {}_nY_1\ ),\ (\ {}_nX_2,\ {}_nY_2\ )$ be the intersection of the n^{th} approximate curve $y = y_n\ (\ x\ )$ and given curves $y = \varphi_1\ (\ x\ ),\ y = \varphi_2\ (\ x\ )$ respectively, then we have

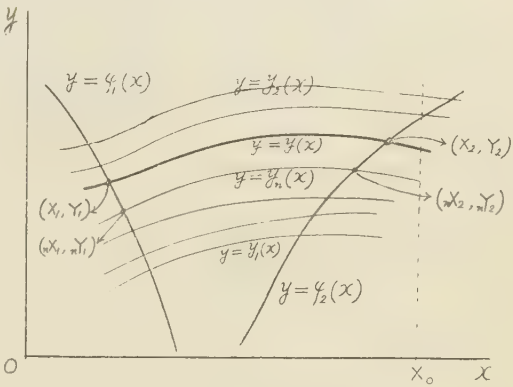

Fig. 1

$$q_n\ (\ {}_nX_1\ ) + c_n = k_1\ (\ {}_nX_1\ )$$
$$q_n\ (\ {}_nX_2\ ) + c_n = k_2\ (\ {}_nX_2\ )$$
$$r_n\ (\ {}_nX_1\ ) + c_n\ {}_nX_1 + d_n = \varphi_1\ (\ {}_nX_1\ )$$
$$r_n\ (\ {}_nX_2\ ) + c_n\ {}_nX_2 + d_n = \varphi_2\ (\ {}_nX_2\ ),$$

and solving these simultaneous equations with respect to ${}_nX_1,\ {}_nX_2,\ c_n,\ d_n$ we get $c_n,\ d_n$.

We can take any known algebraic, graphical or other method to find the numerical solutions of these simultaneous equations, and also the following method is a convenient one. Putting

$$\left.\begin{aligned} A_n\ (\ x\ ) &= k_1\ (\ x\ ) - q_n\ (\ x\ ),\quad B_n\ (\ x\ ) = k_2\ (\ x\ ) - q_n\ (\ x\ ) \\ D_n\ (\ x\ ) &= \varphi_1\ (\ x\ ) - r_n\ (\ x\ ),\quad E_n\ (\ x\ ) = \varphi_2\ (\ x\ ) - r_n\ (\ x\ ) \end{aligned}\right\} \cdots\cdots\cdots\cdots\cdots\cdots (\mathrm{I})$$

we have

$$\left.\begin{aligned} c_n &= A_n\ (\ {}_nX_1\ ) = B_n\ (\ {}_nX_2\ ) \\ d_n &= D_n\ (\ {}_nX_1\ ) - c_n\ {}_nX_1 = E_n\ (\ {}_nX_2\ ) - c_n\ {}_nX_2 \end{aligned}\right\} \cdots\cdots\cdots\cdots\cdots\cdots\cdots\cdots (\mathrm{II}).$$

Solving $A_n\ (\ {}_nX_1\ ) = B_n\ (\ {}_nX_2\ )$ with respect to ${}_nX_2$ we have ${}_nX_2 = B_n^{-1}\ (\ A_n\ (\ {}_nX_1\ )\ ) = G_n\ (\ {}_nX_1\ )$,

then from (II) we get

$$A_n\,(\,{}_nX_1\,)\,[\,G_n\,(\,{}_nX_1\,)-{}_nX_1\,]-E_n\,(\,G_n\,(\,{}_nX_1\,)\,)+D_n\,(\,{}_nX_1\,)=0,$$

therefore ${}_nX_1$ is a root of the equation

$$S_n\,(\,x\,)\equiv A_n\,(\,x\,)\,[\,G_n\,(\,x\,)-x\,]-E_n\,(\,G_n\,(\,x\,)\,)+D_n\,(\,x\,)=0,$$

then from (II) we have the values of c_n, d_n.

5. Examples

In the following, we show some examples for the sake of better understanding.

EX 1.

$$\frac{dy}{dx}=p,\quad \frac{dp}{dx}=-y$$

conditions ····· $y=0$ when $x=0$

$p=1$ at the intersection of the solution curve and the straight line $y=1-x$.

This problem is in the case (iv) and $m_1\,(\,p\,)=0$, $k_2\,(\,x\,)=1$, $\varphi_2\,(\,x\,)=1-x$, $f\,(\,x,\,y,\,p\,)=-y$, therefore

$$q_n\,(\,x\,)=-\int_0^x y_{n-1}\,(\,x\,)\,dx,\quad r_n\,(\,x\,)=\int_0^x q_n\,(\,x\,)\,dx$$

$$s_n\,(\,x\,)=r_n\,(\,x\,)-x\,q_n\,(\,x\,)+2x-1$$

and

$$p_n\,(\,x\,)=q_n\,(\,x\,)+1-q_n\,(\,{}_nX_2\,),\ y_n\,(\,x\,)=r_n\,(\,x\,)+\{\,1-q_n\,(\,{}_nX_2\,)\}\,x,$$

where ${}_nX_2$ is a root of $s_n\,(\,x\,)=0$.

In the follouing table, taking $y_1\,(\,x\,)=x$ as the first approximation of $y\,(\,x\,)$, calculated the values of $q_2\,(\,x\,)$, $r_2\,(\,x\,)$ for each value of x by ordinarly numerical integration, then the values of $s_2\,(\,x\,)$ for each value of x is calculated by the formula $s_2\,(\,x\,)=r_2\,(\,x\,)-x\,q_2\,(\,x\,)+2x-1$ and from the values of $s_2\,(x)$, the value (0.483) of ${}_2X_2$ is founded by interpolation and then the value (-0.118) of $q_2\,(0.483)$ is founded by interpolation, therefore

$$p_2\,(\,x\,)=q_2\,(\,x\,)+1.118,\qquad y_2\,(\,x\,)=r_2\,(\,x\,)+1.118x.$$

Similarly

$$p_3\,(\,x\,)=q_3\,(\,x\,)+1.128,\qquad y_3\,(\,x\,)=r_3\,(\,x\,)+1.128x$$

$$p_4\,(\,x\,)=q_4\,(\,x\,)+1.1280,\quad y_4\,(\,x\,)=r_4\,(\,x\,)+1.1280x.$$

Table. 1.

		${}_2X_2 = 0.483$					${}_3X_2 = 0.480$		
		$q_2({}_2X_2) = -0.118$					$q_3({}_3X_2) = -0.128$		
x	$y_1 = -F_1$	q_2	r_2	s_2	p_2	$y_2 = -F_2$	q_3	r_3	s_3
0.00	0.00	0.000	0.0000	−1.0000	1.118	0.000	0.000	0.0000	
0.05	0.05	−0.001	0.0000	−0.9000	1.117	0.056	−0.001	0.0000	
0.10	0.10	5	2	7997	1.113	0.112	6	−0.0002	
0.15	0.15	11	6	6989	1.170	167	13	7	
0.20	0.20	20	14	5974	1.098	222	22	16	
0.25	0.25	31	27	4948	1.087	277	35	30	
0.30	0.30	45	46	3911	1.073	331	50	15	
0.35	0.35	61	72	2858	1.057	384	68	81	
0.40	0.40	−0.080	108	1788	1.038	437	89	−0.0120	−0.1764
0.45	0.45	−0.101	153	−0.0697	1.017	488	−0.112	171	−0.0667
0.50	0.50	125	209	0.0416	0.993	539	138	233	0.0457
0.55	0.55	151	279	1554	0.967	588	166	−0.0309	0.1604
0.60	0.60	−0.180	−0.0361	0.2719	0.938	0.635	−0.197		

		${}_4X_2 = 0.4796$						
		$q_4({}_4X_2) = -0.1280$						
x	p_3	$y_3 = -F_3$	q_4	r_4	s_4	p_4	y_4	y
0.00	1.128	0.000	0.000	0.0000		1.128	0.0000	0.0000
0.05	1.127	0.056	−0.001	0.0000		1.127	0.0564	0.0564
0.10	1.122	0.113	6	−0.0002		1.122	0.1126	0.1125
0.15	1.115	169	13	7		1.115	1685	1684
0.20	1.106	224	23	16		1.105	2240	2240
0.25	1.093	279	35	30		1.093	2790	2789
0.30	1.078	333	50	52		1.078	3333	3331
0.35	1.060	387	68	81		1.060	3868	3865
0.40	1.039	439	89	−0.0120	−0.1764	1.039	4393	4389
0.45	1.016	491	−0.112	171	−0.0667	1.016	4907	4903
0.50	0.990	541	138	233	0.0457	0.990	5409	5404
0.55	0.962	590	167	−0.0310	0.1609	0.961	5897	5891
0.60	0.931	0.637	−0.197			0.931	0.6370	0.6364

We can solve this differential equation directly, and the result is $y = 1.1272\ \sin x$. The last figures in this table are the values which are calculated by this formula.

EX 2.

$$\frac{dy}{dx} = p,\quad \frac{dp}{dx} = \frac{1+p}{y-x+6} - 1.5(1-x)$$

conditions ····· $y = 0$ when $x = 0$ and the solution curve is in contact with the parabola $y = 0.1 - 10\ (x - 0.3)^2$.

Solution curves of this equation which pass the origin form a family of curves as shown in Fig. 2., and from this family we ought to find the curve which touches to the parabola.

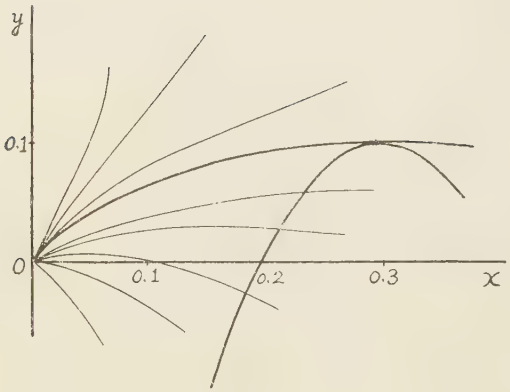

Fig. 2.

This problem is in the case (iv) also, and

$$m_1(p) = 0,$$

$$\varphi_2(x) = 0.1 - 10(x - 0.3)^2,$$

$$k_2(x) = \frac{d}{dx}\varphi_2(x) = 6 - 20x,$$

and

$$F_{n-1}(x) = \frac{1 + p_{n-1}(x)}{y_{n-1}(x) - x + 6} - 1.5(1-x), \quad q_n(x) = \int_0^x F_{n-1}(x)dx,$$

$$r_n(x) = \int_0^x q_n(x)\,dx,$$

$$s_n(x) = r_n(x) - x\,q_n(x) - (x - 0.3)(10x + 3) - 0.1,$$

$$c_n = 6 - 20\,{}_nX_2 - q({}_nX_2), \quad d_n = 0.$$

The following table is obtained by similar method as EX. 1., starting from the straight line $y_1(x) = 0.33x$, that is

$$p_1(x) = 0.33, \quad y_1(x) = 0.33x,$$

and from these, calculated the values of $F_1(x)$, $q_2(x)$, $r_2(x)$ and $s_2(x)$ for each value of x ($x = 0.00,\ 0.02,\ \cdots\cdots\cdots\ 0.40$). And then by interpolation we get

$${}_2X_2 = 0.290, \quad q_2({}_2X_2) = -0.305 \quad \therefore\ c_2 = 6 - 20\,{}_2X_2 - q_2({}_2X_2) = 0.505$$

$$\therefore\ p_2(x) = q_2(x) + 0.505, \quad y_2(x) = r_2(x) + 0.505x.$$

Similarly

$${}_3X_2 = 0.2902, \quad q_3({}_3X_2) = -0.306, \quad \therefore\ c_3 = 0.502$$

$$\therefore\ p_3(x) = q_3(x) + 0.502, \quad y_3(x) = r_3(x) + 0.502x$$

$${}_4X_2 = 0.2902, \quad q_4({}_4X_2) = -0.306 \quad \therefore\ c_4 = 0.502$$

$$\therefore\ p_4(x) = q_4(x) + 0.502, \quad y_4(x) = r_4(x) + 0.502x,$$

and within 0.2%, $y_3(x) \equiv y_4(x)$ is satisfied.

Table. 2.

x	p_1	y_1	F_1	q_2	r_2	s_2	p_2	y_2	F_2	q_3
0.00	0.33	0.000	−1.28	0.000	0.000	0.800	0.505	0.000	−1.249	0.000
0.02	33	0.007	−1.25	−0.025	0.000	797	480	0.010	−1.223	−0.025
4	33	0.013	−1.22	50	−0.001	785	455	19	−1.193	49
6	33	20	−1.19	74	2	766	431	28	−1.170	73
8	33	26	−1.16	98	4	740	407	37	−1.144	96
0.10	33	33	−1.13	−0.121	6	706	384	44	−1.117	−0.118
12	33	39	1.09	143	9	664	362	52	−1.090	140
14	33	46	1.06	164	−0.012	615	341	59	−1.063	162
16	33	52	−1.03	185	16	558	320	66	−1.036	183
18	33	59	−1.00	205	19	494	300	72	−1.009	203
0.20	33	66	−0.97	225	24	421	280	78	−0.982	223
22	33	72	0.94	244	28	342	261	83	−0.955	242
24	33	79	−0.91	263	34	253	242	88	−0.928	261
26	33	85	0.88	281	39	168	224	93	−0.900	280
28	33	92	0.85	298	45	0.054	207	97	−0.873	297
0.30	33	99	0.82	315	51	−0.056	190	0.101	−0.845	315
32	33	0.105	−0.79	331	57	−0.175	174	104	−0.817	331
34	33	112	0.76	346	64	−0.302	159	108	−0.789	347
36	33	118	0.73	361	71	−0.437	144	111	−0.761	362
38	33	125	0.70	375	79	−0.680	130	113	−0.733	378
0.40	0.33	0.132	−0.67	−0.389	−0.086	−0.730	0.116	0.116	−0.705	−0.392

x	r_3	s_3	p_3	y_3	F_3	q_4	r_4	s_4	p_4	y_4
0.00	0.0000		0.502	0.0000	−1.250	0.000	0.0000		0.502	0.0000
0.02	−0.0003		477	0.0098	−1.224	−0.025	−0.0003		477	0.0098
4	−0.0010		453	0.0191	−1.197	49	−0.0010		453	0.0191
6	22		429	279	−1.171	73	22		429	279
8	39		406	363	−1.144	96	39		406	363
0.10	60		384	443	−1.117	−0.118	60		384	442
12	86		362	517	−1.090	141	86		361	516
14	−0.0116		340	587	−1.063	162	−0.0117		340	586
16	151		319	653	−1.037	183	151		319	652
18	190		299	715	−1.010	203	190		299	714
0.20	233		279	773	−0.982	223	232		279	772
22	280		259	827	−0.955	243	279		259	826
24	330		241	877	−0.928	262	329		240	875
26	384	0.1584	222	923	−0.900	280	383	0.1585	222	922
28	442	0.0550	205	966	−0.873	297	441	0.0551	205	964
0.30	503	−0.0558	186	0.1005	−0.846	315	502	−0.0558	187	0.1004
32	568	−0.1749	171	1041	−0.818	331	567	−0.1748	171	1039
34	636		155	1074	−0.790	347	635		155	1072
36	707		139	1103	−0.762	363	706		139	1101
38	781		124	1129	−0.734	378	780		124	1128
0.40	−0.0858		0.110	0.1153	−0.705	−0.392	−0.0857		0.110	0.1151

EX 3.

$$\frac{dy}{dx} = p, \quad \frac{dp}{dx} = \frac{1}{1+y^2}$$

conditions ····· the solution curve and the parabola $y = 3(x+0.2)^2$ intersect perpendicularly and

the solution curve and the circle $y = \sqrt{1-(x-2)^2}$ touch each

other.

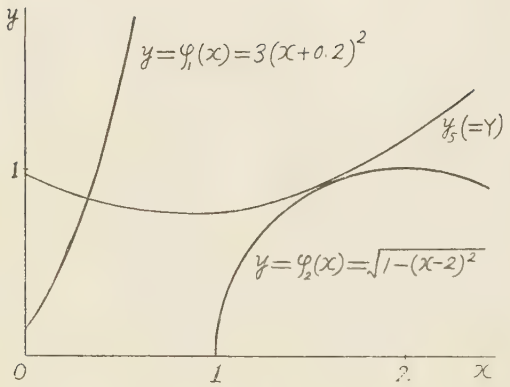

Fig. 3.

This problem is in the case (vi) and

$$\varphi_1(x) = 3(x+0.2)^2$$

$$\varphi_2(x) = \sqrt{1-(x-2)^2}$$

$$k_1(x) = \frac{-1}{\frac{d}{dx}\varphi_1(x)} = \frac{-1}{6(x+0.2)}$$

$$k_2(x) = \frac{d}{dx}\varphi_2(x) = \frac{2-x}{\sqrt{-3+4x-x^2}}$$

and

$$\left.\begin{aligned} &F_{n-1}(x) = \frac{1}{1+[y_{n-1}(x)]^2},\quad q_n(x) = \int_0^x F_{n-1}(x)\,dx,\\ &r_n(x) = \int_0^x q_n(x)\,dx \\ &A_n(x) = \frac{-1}{6(x+0.2)} - q_n(x),\ B_n(x) = \frac{2-x}{\sqrt{-3+4x-x^2}} - q_n(x)\\ &D_n(x) = 3(x+0.2)^2 - r_n(x),\ E_n(x) = \sqrt{-3+4x-x^2} - r_n(x)\\ &c_n = A_n({}_nX_1),\quad d_n = D_n({}_nX_1) - c_n\,{}_nX_1 \end{aligned}\right\} \cdots (\mathrm{I})$$

where ${}_nX_1$ is a root of

$$s_n(x) \equiv A_n(x)[G_n(x) - x] - E_n(G_n(x)) + D_n(x) = 0 \cdots (\mathrm{II}).$$

As the first approximation, let us take $y_1(x) = 1$, and calculate the values of $F_1(x)$, $q_2(x)$, $r_2(x)$, $A_2(x)$ ..... for each value of x ($x = 0.0, 0.1, 0.2, 0.4, 0.6, \cdots\cdots 3.0$) by the following order successively.

(1) calculate the values of $F_1(x)$ and integrate $q_2(x) = \int_0^x F_1(x)\,dx$

$r_2(x) = \int_0^x q_2(x)\,dx$ numerically

(2) by the formula (I) calculate the values of $A_2(x)$, $B_2(x)$, $D_2(x)$ and $E_2(x)$

(3) from the table of the values of $A_2(x)$, $B_2(x)$, by interpolation, find the values of $G_2(x)$ which satisfies the relation $A_2(x) = B_2(G_2(x))$ for each value of x ($x = 0.0,\ 0.1,\ 0.2,\ 0.4,\ \cdots\cdots\cdots\cdots\ 1.0$)

(4) from the table of the values of $E_2(x)$, find the values of $E_2(G_2(x))$ by interpolation

(5) calculate the values of $s_2(x)$ using the formula (II) and above values, and by interpolation, solve the equation $s_2(x) = 0$ numerically, and we get ${}_2X_1 = 0.345$, then

$c_2 = A_2(0.345) = -0.480,\ d_2 = D_2(0.345) - c_2 \times 0.345 = 1.043$

and we have

$p_2(x) = q_2(x) - 0.480,\ y_2(x) = r_2(x) - 0.480x + 1.043.$

Similarly

${}_3X_1 = 0.327,\ c_3 = -0.489,\ d_3 = 0.983$

$\therefore\ p_3(x) = q_3(x) - 0.489,\ y_3(x) = r_3(x) - 0,489x + 0.983$

${}_4X_1 = 0.323,\ c_4 = -0.501,\ d_4 = 0.969$

$\therefore\ p_4(x) = q_4(x) - 0.501,\ y_4(x) = r_4(x) - 0.501x + 0.969$

${}_5X_1 = 0.323,\ c_5 = -0.504,\ d_5 = 0.967$

$\therefore\ p_5(x) = q_5(x) - 0.504,\ y_5(x) = r_5(x) - 0.504x + 0.967.$

The last figures Y in the table. 5., are the values which are calculated by the ordinarly method under the conditions that

"$p = c_5 = -0.504,\ y = d_5 = 0.967$ when $x = 0$"

and y_5 coinsides with Y about within 0.1%, therefore y_5 is the required solution.

Table. 3.

x	$\frac{-1}{6(x+0.2)}$	$3(x+0.2)^2$	$\sqrt{-3+4x-x^2}$	$\frac{2-x}{\sqrt{-3+4x-x^2}}$	y_1	q_2	r_2	A_2	B_2	D_2
0.0	−0.8333	0.1200			1.0	0.000	0.000	−0.833		0.120
0.1	−−0.5556	0.2700			1.0	0.050	0.003	−0.606		0.257
0.2	−0.4167	0.4800			1.0	0.100	0.010	−0.517		0.470
0.4	−0.2778	1.0800			1.0	0.200	40	−0.478		1.040
0.6	−0.2083	1.9200			1.0	300	90	−0.508		1.830
0.8	−0.1667	3.0000			1.0	400	160	−0.567		2.840
1.0	−0.1389	4.3200	0.0000	$+\infty$	1.0	500	250	−0.639		4.070
1.2	−0·1191	5.8800	0.6000	1.3333	1.0	600	360		0.733	
1.4	−0.1042	7.6800	0.8000	0.7500	1.0	700	490		0.050	

1.6	−0.0926	9.7200	0.9165	0.4364	1.0	800	640	−0.364
1.8	−0.0833	12.000	0.9798	0.2041	1.0	900	810	−0.696
2.0	−0.0758	14.520	1.0000	0.0000	1.0	1.000	1.000	−1.000
2.2			0.9798	−0.2041	1.0	1.100	1.210	−1.304
2.4			0.9165	−0.4364	1.0	1.200	1.440	−1.636
2.6			0.8000	−0.7500	1.0	1.300	1.690	−2.050
2.8			0.6000	−1.3333	1.0	1.400	1.960	−2.733
3.0			0.0000	−∞	1.0	1.500	2.250	

$_2X_1 = 0.345$, $_2X_2 = 1.665$, $c_2 = -0.480$, $d_2 = 1.043$

Table. 4.

x	E_2	G_2	$E_2(G_2(x))$	s_2	p_2	y_2	q_3	r_3	A_3	B_3	D_3
0.0		1.885	0.106	−1.558	−0.480	1.043	0.000	0.000			
0.1		1.745	0.204	−0.934	−0.430	0.996	0.049	0.003	−0.605		0.267
0.2		1.685	0.240	−0.537	−0.380	955	100	10	−0.517		0.470
0.4		1.625	0.268	0.186	−0.280	889	208	41	−0.486		1.039
0.6		1.680	0.242	1.040	−0.180	843	323	94	−0.513		1.826
0.8		1.715	0.222	2.099	−0.080	817	441	170	−0.608		2.830
1.0	−0.250	1.765	0.192	3.390	0.020	811	561	270			
1.2	0.240				120	825	681	395			
1.4	0.310				220	859	798	543		−0.048	
1.6	0.277				320	913	910	713		−0.474	
1.8	0.170				420	987	1.015	906		−0.811	
2.0	0.000				520	1.081	1.112	1.119		−1.112	
2.2	−0.230				620	1.195	1.199	1.350			
2.4	−0.523				720	1.329	1.276	1.597			
2.6	−0.890				820	1.483	1.344	1.859			
2.8	−1.360				920	1.657	1.402	2.134			
3.0	−2.250				1.020	1.851	1.451	2.419			

$_3X_1 = 0.327$, $_3X_2 = 1.608$, $c_3 = -0.489$, $d_3 = 0.983$

Table. 5.

x	E_3	G_3	$E_3(G_3(x))$	s_3	y_3 ·····	y_4	y_5	Y
0.0					0.983 ·····	0.969	0.967	0.967
0.1		1.680	0.158	−0.847	937	922	920	919
0.2		1.625	0.192	−0.458	895	880	877	877
0.4		1.605	0.202	0.251	828	812	809	809
0.6		1.635	0.186	1.090	784	768	766	766
0.8		1.680	0.158	2.137	762	749	748	748
1.0					764	755	754	755
1.2					791	786	787	787
1.4	0.257				841	842	843	844
1.6	0.204				914	920	924	925
1.8	0.074				1.009	1.020	1.026	1.027
2.0	−0.119				1.124	1.141	1.147	1.148
2.2					1.257	1.278	1.286	1.286
2.4					1.406	1.431	1.439	1.440
2.6					1.571	1.596	1.607	1.607
2.8					1.748	1.774	1.785	1.785
3.0					1.935 ·····	1.962	1.973	1.973

$_4X_1 = 0.323$, $_4X_2 = 1.593$, $c_4 = -0.501$, $d_4 = 0.969$

$_5X_1 = 0.323$, $_5X_2 = 1.595$, $c_5 = -0.504$, $d_5 = 0.967$

6. Convergency of solutions

We can prove the convergency of solutions under some conditions. For the n^{th} approximate solution, we have

$$\left.\begin{aligned} q_n(x) &= \int_0^x F_{n-1}(x)\,dx, \quad r_n(x) = \int_0^x q_n(x)\,dx \\ p_n(x) &= q_n(x) + c_n, \qquad y_n(x) = r_n(x) + c_n x + d_n \end{aligned}\right\} \cdots\cdots (I)$$

and for the accurate solution, we have

$$\left.\begin{aligned} q(x) &= \int_0^x f(x, y, p)\,dx, \quad r(x) = \int_0^x q(x)\,dx \\ p(x) &= q(x) + c, \qquad y(x) = r(x) + cx + d \end{aligned}\right\} \cdots\cdots (II).$$

Putting

$$\begin{aligned} &p_n(x) - p(x) = \delta_n(x), \quad y_n(x) - y(x) = \varepsilon_n(x) \\ &q_n(x) - q(x) = \beta_n(x), \quad r_n(x) - r(x) = \gamma_n(x) \\ &c_n - c = \sigma_n, \quad d_n - d = \tau_n \\ &{}_nX_1 - X_1 = \lambda_n, \quad {}_nX_2 - X_2 = \mu_n \end{aligned} \qquad \cdots\cdots (III)$$

we get

$$\delta_n(x) = \beta_n(x) + \sigma_n, \quad \varepsilon_n(x) = \gamma_n(x) + \sigma_n x + \tau_n \qquad \cdots\cdots (IV)$$

while

$$\begin{aligned} \beta_n(x) &= \int_0^x [f(x, y_{n-1}(x), p_{n-1}(x)) - f(x, y(x), p(x))]\,dx \\ &= \int_0^x [M_{n-1}(x)\varepsilon_{n-1}(x) + N_{n-1}(x)\delta_{n-1}(x)]\,dx \end{aligned}$$

where

$$M_{n-1}(x) = \frac{\partial}{\partial y} f(x, y_0(x), p_0(x)), \quad N_{n-1}(x) = \frac{\partial}{\partial p} f(x, y_0(x), p_0(x))$$

and $y_0(x)$, $p_0(x)$ are between $[y(x), y_{n-1}(x)]$, $[p(x), p_{n-1}(x)]$ respectively.

Let the interval of x be $0 \leqq x \leqq X_0$ and in this interval, the maximum values of $|\delta_n(x)|$, $|\varepsilon_n(x)|$ be δ_n', ε_n' respectively, and the following relations be satisfied independently of x, y, p and n

$$|M_{n-1}(x)| \leqq M, \quad |N_{n-1}(x)| \leqq N \qquad \cdots\cdots (V)$$

where M, N are some fixed constants. And if we put

$$\rho_n = M\varepsilon_n' + N\delta_n' \quad \cdots\cdots \text{(VI)}$$

then

$$|\beta_n(x)| \leqq |\rho_{n-1}\int_0^x dx| = \rho_{n-1}\, x \leqq \rho_{n-1} X_0$$

that is

$$|\beta_n(x)| \leqq \rho_{n-1}\, x \leqq \rho_{n-1} X_0$$

similarly

$$|\gamma_n(x)| \leqq \rho_{n-1}\frac{x^2}{2} \leqq \rho_{n-1}\frac{X_0^2}{2} \quad \cdots\cdots \text{(VII)}.$$

Therefore, if we put $|\sigma_n| = \sigma_n'$, $|\tau_n| = \tau_n'$, and x' be the value of x when $|\delta_n(x)| = \delta_n'$, then

$$\delta_n' = |\beta_n(x') + \sigma_n| \leqq |\beta_n(x')| + \sigma_n'$$

that is

$$\delta_n' \leqq \rho_{n-1} X_0 + \sigma_n'$$

similarly

$$\varepsilon_n' \leqq \rho_{n-1}\frac{X_0^2}{2} + \sigma_n' X_0 + \tau_n' \quad \cdots\cdots \text{(VIII)}.$$

Next, it is obvious that if $\lim_{n\to\infty}\rho_n = 0$, then $\lim_{n\to\infty}\delta_n' = 0, \lim_{n\to\infty}\varepsilon_n' = 0$ that is $\lim_{n\to\infty} y_n(x) = y(x)$, $\lim_{n\to\infty} p_n(x) = p(x)$. Consequently in the following, in order to converge the solutions, it is sufficient that we show $\lim_{n\to\infty}\rho_n = 0$.

case (i)

$$\text{Conditions} \begin{cases} y = m_1(p) \cdots\cdots \text{when } x = 0 \\ y = m_2(p) \cdots\cdots \text{when } x = a_2. \end{cases}$$

For the n^{th} approximate solution

$$d_n = m_1(c_n),\ r_n(a_2) + c_n a_2 + d_n = m_2(q_n(a_2) + c_n)$$

and for the accurate solution

$$d = m_1(c),\ r(a_2) + c a_2 + d = m_2(q(a_2) + c)$$

therefore

$$\tau_n = m_1(c_n) - m_1(c) = \sigma_n m_1'(c + \theta\sigma_n),\ 0 \leqq \theta \leqq 1$$

that is

$$\tau_n = \sigma_n \, m_1'(c + \theta \sigma_n).$$

Similarly

$$\gamma_n(a_2) + a_2\sigma_n + \tau_n = \{\beta_n(a_2) + \sigma_n\} m_2'(q(a_2) + c + \theta'\{\beta_n(a_2) + \sigma_n\}) \qquad 0 \leqq \theta' \leqq 1$$

therefore, if we put

$$m_1'(c + \theta\sigma_n) = A_{1\cdot n},\ m_2'(q(a_2) + c + \theta'\{\beta_n(a_2) + \sigma_n\}) = A_{2\cdot n} \cdots (1)$$

then

$$\left.\begin{aligned} &\tau_n = A_{1\cdot n}\sigma_n \\ &\gamma_n(a_2) + a_2\sigma_n + \tau_n = A_{2\cdot n}\{\beta_n(a_2) + \sigma_n\} \end{aligned}\right\} \cdots\cdots (2)$$

and putting

$$a_2 + A_{1\cdot n} - A_{2\cdot n} = A_n \cdots\cdots (3)$$

if $A_n \neq 0$, then from (2) we get

$$\left.\begin{aligned} &\sigma_n = \frac{1}{A_n}[A_{2\cdot n}\beta_n(a_2) - \gamma_n(a_2)] \\ &\tau_n = \frac{A_{1\cdot n}}{A_n}[A_{2\cdot n}\beta_n(a_2) - \gamma_n(a_2)] \end{aligned}\right\} \cdots\cdots (4).$$

If there exist some fixed constans A_1, A_2, A_0 which satisfy

$$0 < A_0 \leqq |A_n|,\ |A_{1\cdot n}| \leqq A_1,\ |A_{2\cdot n}| \leqq A_2 \cdots\cdots (5)$$

independently of n, then from (4) we get

$$\sigma_n' \leqq \frac{1}{A_0}\left(A_2 + \frac{X_0}{2}\right)X_0\,\rho_{n-1},\ \tau_n' \leqq \frac{A_1}{A_0}\left(A_2 + \frac{X_0}{2}\right)X_0\,\rho_{n-1},$$

therefore from (VIII) we have

$$\delta_n' \leqq \left[1 + \frac{1}{A_0}\left(A_2 + \frac{X_0}{2}\right)\right]X_0\rho_{n-1},\ \varepsilon_n' \leqq \left[\frac{X_0}{2} + \frac{X_0 + A_1}{A_0}\left(A_2 + \frac{X_0}{2}\right)\right]X_0\rho_{n-1}$$

and

$$\rho_n = M\varepsilon_n' + N\delta_n' \leqq \left[M\left\{\frac{X_0}{2} + \frac{X_0 + A_1}{A_0}\left(A_2 + \frac{X_0}{2}\right)\right\} + N\left\{1 + \frac{1}{A_0}\left(A_2 + \frac{X_0}{2}\right)\right\}\right]X_0\,\rho_{n-1}$$

that is

$$\rho_n \leqq RX_0\,\rho_{n-1},\quad \rho_n \leqq (RX_0)^{n-1}\rho_1$$

where

$$R = M\left\{\frac{X_0}{2} + \frac{X_0 + A_1}{A_0}\left(A_2 + \frac{X_0}{2}\right)\right\} + N\left\{1 + \frac{1}{A_0}\left(A_2 + \frac{X_0}{2}\right)\right\} \cdots (6).$$

Consequently if

$$RX_0 < 1 \quad \cdots (7)$$

then

$$\lim_{n\to\infty} \rho_n = 0.$$

Case (ii)

$$\text{Conditions} \begin{cases} p = 0 & \cdots\cdots \text{ when } x = 0 \\ y = m_2(p) & \cdots\cdots \text{ when } x = a_2. \end{cases}$$

Similarly in case (i), we have

$$c_n = 0,\ r_n(a_2) + d_n = m_2(q_n(a_2))$$

$$c = 0,\ r(a_2) + d = m_2(q(a_2))$$

and

$$\sigma_n = 0,\ \gamma_n(a_2) + \tau_n = \beta_n(a_2)\, m_2'(q(a_2) + \theta\beta_n(a_2)).$$

If there esists a fixed constant A_2 which satisfies

$$|m_2'(q(a_2) + \theta\beta_n(a_2))| \leqq A_2 \quad \cdots (1)$$

independently of n, then

$$\tau_n' = |\beta_n(a_2)\, m_2'(q(a_2) + \theta\beta_n(a_2)) - \gamma_n(a_2)| \leqq \left(A_2 + \frac{X_0}{2}\right) X_0 \rho_{n-1}$$

therefore from (VIII) we get

$$\delta_n' \leqq X_0 \rho_{n-1},\ \varepsilon_n' \leqq (X_0 + A_2) X_0 \rho_{n-1}$$

therefore

$$\rho_n = M\varepsilon_n' + N\delta_n' \leqq RX_0 \rho_{n-1} \leqq (RX_0)^{n-1} \rho_1$$

where

$$R = M(X_1 + A_2) + N \quad \cdots (2).$$

Consequently if

$$RX_0 < 1 \quad \cdots (3)$$

then

$$\lim_{n\to\infty} \rho_n = 0.$$

For example, if

$$f(x, y, p) = \frac{1}{1+x^2+y^2+p^2}, \quad m_2(p) = p$$

then

$$f_y = \frac{-2y}{(1+x^2+y^2+p^2)^2}, \quad f_p = \frac{-2p}{(1+x^2+y^2+p^2)^2}$$

and $|f_y| \leqq \frac{3\sqrt{3}}{8}$, $|f_p| \leqq \frac{3\sqrt{3}}{8}$, therefore we put $M = N = \frac{3\sqrt{3}}{8}$. Next $m_2'(p) = 1$ and we can put $A_2 = 1$, therefore

$$R = (X_0 + 1)\frac{3\sqrt{3}}{8} + \frac{3\sqrt{3}}{8} = \frac{3\sqrt{3}}{8}(X_0 + 2)$$

and $RX_0 < 1$ becomes $X_0^2 + 2X_0 - \frac{8}{3\sqrt{3}} < 0$ that is $X_0 < \sqrt{1 + \frac{8}{3\sqrt{3}}} - 1 \fallingdotseq 0.6$.

Consequently if $a_2 < 0.6$ then $\lim_{n\to\infty} \rho_n = 0$.

Case (v)

Conditions $\begin{cases} p = 0 \cdots\cdots\cdots\cdots\cdots \text{ when } x = 0 \\ p = k_2(x) \cdots\cdots\cdots \text{ at the intersection of } y = y(x) \text{ and } y = \varphi_2(x). \end{cases}$

Similarly

$$c_n = 0, \quad r_n({}_nX_2) + d_n = \varphi_2({}_nX_2), \quad q_n({}_nX_2) = k_2({}_nX_2)$$
$$c = 0, \quad r(X_2) + d = \varphi_2(X_2), \qquad q(X_2) = k_2(X_2)$$

and from these equations we have

$$\mu_n \varphi_2'(X_2 + \theta\mu_n) = r_n({}_nX_2) - r(X_2) + \tau_n = \tau_n + r_n({}_nX_2) - r_n(X_2)$$
$$+ r_n(X_2) - r(X_2) = \tau_n + \mu_n q_n(X_2 + \theta'\mu_n) + r_n(X_2), 0 \leqq \theta, \ \theta' \leqq 1$$
$$\therefore [\varphi_2'(X_2 + \theta\mu_n) - q_n(X_2 + \theta\mu_n)]\mu_n = \tau_n + r_n(X_2),$$

similarly

$$[k_2'(X_2 + \theta''\mu_n) - F_{n-1}(X_2 + \theta'''\mu_n)]\mu_n = \beta_n(X_2),$$

and putting

$$\left.\begin{aligned} \varphi_2'(X_2 + \theta\mu_n) - q_n(X_2 + \theta'\mu_n) &= A_n \\ k_2'(X_2 + \theta''\mu_n) - F_{n-1}(X_2 + \theta'''\mu_n) &= B_n \end{aligned}\right\} \cdots\cdots\cdots\cdots\cdots\cdots (1)$$

we get

$$\sigma_n = 0 \text{ and } A_n\mu_n = r_n(X_2) + \tau_n, \quad B_n\mu_n = \beta_n(X_2),$$

and if $B_n \neq 0$, we have

$$\left.\begin{aligned}\delta_n(x) &= \beta_n(x)\\ \varepsilon_n(x) &= \gamma_n(x) + \frac{A_n}{B_n}\beta_n(X_2) - \gamma_n(X_2)\end{aligned}\right\} \quad \cdots\cdots (2).$$

If there exist some fixed constants A, B_0 which satisfy following relations independently of n

$$|A_n| \leqq A,\ 0 < B_0 \leqq |B_n| \quad \cdots\cdots (3)$$

then

$$|\varepsilon_n(x)| \leqq |\gamma_n(x) - \gamma_n(X_2)| + \frac{A}{B_0} X_0 \rho_{n-1}$$

while

$$|\gamma_n(x) - \gamma_n(X_2)| = \left|\int_{X_2}^{x} \beta_n(x)\,dx\right| \leqq \rho_{n-1}\frac{x^2 \sim X_2^2}{2} \leqq \frac{X_0^2}{2}\rho_{n-1},$$

therefore

$$\varepsilon_n' \leqq \left(\frac{X_0}{2} + \frac{A}{B_0}\right) X_0 \rho_{n-1},\quad \delta_n' \leqq X_0 \rho_{n-1}$$

so that

$$\rho_n = M\varepsilon_n' + N\delta_n' \leqq RX_0 \rho_{n-1} \leqq (RX_0)^{n-1}\rho_1$$

where

$$R = \left(\frac{X_0}{2} + \frac{A}{B_0}\right)M + N \quad \cdots\cdots (4)$$

and if

$$RX_0 < 1 \quad \cdots\cdots (5)$$

then

$$\lim_{n\to\infty} \rho_n = 0.$$

For example, when $f(x, y, p) = \frac{1}{1+p^2}$ we get $f_y = 0$, $f_p = \frac{-2p}{(1+p^2)^2}$, and $|f_p| \leqq \frac{3\sqrt{3}}{8}$ for all value of p, therefore we can put $M = 0$, $N = \frac{3\sqrt{3}}{8}$ then if there exist A, B_0 we have $R = N = \frac{3\sqrt{3}}{8}$ and from $RX_0 < 1$ we get $X_0 < \frac{8}{3\sqrt{3}} \fallingdotseq 1.54$. While, evidently $0 < F_{n-1}(x) < 1$, $0 < q_n(x) < x$ for all positive value of x. So that if $k_2'(x) \leqq -\Delta$ or $1 + \Delta \leqq k_2'(x)$, $\Delta > 0$ is satisfied independently of x, then we can put $B_0 = \Delta$. (e.g if $k_2(x) = 2x$ then $k_2'(x) = 2$ therefore we can put $\Delta = 1$). And if $\varphi_2'(x)$ is finite, then a constant A exists which satisfies $|A_n| \leqq A$. Consequent-

ly, when $k_2'(x) \leqq -\Delta$ or $1+\Delta \leqq k_2'(x)$ and $\varphi_2'(x) =$ finite, if we can recognize that $X_2 \leqq X_0 < 1.54$ by some suitable method, then we can assert that $\lim_{n\to\infty} \rho_n = 0$.

In regard to other cases we can introduce similar results.

7. Conclusion

It is meaningless that the functions $y_1(x)$, $y_2(x)$, ……, $y_n(x)$, …… obtained by our method do not converge to a definite function uniformly. The sufficient conditions which are mentioned in the preceding section, are so narrow that in most cases they do not be satisfied, but in fact, as example shows, in most acses the numerical values approach to definite values. And if $\lim_{n\to\infty} y_n(x) = y(x)$, it is obvious that the limitting function $y(x)$ is the required solution. Therefore we propose the following procedure.

At the beginning, take $y_1(x)$ considerably near the accurate solution by a suitable method, then calculate $y_2(x)$, $y_3(x)$, ……, $y_n(x)$, …… successively by the method mentioned above, and if within required accuracy, $y_{i-1}(x) \equiv y_i(x)$ is reached, stop this procedure. Next find the solution $Y(x)$ of the given differential equation under the condition "$y = d_i$, $p = c_i$ when $x = 0$" by ordinarly method, and if $Y(x) \equiv y_i(x)$, then $y_i(x)$ is the required solution.

Of course, it may occur that $y_2(x)$, $y_3(x)$, ……, $y_n(x)$, …… do not converge, and $s_n(x) = 0$ has no root or many roots in the considered interval of x in spite of the existence of the unique solution.

We want to know more precise condition of the convergency of the solution (if possible, the necessary and sufficient condition), but as far as I know there is no more precise one, and it is our future research.

ON THE ELECTRIC RESISTANCE OF THE CONCRETE

Shigeo- MATSUMAE

(Received Sept. 3, 1953)

(I) Introduction.

It was reported that the electric resistance of the concrete changes, when the direction of the electric current is reversed, and that this occurs when the direction of the electric current passing through the contact surface of two different materials, namely the stone and the cement, is changed.

As the above-stated is very doubtful to us, we study the electric resistance of the concrete. According to our investigations, the experimental results which are different from the above-stated are obtained. The details are as follows.

(II) Measurements and Discussions.

(1) At first, we take measurement of the electric potential distribution of the specimen, containing the pure cement and the water, in two cases when the electric direct voltage is either applied to the specimen or not. The specimen is a square rod, 5.7 cm square by 21 cm in length, and six columnar carbon rods, 0.4 cm in diameter and 7 cm long, are inserted lengthwise at the intervals of 2.7 cm in the middle part of the specimen. Two electrodes are made in such a manner that the surfaces of two ends of the specimen are plastered about 1 mm thick with a paste which is made out of graphite-powder, a small quantity of the cement and a little water.

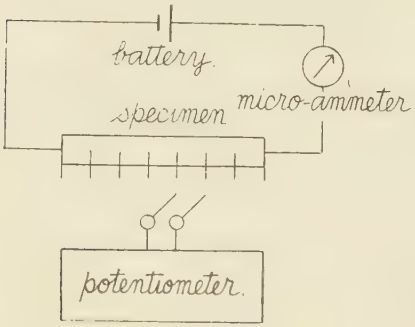

Fig. 1.

As shown in Fig. 1, the strength of the electric current is measured by a micro-ammeter and the electric potential distribution is measured by a potentiometer.

(i) When a certain constant electric direct voltage is applied to the specimen, the electric current flowing through the specimen decreases at first rapidly and then slowly, becoming at last almost contant, and herewith the electric potential distribution changes with the lapse of time.

From this reason, the experimental results in this paper are such as measured 30 minutes after applying the electric direct voltage to the specimen.

The results of the measurements taken I day and about 20 days later after drawing the specimen up from the water are shown in Fig. 2, in which the curve of the potential

distribution denoted by (1) is the experimental result in the former case and the curve denoted by (2) is the experimental result in the latter case. As shown in the figure, these two curves have the same tendency that the potential differences between each carbon rod respectively, existing side by side, are almost the same but the potential differences between the electrode and the carbon rod, nearest to the electrode, are fairly large, compared with the above potential differences between each carbon rod respectively.

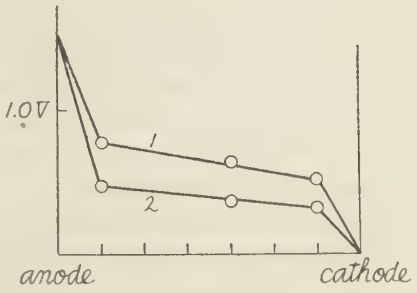

Fig. 2.

This is caused chiefly by the fact that the polarizations take place in the parts of the electrodes and to some extent by the fact that the electric resistance in the part of the surface of the specimen increases as the result of the drying of the surface.

Ordinarily, the electric conduction of the settled cement is chiefly due to the water from which the water of crystalization is excluded- namely, the free water and the colloidal water—and, furthermore, may be considered to be the electric conduction in the electrolytic solution, as the cement is alkaline. As shown in the figure, the potential fall at the side of the anode is always greater than that at the side of the cathode and this shows that over-potential on the anode is greater than the over-potential on the cathode.

(ii) When the specimen is on an open circuit without applying of the external electric voltage, the potential distribution of the specimen is measured and the experimental result measured several days later after drawing the specimen up from the water is shown in Fig. 3. As shown in the figure, the potentential difference exists to some degree between two electrodes and, at the same time, the potential differences, several times larger than that between two electrodes, are found between electrode and each carbon rod respectively. This fact shows that, as the result of the drying of the outer part of the specimen, the amount of the free water and the colloidal water becomes smaller in the outer part than in the inner part and, consequently, the alkalinity in the outer of the specimen seems to become so stronger than the alkalinity in the inner part that the so-called concentration-cell is formed between electrode and each carbon rod in the specimen. From this reason, it is easy to understand that the electric potentials of the electrodes on the

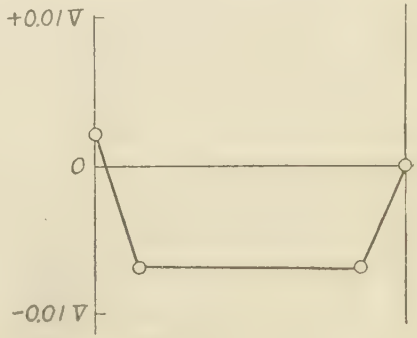

Fig. 3.

surface are higher than that of the carbon rods in the inner part. And, as the potential difference exists between two electrodes, the component—probably, the free water and the colloidal water—is considered to be unequal in the parts of these two electrodes.

(iii) When one electrode of the specimen is moistened and then the electric current is flown through the specimen by the external electro-motive force, the electric potential distribution of the specimen is shown in Fig. 4. The measurement is taken 20 days later after drawing the specimen up from the water. In this figure, the dotted curve shows the potential distribution of the specimen measured before moistening one electrode of the specimen. The curve denoted by (1) shows the potential distridution in the case when the positive voltage is applied to the wet electrode and, at the same time, the curve denoted by (2) shows also the potential distribution in the case when the negative voltage is applied to the wet electrode.

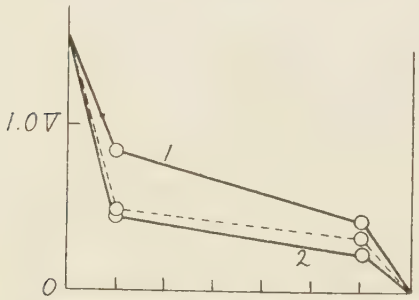

curve 1
effective voltage. 0.42V
electric current. 370μA
curve 2
effective voltage. 0.22V
electric current. 205μA

Fig. 4.

With the exception of the potential drops in the parts of the electrodes, the effective voltage, which is applied substantially to the specimen, is greatly different and consequently the electric current flowing through the specimen is also greatly different between in the case of (1) and in the case of (2), as the strength of the electric current flowing through the specimen is proportional to the effective voltage

The electro-motive force between two electrodes which is produced by the ununiformity of the free water and the colloidal water is below several hundredth Volt. Therefore, it is concluded that the large difference of the effective voltage between in the case of (1) and in the case of (2) is chiefly caused by the difference of the magnitudes of the polarizations in the parts of the two electrodes.

As the magnitude of the anode-polarization is greater than that of the cathode-polarization in the same condition and, furthermore, the amount of the free water and the colloidal water in the part of one electrode is not the same as in the part of the other electrode, the magnitudes of the potential drops produced by the polarizations on the electrodes are different between the curve (1) and the curve (2) and, therefore, the effective voltage, from

which the potential drops of the polarizations in the parts of the electrodes are excluded, is different between the curve (1) and the curve (2).

(2) The above-mentioned is the results of the measurements on the specimen, containing the water and the pure cement, and now the experimental results of the concrete are described below.

The specimen contains about 40% pebble, about 25% cement, about 20% sand and about 15% water at first but the amount of the water changes in the lapse of time. The dimension of the specimen is the same as in the previous paragraphs.

The specimen is settled in making the axis of the column of the specimen perpendicular to the horizontality and the electrode on the upper surface of the specimen and also the electrode on the lower surface of the specimen are denoted arbitrarily by (A) and (B) respectively.

The measurement are taken about 80 days after drawing the specimen up from the water. The experimental results are as follows.

The electric potential distribution of the specimen of the concrete is shown in Fig. 5, when the external electro-motive force is applied to the specimen. In the figure, the curve denoted by (1) is the potential distribution of the specimen in the case when the direct positive voltage is applied to the electrode (A) and the curve denoted by (2) is also the potential distribution of the specimen in the case when the negative direct voltage is applied to the electrode (A). As shown in the figure, the effective voltage is higher in the curved denoted by (1) than in the curve denoted by (2) and consequently the strength of the electric current flowing through the specimen is greater in the case of (1) than in the case of (2), in proportional to the effective voltage.

curve 1

effective voltage 0.53V
electric current 9.9μA

curve 2

effective voltage 0.47V
electric current 8.6μA

Fig. 5.

The potential distribution of the specimen is measured, when the specimen is on an open circuit without applying of the external electric voltage. The potential difference of 0.035V is observed between two electrodes on the surface and, as in the specimen containing the water and the cement, tbe electric potential of the inner part of the specimen is several times lower than that of the outer part of the specimen, as compared with the potential difference between two electrodes.

The fairly large potential difference between two electrodes is always observed and the potential of the electrode (B) is always higher than that of the electrode (A). From the above facts, the amount of the free water and the colloidal water is considered to be larger in the part of the electrode (A) than in the part of the electrode (B), that is caused chiefly by the ununiformity of the pebble which is obviously affected by the gravity.

As in the case of the paragraph (iii), the strength of the electric current is greater in the case of appling the positive direct voltage to the electrode (A), in the part of which the amount of the free water and the colloidal water is considered to be greater than in the part of the other electrode (B), than in the case of applying the negative direct voltage to the same electrode.

In the specimen of the concrete, the difference of the effective voltage between in the case of (1) and in the case of (2) is considered to be caused by the difference of the magnitudes of the polarizations in the parts of the electrodes, as in she paragraph (iii), and also by the electro-motive force between two electrodes which is due to the difference of the amount of the free water and the colloidal water in the parts of these two electrodes.

(III) Conclusion

When the electric current is flown through the specimen of the concrete, the polarizations are produced in the parts of the electrodes. If the potential drops of the polarizations in the parts of the electrodes are excluded, the electric current flowing through the specimen is proportional to the effective voltage which is substantially applied to the specimen, in two cases when the direction of the electric current is reversed or not.

Namely, the electric resistance of the concrete does not change, when the direction of the electric current flowing through the specimen is reversed.

In conclusion, the writer wishes, to express his cordial thanks to Professors. Mukai and Ochiai for their discussions.

ON THE BALLOONING PROBLEM (I)

Akira ONUKI

(Received Oct. 1. 1953)

Introduction

The calculation of the shapes of the ballooning thread is one of the very important problems to be considered in any cap spinning system, and chiefly due to the great difficulties of mathematical treatment, the perfect solutions of problem have not yet been given until the recent work of J. Crank *[1]) appeared.

This paper treats just the same problem as J. Crank's, the only difference is that, my calculation is taking into account the variation of air drag with the angle between the thread and rotating velocity vector, and consequently my equations contain an additional parameter refering to these angles.

J. Crank's equations are as follows:

$$\frac{d}{ds}\left(T_1 \frac{dx}{ds}\right) + \frac{fy}{r} + 2m\omega v \frac{dy}{ds} + m\omega^2 x = 0$$

$$\frac{d}{ds}\left(T_1 \frac{dy}{ds}\right) - \frac{fx}{r} - 2m\omega v \frac{dx}{ds} + m\omega^2 y = 0$$

$$\frac{d}{ds}\left(T_1 \frac{dz}{ds}\right) + mg = 0$$

$$T_1 = T - mv^2$$

where T_1 : true tension of the thread in grams.

m : mass in grams per cm.

v : moving velocity of the thread along itself.

ω : rotational speed in radian per second.

s : distance measured along the thread.

f : air-drag acting on the unit length of the thread.

g : gravitational acceleration constant.

In practice it can be put in most cases $T_1 = T$ and $mg = 0$. The third term of upper two equations originated from Coriolis force, and the fourth from the rotating potential. In my calculation the third term is neglected, but sometimes questions arise here and I shall discuss these points fully in the following reports. As the result of this assumption, the variable v in the Crank's equations disappeared in my equations, that is, we are treating the threads which are not moving along themselves.

* See the references at the end of this paper

1. Fundamental equations.

Taking the coordinate axis as shown in Fig. 1 the fundamental equations are

$$\frac{d}{ds}\left(T\frac{dx}{ds}\right)+m\omega^2 x+P\sin\tau\,\omega^2 r y=0 \tag{1.1}$$

$$\frac{d}{ds}\left(T\frac{dy}{ds}\right)+m\omega^2 y-P\sin\tau\,\omega^2 r x=0 \tag{1.2}$$

$$\frac{d}{ds}\left(T\frac{dz}{ds}\right)=0 \tag{1.3}$$

$$\left(\frac{dx}{ds}\right)^2+\left(\frac{dy}{ds}\right)^2+\left(\frac{dz}{ds}\right)^2=1 \tag{1.4}$$

$$\cos\tau=\frac{1}{r}\left(x\frac{dy}{ds}-y\frac{dx}{ds}\right) \tag{1.5}$$

$$r^2=x^2+y^2 \tag{1.6}$$

where T, m, ω have the same meanings as in the Crank's equation shown above.

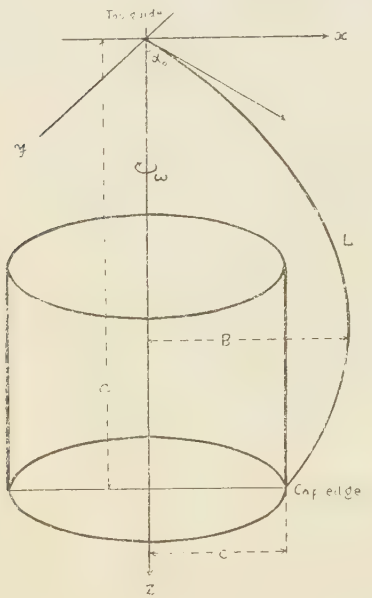

Fig. 1.

P is the coefficient of the air-drag acting on the thread of unit length per square of the rotating linear velocity. Therefore, P is given by 1/2 × air density × diameter of the thread × numerical coefficient

This numerical coefficient itself depends upon the Reynolds number in some unknown way, but this coefficient can be estimated in practice easily by comparing with the experiments. The experiments show that, through wide interval of rotating linear velocities, this coefficient takes the value between 1 and 2. τ is the angle between the directions of the thread and of the velocity vector of thread element.

Putting

$$T_1=T/T_0 \tag{1.7}$$

$$x=cX \quad y=cY \quad z=aZ \tag{1.8}$$

where To is the tension of the thread at the top guide, c is the radius of cap edge and a is the distance between the top guide and cap edge (see the Fig. 1), above equations take the dimensionless form. And after some reductions and calculations, these lead

$$\left.\begin{aligned} U&=\rho T_1\cos\tau \\ V&=T_1+\frac{2c^2}{a}\eta^2\rho^2 \end{aligned}\right\} \tag{1.9}$$

$$\frac{dU}{dZ} = \frac{c\gamma}{a\cos\alpha_0} T_1 \rho^3 \sin\tau \tag{1.10}$$

$$\frac{d\rho}{dZ} = \pm \frac{a}{c}\left\{ T_1^2 \sec^2\alpha_0 \sin^2\tau - 1 \right\}^{-\frac{1}{2}} \tag{1.11}$$

$$\frac{dV}{dZ} = \frac{c\gamma}{a\cos\alpha_0} \rho^2 T_1 \sin\tau\cos\tau \tag{1.12}$$

$$\frac{d\theta}{dZ} = \frac{a}{c\cos\alpha_0} \frac{T_1\cos\tau}{\rho} \tag{1.13}$$

where

$$c\rho = r \quad X = \rho\cos\theta \quad Y = \rho\sin\theta \tag{1.14}$$

$$\left.\begin{aligned} \eta &= \frac{1}{2}\sqrt{\frac{m}{T_0}}\, a\omega \\ \gamma &= \frac{P\omega^2 a^2 c}{T_0} \end{aligned}\right\} \tag{1.15}$$

and α_0 is the angle between the direction of thread and Z axis at the top guide.

η and γ are clearly the numerical numbers which, with the parameters α_0 and c/a, affect the shape of the ballooning seriously. Therefore, our object of calculations are to obtain the inner relation lying between these parameters and tension of the threads under suitable boundary conditions. The boundary conditions corresponding the actual circumstances are as follows

$$\left.\begin{aligned} &\tau = \frac{\pi}{2} \quad \rho = 0 \quad \theta = 0 \quad T_1 = \sec\alpha_0 && \text{when } Z = 0 \\ &\rho = 1 && \text{when } Z = 1 \end{aligned}\right\} \tag{1.16}$$

2. Solutions in vacuum.

when we neglect the terms describing the air drag in the equations from (1.9) to (1.13), the solutions will be easily obtained by quadrature which lead

$$\rho = \frac{a}{c\eta} \sin\frac{\alpha_0}{2}\, sn\left\{ \frac{\eta\tan\alpha_0}{\sin\frac{\alpha_0}{2}} Z,\ \tan^2\frac{\alpha_0}{2} \right\} \tag{2.1}$$

$$\tau = \frac{\pi}{2}, \quad \theta = 0, \tag{2.2}$$

and this shows that the moving threads always lie in one plane. $\tan^2\frac{\alpha}{2}$ in the right hand bracket of (2.1) is the modulus of Jacobi's elliptic function.

It is evident from (2.1) that, when Z increases from 0 to 1, $c\rho$ increases also from 0 to some maximum value, (which we call provisionally "the maximum ballooning B,") and then begins to decrease to c.

Whether the value of $c\rho$ takes the maximum only once or more than twice, determines the value of coefficient of Z in the argument of function sn, and in case of more than twice the "licking" balloon arises. In order to avoid the licking and to make $c\rho$ take the value c at the cap edge precisely in the second quadrant of function sn, η must satisfy the condition

$$\frac{K(\alpha_0)}{\tan\alpha_0 \cos ec\frac{\alpha_0}{2}} \leqq \eta \leqq \frac{2K(\alpha_0)}{\tan\alpha_0 \cos ec\frac{\alpha_0}{2}} \tag{2.3}$$

where $4K(\alpha_0)$ is the period of function sn corresponding to α_0.

The value of B is given by

$$B = \frac{a}{\eta} \sin\frac{\alpha_0}{2} \tag{2.4}$$

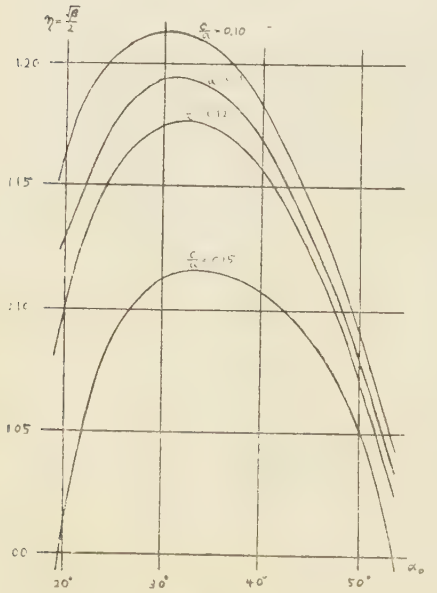

Fig. 2.

Though the "vacuum" cases of course are rather different from actual states, it is of some interest that we can roughly estimate the order of η by inserting the experimental values of B and α_0 in both sides of equation (2.4).

The Fig. 2 shows the relation of α_0 and η which strictly satify the boundary conditions adopted in practical case. Using this Fig. 2, the tension at the top guide will be easily obtained from η if one measures the value of angle. α_0. Numerical example shows that this procedure will give T_0, the value about 30% less than the reasonable value which will be obtained in the later calculation.

3. Solutions in general cases.

When one takes the air drag term into acconnt, the problem to be considered presents itself in the following form;

1) to find the integrals which satisfy the boundary conditions (1.16)

Table 1

α_0	$K(\alpha_0)\frac{\sin\frac{\alpha_0}{2}}{\tan\alpha_0}$	$2K(\alpha_0)\frac{\sin\frac{\alpha_0}{2}}{\tan\alpha_0}$	α_0	$K(\alpha_0)\frac{\sin\frac{\alpha_0}{2}}{\tan\alpha_0}$	$2K(\alpha_0)\frac{\sin\frac{\alpha_0}{2}}{\tan\alpha_0}$
10^0	0.779	1.558	60^0	0.504	1.008
20^0	756	1.513	65	441	0.882
30^0	722	1.444	70	378	0.757
38^0	690	1.380	75	317	0.635
46^0	624	1.248	82	204	0.408
53^0	565	1.131	88	067	0.133

Limit of η in "vacuum" solution.

Table 2

c/a / α_0	0.10	0.11	0.12	0.15
	η	η	η	η
19.°7	1.1568	1.1250	1.0934	1.0006
22. 0		1.1534		
26. 0		1.1834		
29. 1	1.2144	1.1936	1.1731	1.1116
33. 0		1.1946		
35. 1		1.1905		
37. 8	1.1951	1.1805	1.1661	1.1235
45. 8	1.1354	1.1250	1.1173	1.0838
53.1	1.0511	1.0435	1.0360	1.0139

Relation of η and α in "vacuum" solution.

2) to get some functional relations existing between those parameters contained in the equations in order to fulfil the requirements of boundary conditions.

Essential difficulties arise, of course, from the nonlinearity of the simultaneous equations, and only we can do is to integrate numerically step by step. Whole program of calculations are now in progress, but it may be not worthless to anticipate several properties or behaviours of the solution and to compare it with "vacuum" solutions obtained already in §2.

Some remarkable features obtained at the present stage are as follows.

1) the parameter η becomes abont 20% larger than in the vacuum case for the same α,

and consequently the tension of top guide T_0 slightly diminishes.

2) angle τ decreases monotonously from 90° to some 60°, so the effect of inserting this τ in the equations seems to be never negligible.

3) functional relation between B and $\eta(\alpha_0)$ becomes more complicate in some unknown way, but numerically, this will not be so seriously changed that we must abdicate the relation (2.4) entirely.

Table 3

Z	ρ	τ	cos τ	θ
0.00	0.0000	0.000	0.0000	0.00
5	1661	1.296	0000	0. 02
10	3290	2.566	0013	0. 08
15	4871	3.799	0024	0. 16
20	6360	4.961	0087	0. 35
25	7740	6.037	0183	0. 72
30	8961	6.990	0317	1. 31
35	1.0064	7.850	0485	2. 14
40	1.1002	8.582	0706	3. 23
45	1.1767	9.178	0968	4. 64
50	1.2355	9.637	1267	6. 41
55	1.2756	9.950	1598	8. 58
60	1.2960	10.109	1955	11. 20
65	1.2969	10.116	2330	14. 36
70	1.2774	9.964	2719	18. 17
75	1.2435	9.699	3113	22. 72
80	1.1982	9.346	3510	28. 17
85	1.1455	8.935	3909	34. 64
90	1.0901	8.503	4305	42. 31
95	1.0408	8.118	4675	51. 27
1.00	1.0000	7.800	5008	61. 54

solution for $c/a = 0.11$ in general case

References

1. Hall H. W. Nature vol. 138, 933. (1936)
2. Hall H. W. Hunter W. phil. Mag. vol. 25, 193 (1938)
3. Goshawk E. R. Nature vol. 140, 194 (1937)
4. Honegger E. Fehr A. J. Text. Inst. 38, 353, (1947)
5. Hanner M. J. Text. Inst. 43, No 10 (1952)
6. J. Crank J. Text. Inst. (1953) 266

SOME STUDIES ON VOLCANO ASO AND KUJIU (PART 6)

A Consideration to the process of Volcanic Explosion.

Munetosi NAMBA

(Received Aug. 31, 1953)

Abstract.

The writer observed volcanic explosions dividing into two stages Boring and Magma stages. He could learn the fact that both stages differed in their mechanisms by studying the relatiou between the change of atmospheric pressure and the two stages in a volcanic explosion. Then it will be able to say that the square reciprocal of the frequency is proportional to time t, therefore the boring stage comes to its end when $t = \frac{R_0}{2aP_0(cP_0 - b/R_0)}$ and the explosion becomes to the most energetic stage at this moment.

1. Foreword.

Volcanic explosion is regarded as the phenomenon that high compressed volcanic gas congested under the plug of a volcanic conduit tube excludes its volcanic plug, begins what is called a surface eruption and ceases it as the containing gas pressure decleases. According to the result of observation of the process in a surface eruption, the writer will divide the process of velcanic explosion into two stages and investigate their natures. But the writer has not had the perfact observation of the curve of frequency of volcanic explosion, so that he will reason about it by supplement of materials from the observation of a geyser (Yunotani Geyser in Aso) which has the similar phenomenon as a volcanic explosion.

2. Volcanic Activity in the Stage of Sweeping of the Volcanic Vent Tube (shortly "Boring Stage").

When the accumulation of volcauic gas under a volcanic vent is at the height, it breaks up and disperses the plug with explosions and, when the explosion is very powerful, emits flash arcs of light into the atmosphere caused to the compression of the atmosphere; it shatters the rocks from the plug to pieces and disperses them, and the volcanic ashes sprung up in this case are generally light colourod lava-ashes. The numbers of frequency of explosion dN/dt increases more and more, so that intermittent time becomes shorter and shorer. The curve dN/dt and time t take the form of convex to time axis, and the curve of number of explosion N and time t are also convex to time axis. The ejectors are thrown up

higher and higher in the atmosphere untill they are almost successively thrown up, and the aspect pressents one of the grandest scene; that is, the initial velocity of eruption increases by degrees. Volcanic activity in this stage has a tendency to be suppressed by rising of atmospheric pressure.

3. Volcanic Activity in the Main Active Stage ("Magma-stage").

When volcanic activity finishes the sweeping action in Boringstage and reaches to the stratum of plastic magma, explosion at the maximum becomes lulled by degrees. If pumices are erupted, they will be thrown up at the beginning of the magma-stage. After the eruption of pumices, there begins the issue of rather compact stream of lava or the eruption of plastic magma. Then the explosions are conspiciously in a low tone, and volcanic ashes increase in the content of magma ash and $F_{e3}O_4$, therefore, they are tinged with rich black. The frequency of exqlosions are decreased in proportion tothe lapse of time; Green ash with $F_e O$ often appears in this stage.

The curve of frequency and time forms itself into convex to time axis, and the curve of the number N of explosions and t rises in concave to time axis. The height of ejectors gradually lowers; that is the initial velocity of eruption decreases in turn. The volcanic activity usually ceases after a week or thereabout and then, for a while, volcanic ashes are blown off intermittently as embers, but they cease soon after and volcano regains the silence. The volcanic activity in the magma stage is seems to have a tendency to be promoted by rising of the atmospheric pressure.

4. The Expolsion of Volcano Aso on February, 1933.

On February, 1933 the first and second craters of Volcano Aso began the activity at almost the same time; the second crater has been called "Naka-no-miike" from time immemorial. It seems that the second crater had been active already at midnight of February 23; the margine of the crater vibrated so violently that the dwellers of a resting-place in the northwest margine of the crater (near the monument of an Imperial visit) packed the houshold effects and went down the volcano to take refuge. About half past two o' clok, February 24, it was possible to hear the explosions at the shrine (abut 800 meters west from the crater) and the neighbouring place, but was impossible to have a view of the condition of eruption because of the dense fog. According to the phograph taken about half past fourteen o'clock, February 24, the interval of clean wether in fog, the volcano is violently spouting the plastic magma pieces, and it is clear that the volcanic activity is already in the magma atage[1].

At sixteen o'clock, February 24, Mr. Yasuhisa Oyama, the manager of Tochinoki Hot

spring Resort at the foot of Volcano Aso, came hurriedly to the scene and took a moving picture of the aspects of the volcanic eruption in 16 m.m. film. Since February 25, the numbers of exlosions began to be observed in Branch Office of Kumamoto Meteorogical Station, present Aso Meteorogical Station's antecedents, about one kilometer West from the crater[1]. The diagram of frequency of explosions, which was transcribed through the kindness of Mr. Hiroe, the person in charge of the Branch Office, is descripted in Figure 1. But the frequeny of explosions in Boring stage is indistinct for the imperfectness of the observation.

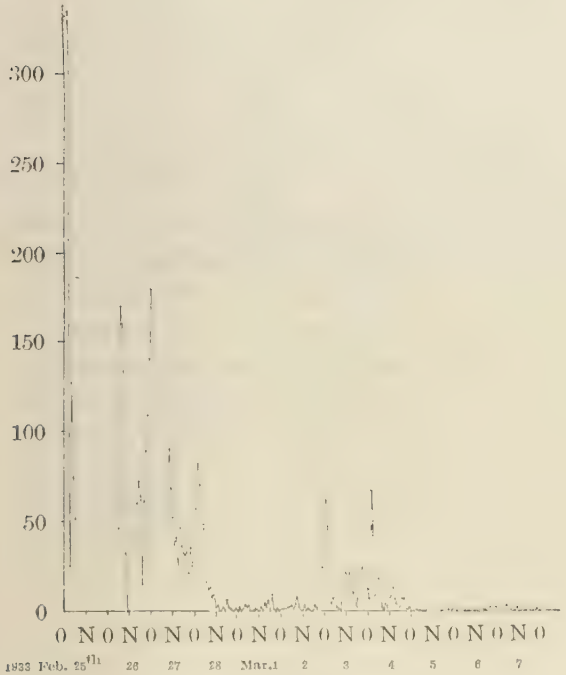

Fig 1. Frequency of eruption per hour in II crater, Aso Volcano.

Both the first crter called "Kita-no-miike" since olden times and the fourth one, "Minami-no-miike", among many craters of Naka-dake in Aso are famous for their incessant and Vesuvian activity. The second diagrams show the frequency of explosions in the first crater and the progress of activity of Vesuvius, which was obseved by Mr. Rittman.

The former half of the diagram is Boring stage and the latter half is the magma stage; the transition stage from boring stage to the magma stage presents the most splendid sight.

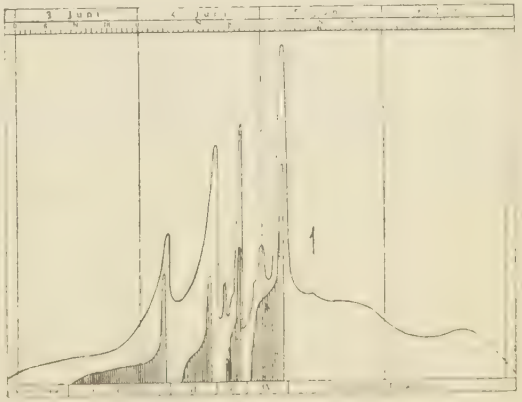

Fig. 2. B. Eruption of vesuvius (1929, by A. Rittmann)

5. Investigation of Boring-stage.

If volcanic gas pressure is P, resistance of volcanic tube (mainly mass of the plug) is R, numbers of explosion is N, and time is t, it might be no great error to say that the following three equations show their correlation

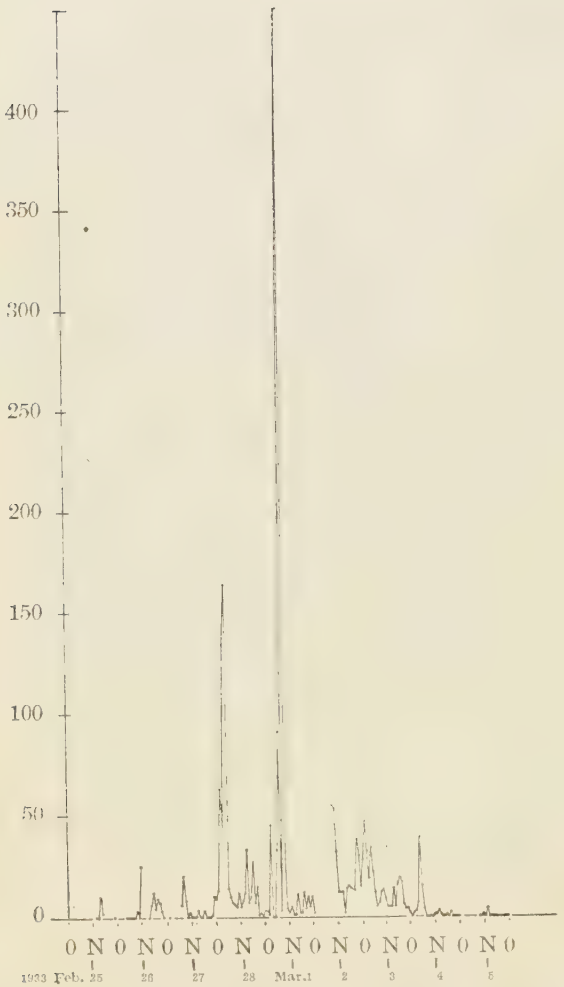

Fig 2. A. Frequency of eruption per hour in The I-crater (Aso-volcano)

most simply:
that is

$$\frac{dN}{dt} = a.\ \frac{P}{R} \quad \cdots\cdots(1)$$

$$-\frac{dP}{dN} = b.\ \frac{P}{R} \quad \cdots\cdots(2)$$

$$-\frac{dR}{dN} = c.\ PR \quad \cdots\cdots(3)$$

The equation (1) means that explosion is apt to break out in direct proportion and in inverse prorortion to its resistance; the equation (2) means that quantity of pressure decreases by an explosion is also proportionate to P and $1/R$; and the equation (3) means that quantity of diminution of the resistance of the plug proportionate to both P and R. Solving the equations (2) and (3)

$$P = P_0 + \frac{b}{c}\left(\frac{1}{R_0} - \frac{1}{R}\right) \quad \cdots\cdots(4)$$

$$R = \frac{b}{cP_0 + b/R_0} + \left(R - \frac{1}{cP_0 + b/R_0}\right) e^{-\left(cP_0 + \frac{b}{R_0}\right)N} \quad \cdots\cdots(5)$$

P_0 and R_0 are the value of P and R at $t = 0$, therefore from (1)

$$\left(cP_0 + \frac{b}{R_0}\right)N - \left(cP_0 + \frac{b}{R_0}\right)N + 2\left(cP_0 + \frac{b}{R_0}\right)N$$

$$= \left(cP_0 + \frac{b}{R_0}\right)\frac{a}{bc}t + \frac{b}{cP_0R_0} - \frac{cP_0R_0}{b} \quad \cdots\cdots(6)$$

When the value of $(cP_0 + bR_0)N$ is small, the term below cube is to be neglected.

$$(cP_0R_0 - b)N^2 - 2R_0N + 2aP_0t = 0 \quad \cdots\cdots (7)$$

therefore

$$N = \frac{1}{cP_0 - b/R_0} + \sqrt{\frac{1}{(cP_0 - b/R_0)^2} - \frac{2aP_0}{R_0\left(cP_0 - \frac{b}{R_0}\right)}t} \quad \cdots\cdots (8)$$

$$\frac{dN}{dt} = +\frac{aR_0}{R_0}\frac{1}{\sqrt{1 - \frac{2aP_0}{R_0}\left(cP_0 - \frac{b}{R_0}\right)t}} \quad \cdots\cdots (9)$$

As the above mentioned observation of explosion in both the first and the second craters of Volcano Aso is deficient in the beginning of observation, there is an inclination to be wanting in certainty; therefeore, the writer tried to observe the numbers of spouting in Aso Geyser regarded as a kind of explosive activity. When he examines in the general state about the spouting No. 19 which began at twelve o'clock, June 30 th, 1943, the curve of N, t is like that is shown at Figure 3; therefore the mark of the equation (8) is to taken as follows;

$$N = \frac{1}{cP_0 - \frac{b}{R_0}} - \sqrt{\frac{1}{\left(cP_0 - \frac{b}{R_0}\right)^2} - \frac{2aP}{R_0\left(cP_0 - \frac{b}{R_0}\right)}t} \quad \cdots\cdots (10)$$

$$\frac{dN}{dt} = \frac{aP_0}{R_0}\left\{1 - \frac{2aP_0}{R_0}\left(cP_0 - \frac{b}{R_0}\right)t\right\}^{-\frac{1}{2}}$$

provided that $cP_0 > b/R_0$.

Considering from this result, the writer can reason about the fact that the frequency of explosions in the second crater is Vesuvian type as that in the first crater, and both the curves $(dN/dt, t)$ and (N, t) are convex to time axis.

From the equation (10) we have

$$t = \frac{R_0}{2aP_0(cP_0 - b/R_0)} \quad \cdots\cdots (11)$$

At this time (the equation 11) dN/dt comes up to maximum, and at the same time, the activity in boring stage ceases; that is, the atmosphere makes a junction with the plastic maga, and the volcanic activity moves from boring atage to the magma stage. Though the

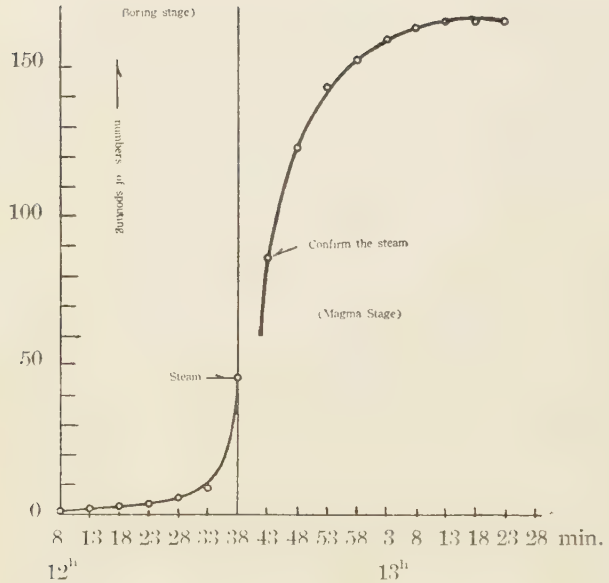

Fig 3A. Curve of Numbers of spouting in Aso Geyser (No. 19) (1943, June 13th, 12h)

twelve o'clock. Getting the position of maximum frequency of exqlosions by smoothing the first half of the curve dN/dt and t, $\tau = 31$ mimutes, $F_\tau = 11$; therefore, putting in this value to the equation (11) and

$$F_\tau = \sqrt{\frac{2aP_0}{R_0(cP_0 - b/R_0)}} \qquad \cdots\cdots\cdots\cdots (12)$$

we have

$$ap_0/R_0 = 0.99,\ cp_0 - b/R_0 = \frac{1}{61} \fallingdotseq 1.64 \times 10^{-2}.$$

According to self-register-frequency F which the writer observed in pratical is

$$\int_{t\ 0} \left(\frac{dN}{dt}\right) dt,$$

there seems no appreciable difference between it and dN/dt. Now, he shall try to calculate the constant factors in the above mentioned spouting No. 19 in Aso Geyser. The frnquency of spouting per minute is depicted in Figure 4. About thirty seven minutes past twelve o'clock, the writer found the steam in spouting, but it was at fourty two minutes past twelve that he could clearly confirm it. These spoutings first began at seven past

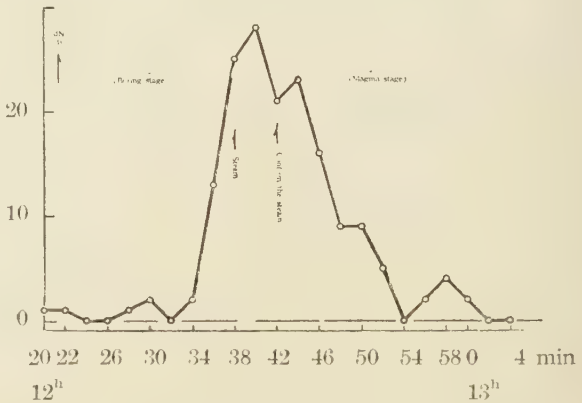

Fig. 3B. Frequency (per two minutes) of spouting in Aso Geyser (1943 June 13th., 12h)
(starts at 12h 07m ceases at 20h 27m).

ing record[3] on Decemcer 4 th., 1939, it became

$$\left(-\frac{dP}{dN}\right)_{t=0} = \frac{1.25}{760}K = 1 \times 10^{-3}K, \quad \therefore b\frac{P_0}{R_0} = 1 \times 10^{-3}K$$

K is a constant and its maximum value is unit (=1.). As the main active source in the tube of Aso Geyser is about 50 meters in depth, it has no objection to think P_0 is five atmospheric pressure and R_0 is about the same water column pressure as P_0 or so; Then we have

$$a = 0.99,\ b = 1 \times 10^{-3},\ b/R_0 = 2 \times 10^{-3},\ cP_0 = 1.66 \times 10^{-2},\ c = 0.33 \times 10^{-2}.$$

Therefore, the initial assumption that $(cP_0 + b/R_0)N$ is small is safe anyway, and there is no objection to think that $cP_0 > b/R_0$ and more $cP_0 \gg b/R_0$.

Putting in this data, we heve

$$\left.\begin{aligned} N &= 61 - 11 \times \quad 31 - t \\ \frac{dN}{dt} &= 0.99 \times \sqrt{\frac{31}{31-t}} \end{aligned}\right\} \cdots\cdots (13)$$

From (4), (5) and (10)

$$R_\tau = \frac{b}{cP_0 + b/R_0} + \left(R_0 - \frac{b}{cP_0 + b/R_0}\right) e^{-(cP_0 + b/R_0)}$$

$$P_\tau - P_0 + \frac{b}{c}\left\{\frac{1}{R_0} - \left[\frac{b}{cP_0 + b/R_0} + \left(R_0 - \frac{b}{cP_0 + b/R_0}\right)\right.\right.$$

$$\left.\left. e^{-\frac{cP_0 + b/R_0}{cP_0 - b/R_0}}\right]^{-1}\right\} \cdots (14)$$

Putting in the former data to the equation (10),

$$R_\tau = 1.8,\ P_\tau = 4.9$$

that is, it is clear that,
in boring stage, gas pressure is not very exhausted yet.

$$R = \frac{b}{cP_0 + b/R_0} + \left(R_0 - \frac{b}{cP_0 + b/R_0}\right)$$

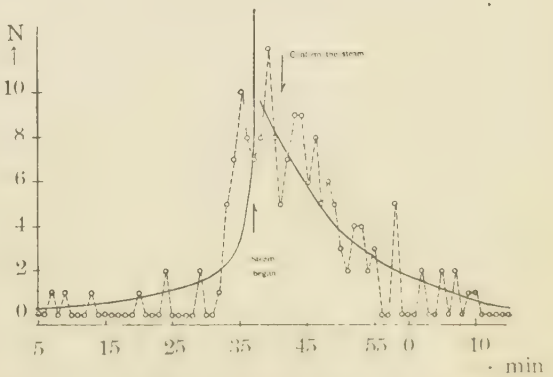

Fig. 4. Frequency of spouting in Aso Geyser
(From 1943 June 13th, $12^h0.0^m$) (start at $12^h0.7^m$ cease at 20^h27^m)

$$\times e^{-\left(cP_0+\frac{b}{R_0}\right)\left\{\frac{1}{cP_0-b/R_0}-\sqrt{\frac{1}{(cP_0-b/R_0)^3}-\frac{2aP_0}{R_0(cP_0-b/R_0)}}t\right\}} \quad \cdots\cdots (15)$$

Therefore the quantity of volcanic ejector dM/dt is ditectly proportional to $(-dR/dt)$ and the change of quantity of ejectors increases with lapse of time and, at τ it is in maximum. The curve $-dR/dt$, t is convex to t- axis, and this fact is the same to that in Geyser.

It is surmised that the state in both dR/dt and dP/dt are disordered for their mixing with the begining of the magma stage.

6. Discussions of The Magma-stage (Eruption-stage).

When the upward pressure of the plug is considerably excluded by the activity of boring stage, the atmosphere comes in contact with the stratum of the plastic magma and the block lava, what is called pahoehoe lavas which contain a large quantity of foams of high compressed volcanic gas are spouted; therefore it seems to the writer that the rate of decrease volcanic gas pressure becomes more larger than that of R. In geyser, it is found that, when activity enters into the the magma stage, a great deal of vapour is spouted together with hot water mingled with vapour. Like in boring atage, it is regarded as that the rudimentary relational expression in the magma stage is as follows. n is the frequency of explosions after boring stage, we have

$$\frac{dn}{dt}=\alpha\frac{P}{R},\quad -\frac{dP}{dn}=\beta\frac{P}{R},\quad -\frac{dR}{dn}=\gamma.P.R \quad \cdots\cdots (16)$$

in which P is the total of the upward pressure of the plug and the pressure of gas emitted from the magma, and R is the resist ance of the magma against the gas pressure; but at the beginning $t=0$, it stands to reason that $P_{t=0}=P_\tau$, $P_{t=0}=R_\tau$.

Threrefore, when $\left(\gamma P_\tau+\frac{\beta}{R_\tau}\right)n$ is small, the relation of (16) is the same as that in boring stage, and from the nafure of the curve (n,t) $(dn/dt,\ t,\ )$ the selection of the sighn is as follows;

$$\left.\begin{aligned} n&=-\frac{-1}{\frac{\beta}{R_\tau}-\gamma P_\tau}+\sqrt{\frac{1}{\left(\frac{\beta}{R_\tau}-\gamma P_\tau\right)^2}+\frac{2\alpha P_\tau}{R_\tau\left(\frac{\beta}{R_\tau}-\gamma P_\tau\right)}t}\\ \frac{dn}{dt}&=\frac{\alpha P_\tau}{R_\tau}\left\{1+\frac{2\alpha P_\tau}{R_\tau}\left(\frac{\beta}{R_\tau}-\gamma P_\tau\right)t\right\}^{-\frac{1}{2}} \end{aligned}\right\} \quad \cdots\cdots (17)$$

in which

$$\beta/R_\tau > \gamma P_\tau.$$

This curve is concave to time axis in (n, t), convex to time axis in (dn/dt). The result of observation is enough for the purpose. In the magma stage, the frequency of explosions is at the maximum in $\left(\frac{dn}{dt} \right)_{t=0} = \alpha . \frac{P_\tau}{R_\tau}$. In No. 19 explosion of Aso geyser, $\alpha \frac{P_\tau}{R_\tau} = 12$, therefor $\alpha = 4.4$, and from the measurement of pressure at the time when the spouting is in the height, the writer got the average value $\left(-\frac{dP}{dt} \right)_{t=0} = \frac{61.K}{760}$ (Aso-Geyser: continued, 1942 May, pp. 57)

When the maximum value of K is one,

$$\beta/R_\tau = 1.64 \times 10^{-2}, \quad \beta = 2.95 \times 10^{-2},$$

$$\left(\frac{dn}{dt} \right)_{t=0} = 5, \text{ therefore } \beta/R_\tau = \gamma P_\tau = 1.99 \times 10^{-2}$$

then $\gamma P_\tau = 0.96 \times 10^{-2}$, $\gamma = 2.1 \times 10^{-4}$

$$\left.\begin{aligned} n &= 50\sqrt{1 + 0.5t} - 50 \\ \frac{dn}{dt} &= 12/\sqrt{1 + 0.5t} \end{aligned}\right\} \quad \cdots\cdots (18)$$

Apparently $\beta/R_\tau > \gamma P_\tau$, and ($\beta/R_\tau + \gamma P_\tau$) are small. Thus it becomes that $P = 0$, $R = 1.5 = \frac{\beta}{(\gamma P_\tau + \beta/R_\tau)}$ *at* $t = \infty$, and therefore it is obvious that the initial velocity is maximum at time is zero.

Then we have;-

$$\left.\begin{aligned} &\text{The maximum initial velocity in boribg stage, } V_{max} = \sqrt{\frac{2bM}{c}} \cdot \frac{1}{R_\tau} \\ &\text{The maximum initial velocity in magma stage, } v_{max} = \sqrt{\frac{2\beta N}{c}} \cdot \frac{1}{R_\tau} \end{aligned}\right\} \quad \cdots\cdots (19)$$

Therefore, in the No. 19 explosion of Aso Geyser:-

$$V_{max} : v_{max} = \sqrt{M} : 11\sqrt{N}$$

In the case of M is equall to N (both are some constants),

$$V_{max} : v_{max} = 1 : 11$$

In either case, it is found that the explosion is violent fora short time when activity entered into the magma stage. In the case of the spouting of geyser, as the activity entered

into magma stage, a thunderous roar arises in the geyser tube. Calculated values of dn/dt in magma stage sre registered in Figure 4.

As the writer received some records of volcanic erution of Miyojin Rock (1952 Sept. 16), he retraced agreeablly with his above results in $(dN/dt, t)$ and even in their energy (dP/dt), (Figure 5). (5)

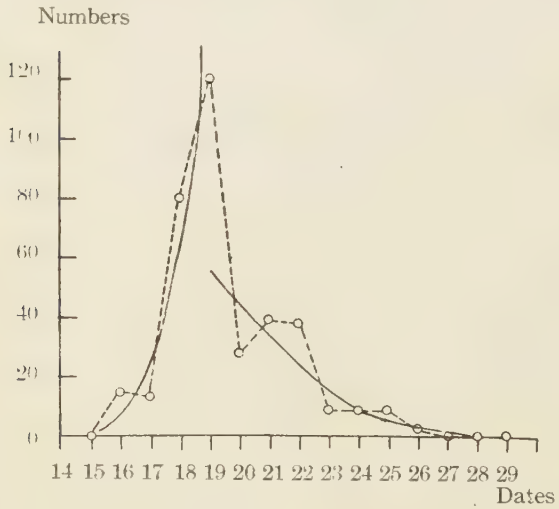

Fig. 5. A. Numbers of Explosions per Day (1952 Septembr Miyo Jin-sho)

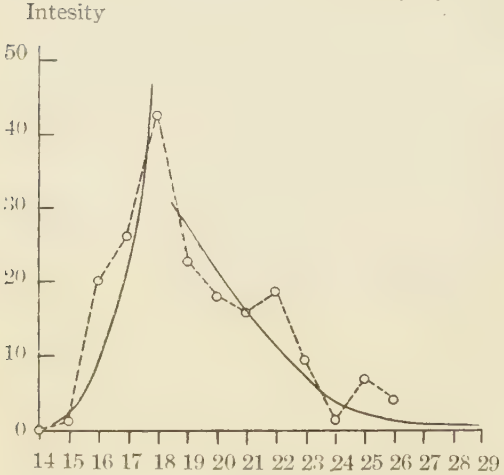

Fig. 5. B. Intensity of Explosion per Day (1952 September Miyo Jin-sho)

7. The Effect of the Atmospheric Pressure in every Stage of a Volcanic Explosion.

The writer could get the frequency of explosion about the first crater in boring stage (from February 25 to 28) and the magma stage (from March 1 to 4), but could not get the freeuency of explosion about the second crater in its boring stage for wanting of observation. Though the number of times of observation is few and the terms of variation for day are rather large, there is very reason to believe that these matters are not impediment to know the general tendency of the influence of the atmospheric pressure in the stage of volcanic eruption.

Putting in order both the first and second craters with respect to the same stage, the writer can find the fact that the former and latter half (boring stage and magma stage) in the second crater have almost the same tendency to the variation of the atmospheric prassure, but, in the first crater, their tendency are contrary to each other; that is, he may say, in boring stage there is a tendency that volcanic activity is suppre-

Feb. 25-28	Mar. 1-4
The First Crater Boring Stage 16.45 Cos (2t-143.3)	Magma Stage 10.07 Cos (2t-288.4)
The Second Crater Magma Stage 10.94 Cos (2t-81.7)	Magma Stage 3.51 Cos (2t-33.7
Change of Atmosph. Pressure in m.m.Hg. 0.37 Cos (2t-291.5)	in m.m.Hg. Cos (2t-296.0)

sseb by rising of atmospheric pressure, while in the magma stage the activity is increased by it.

8. An Example of Volcanic Activity in the Magma-stage.[3]

The writer shall describe the condions of the second crater near upon the ending of the magma stage on March, 1933. At the beginning a column of red hot plastic magma swells about 100 meters high at the top of volcanic vent tube and becomes like as a steamed bean-jum bun, but it does not break up; its surface hollows in a few moment and becomes dark hue in proportion to the refrigeration of it. After the top part repeated to rise up and fall down several tinnes, there start radial fissures on the dark surface, and as soon as red hot plastic magma is seen through the fissures it explodes with a great explosion and many pieces of plastic magma are dispersed and black cloud including a large quantity of magma ashes ascend with terible energy in the atmosphere (a photograph of the state of the crater in this moment has been taken). If at the initial swelling the volcanic gas pressure in the magma is not enough to break up the magma dome, the round top of the dome balances in that condition; after a few minutes the top hollows by the contraction of the gas volume, caused by cooling, and the surface becomes dark hue. When it is supplied with volcanic gas sufficiently, it swells again, but as its surface is hardened by gradual refrigeration, it explosionally breaks out the surface and ejects plastic magma, and many foams in plastic magma break the magma membranes to pieces, (magma ashes), so that the ashes are shot up as blacksmokes. But in this time roaring explosion becomes comparatively low tone. If the atmospheric pressure varies in the course of the explosion there must be some effects as described above. When the writer examines the relation between the number of frequency of volcanic explosion and the variation of atmospheric pressure, which he studied previously, he has such a statical result as that, in general, many great explosions take place when atmospheric pressure is rising.

These facts must explain the mechanism of the volcanic explosion. It may be said that the fact that the boring stage is reverse to the magma stage in the influence to the atmo-

spheric pressure shows, to say the least of it, their mechanisms themselves are different; that is, the two stages reverse each other in the action of atmospheric pressue change to the pressure of magma.

9. Conclusion.

Though it was imperfect, the writer was able to observe the curve of the frequency of volcanic explosions and, therefore, learn about its general property: such being the case, making good the deficiency in observation of the frequency of volcanic explosions by observing a geyser, he could gain the character of the frequency of volcanic explosion. Moreover, he could learn the fact that Boring-stage and Maga-stage in volcanic explosion differed in their mechanisms by study ing the relation between the change of atmospheric pressure and the two stages in volcanic explosion. If it is able to recognize the above mentioned result for the most part, it will be able to say that the square reciprocal of the frequency of volcanic explosions is proportional to time t; the boring stage comes to an end when $t = \dfrac{R_0}{2aP_0(cP_0 - b/R_0)} \equiv \tau$ (this can be calculated by graphically or calculation).

It is so difficult to observe the frequency of volcanic explosions that the writer cannot help to discourse in detail the other day; also it is so difficult to conclude the time on observing Geyser, that ho cannot be relieved of observational error of a few minutes. Moroover, in the proximity of time τ, the frequency of explosions takes a sudden chnge for the confusion of activity in boring and magma stages. The minute observation of the frequency of volcanic explosion is the future problems on Volcano Aso.

But fortunately some self recording data were gained by chance on SOFAR by the explosion of Miyojin Rock (1952 September 16 th.), and it replesents good agreements with the obove discussions.[5]

The writer should like to pay his respect to the members of the staff of Kumamoto Meteorogical Station for their incessant endeavours to observe volcanic explosion, and express his gratitude to the late Prof. Nomitsu who assumed the leadingship of him. Both Mr. Eto and Mori, the staffs of Aso Volcanic Laboratory, endeavoured without sleep or rest to observe Aso Geyser.

Literatues.

1). S. Aoki; Kensin Jiho, Vol. II, No. I, 1934.

2). M. Namba; Aso Geyser Part I, Chikiu Butsuri, Vol. III. No. 4, 1939. part 2, Vol. 6, No. 1. 1942.

3). This kind of observation was done at several times, for example:-

a) S. Aoki: - ditto.
b) K. Sasa: - Chikiu Butsuri, Vol. III, No. 2, and so.
4). M. Namba: - The Effect of Atmospheric pressure on Volcanic Explosion, Chikiu Butsuri, Vol. VI, No. 3, 1938.
5). R. S. Dietz: On the SOFAR, Scientific Asahi, Mar. 1953, -pp. 21-24.

MAGNETIC ANOMALIES ALONG THE BAY OF YATUSIRO, KUMAMOTO PREFECTURE.

Saemon Taro NAKAMURA and Akira ONUKI

(Received September 25 1953)

1. Introduction

Magnetic dip was observed at 48 points distributed in Kumamoto prefecture for the purpose of the earthquake prediction. Of these points, 21 are distributed in the southern part of the prefecture, along the Bay of Yatusiro. In this paper is reported the results of these 21 points only.

The reason why the magnetic dip only was observed is as follows:

(1) The daily variation is generally very small.

(2) Dip circle is quite handy and affords data with sufficiently good accuracy for the authors purpose.

(3) In Japan and other localities where magnetic dip is nearly 45°, the maximum of disturbance observed on the earth's surface appears nearly just above the centre of the source of the disturbance, which is assumed to be a simple magnet.

It was found that the observed magnetic disturbance is sufficiently well explained by assuming a line distribution of simple magnets along the east coast of the bay.

2. Isoclinic chart

Fig. 1 is the isoclinic chart. It is clearly seen that the magnetic dip is remarkably large along the coast of the bay of Yatusiro which runs nearly in the direction of N 30° E refering to the magnetic meridian.

3. General distribution of the magnetic dip

To eliminate the general variation of the magnetic dip in this locality, the observed dip is assumed to be expressed by a linear equation of the longitude (λ) and the latitude (φ) of the point of observation. The coefficients in the equation were determined by the method of the least squares. The result is

$$\Theta = 45°50'.02 + 1.1431\,(\varphi - 32°41'.7) - 0.163\,(\lambda - 130°27'.6) \quad \cdots\cdots\cdots\cdots \quad (1)$$

The residue obtained by subtracting the computed values of Θ given by eq. (1) from the observed values are refered to be the anomaly of dip, ($\Delta\Theta$), which is to be discussed hereafter in this paper.

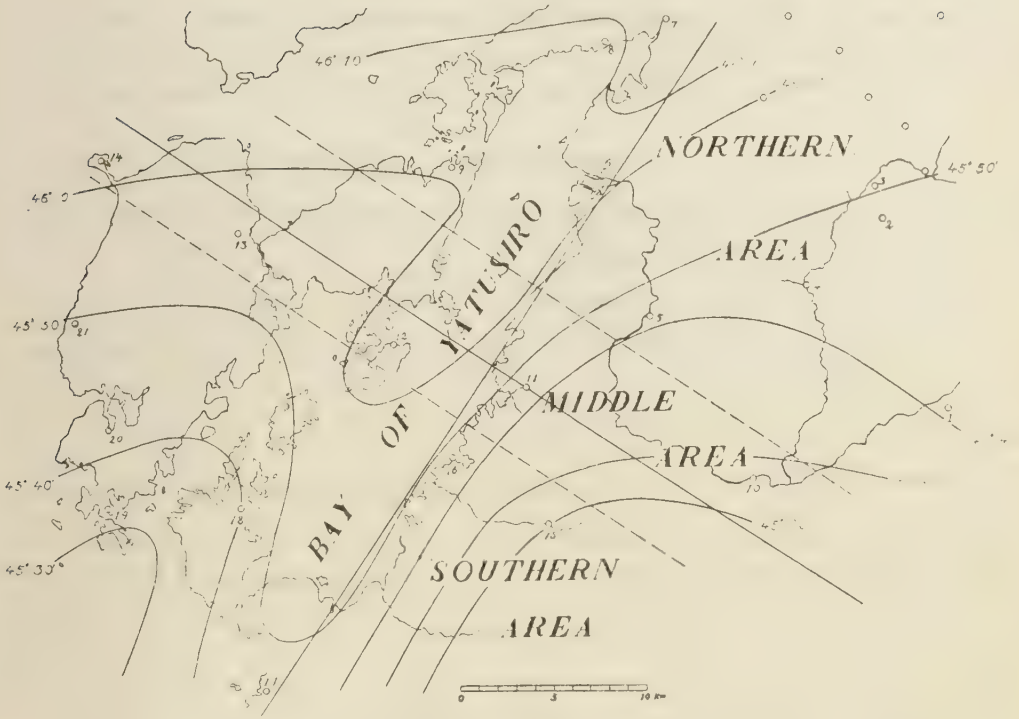

1 Yunomae	8 Matuai	15 Kukino
2 Kureko	9 Aizu	16 Yunoko
3 Siibaru	10 Hitoyosi	17 Akune
4 Ituki	11 Sasiki	18 Nagasima
5 Setoisi	12 Rankuti	19 Usibika
6 Yatusiro	13 Hondo	20 Kamenoura
7 Matubase	14 Tomioka	21 Takahama

4. Magnetic disturbance due to a line double source of infinite length

Take the x-axis on the horizontal surface in the direction perpendicular to the east coast of the bay of Yatusiro and z-axis vertically downwards, and consider a long line double source at $x = x_1$, $z = z_1$, extending infinitely in y-direction or in the direction parallel to the coast line. The axis of the elementary doublet is assumed to be in the direction inclined to horizon an angle θ in the magnetic meridian, to which the y-axis makes an angle α. Then the anomaly of the dip is given by

$$\Delta\theta = -\frac{M}{F}\left[\frac{1}{r^2}\left(\cos^2\alpha\,\cos\theta\,\sin\theta - \cos\theta\,\sin\theta + \sin\theta\,\cos\theta\right)\right.$$
$$+\frac{2}{r^4}\left\{\left(\left(x-x_0\right)^2\sin\theta\,\sin^2\alpha - \left(x-x_0\right)\left(z-z_0\right)\cos\theta\,\sin\alpha\right)\cos\theta\right.$$
$$\left.\left.+\left(\left(x-x_0\right)\left(z-z_0\right)\sin\theta\,\sin\alpha - \left(z-z_0\right)^2\cos\theta\right)\sin\theta\right\}\right] \quad \cdots\cdots(2)$$

where F is the strength of the general magnetic field, M the linear density of the double source and $r^2 = \left(x-x_0\right)^2 + \left(z-z_0\right)^2$.

Put $\alpha = 30°$, $\theta = 45°$ and $z = 0$, then we get

$$\Delta\theta = -A\left[\frac{\sin\theta - 0.25\cos\theta}{r^2} + \frac{1}{r^4}\left\{\left(0.5\left(x-x_0\right)^2 + \left(x-x_0\right)z_0\right)\cos\theta\right.\right.$$
$$\left.\left.-\left(\left(x-x_0\right)z_0 + 2z_0^2\right)\sin\theta\right\}\right], \quad \cdots\cdots(3)$$

where $A = 0.707\,\dfrac{M}{F}$. This equation expresses the anomaly of dip on the earth's surface. Put $\Delta\theta = 0$ in this equation, we get

$$\sin\theta\left\{\left(x-x_0\right)^2 - \left(x-x_0\right)z_0 - z_0^2\right\} + \cos\theta\left\{0.5\left(x-x_0\right)^2\right.$$
$$\left.+\left(x-x_0\right)z_0 - 0.25\,r^2\right\} = 0, \quad \cdots\cdots(4)$$

and $$r^2 = \infty. \quad \cdots\cdots(5)$$

Equation (4) gives two roots of x which are given by

$$x_1 - x_0 = \frac{z_0}{2\left(\sin\theta + 0.25\cos\theta\right)}\left\{\sin\theta - \cos\theta + \frac{\sqrt{5}}{2}\sqrt{1+3\sin^2\theta}\right\}$$
$$\text{and} \quad x_2 - x_0 = \frac{z_0}{2\left(\sin\theta + 0.25\cos\theta\right)}\left\{\sin\theta - \cos\theta - \frac{\sqrt{5}}{2}\sqrt{1+3\sin^2\theta}\right\} \quad (6)$$

Therefore we get

$$x_1 - x_2 = \frac{z_0}{2\left(\sin\theta + 0.25\cos\theta\right)}\cdot\sqrt{5}\,\sqrt{1+3\sin^2\theta}. \quad \cdots\cdots(7)$$

x_1 and x_2 are obtained from observed data, if $\Delta\theta$ is ploted for x and read off two values of x for $\Delta\theta = 0$. z_0 is therefore computed by eq. (7). Using z_0 thus obtained, x_0 can be computed from eq. (6). The most probable value of A is calculated by eq. (3) using all available data.

5. Direction of magnetization of the elementary double source

To solve eqs. (3), (6) and (7), θ the direction of the axis of the elementary double

source must be known. Different values of θ are assumed at first and constants x_0, z_0, and A are calculated for each case, using all data. The sum of the squares of errors of $\Delta\theta$ for each case is computed as shown in Table I.

Table I

θ	0°	30°	60°	90°	120°
x_1 (km)			13		
x_2 (km)			−4		
$x_1 - x_0$ (km)			17		
x_0 (km)	12.1	6.6	3.0	0.7	−1.3
z_0 (km)	3.8	8.2	8.4	7.6	6.3
A	379	1683	1286	943	731
$\Sigma\varepsilon_2$	1116	799	669	626	704

Fig. 2 shows the $\theta - \Sigma\varepsilon^2$ diagram. From this diagram it is seen that the most probable value of θ is between 75° and 90° or the source of disturbance is nearly vertically magnetized.

Put $\theta = 90°$ in eq. (3) we get

$$\Delta\theta = -A\left\{\frac{1}{\xi^2 + z_0^2} - \frac{7.60\,\xi - 115.6}{(\xi^2 + z_0^2)^2}\right\} + B \qquad \cdots\cdots(8)$$

where $\xi = x - x_0$ and B is a constant to correct a systematic error in eq. (1). This constant is neccessary in the next step of discussion.

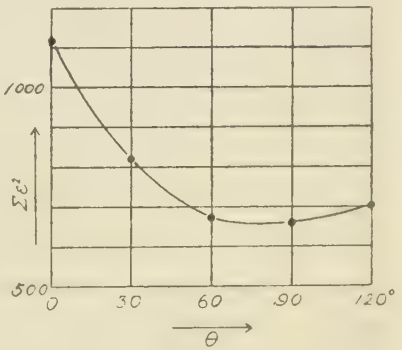

Fig. 2

6. The second approximation

It was found that error is too large in some points when all data are treated as a whole. For the second approximation, therefore, the whole area is devided in three miner areas according as to the value of y, and constants are determined independently. In this case the most probable values of θ are different for the miner areas. The best is found to be 75° for the northern area and 90° for other two areas. The results are given in Table II.

Table II

Area	A	B	z_0 (km)	x_0 (km)	No. of points	$\Sigma\varepsilon_2$	Probable error	x_1 (km)	x_2 (km)	θ
Northern	1321	−1.82′	12.5	−0.26	9	46.26	±1.53′	20	−8	75°
Middle	4083	−3.07′	12.5	3.24	5	6.19	±0.75′	23.5	−4.5	90°
Southern	3523	−7.35′	12.1	0.54	7	38,87	±1.59′	16.5	−5.5	90°

The depth of the linear double source is approximately 12.5 km, which is of the same order of the usual earthquake focus. x_0 is generally very small, largest in the middle area and smallest in the northern area. Or the line source bents very slightly. The linear density of magnetization is largest in the middle area and smallest in the northern area.

7. Magnetic data

The magnetic data used and the results obtained by eq. (8) are given in Table III.

Table III

Station	λ 130°+	φ 32°+	θ 45°+	$\Delta\Theta_{obs.}$	x (km)	y (km)	$\Delta\Theta_{comp.}$	$\varepsilon=\Delta\Theta_{obs.}-\Delta\Theta_{comp.}$
Northern area								
Yunomae	59.2	16.3	41.4	2,7	−42.8	22.6	−2.46	5.2
Kureko	54.9	27.4	46.7	−5.4	−26.0	35.6	−3.14	−2.3
Siibaru	54.5	29.1	50.3	−3.7	−23.2	38.0	−3.30	−0.4
Ituki	49.6	23.5	43.9	−4.6	−23.2	25.4	−3.30	−1.3
Setoisi	38.9	22.0	41.9	−5.9	−11.0	13.6	−5.30	−0.6
Yatusiro	36.2	30.3	64.3	5.9	1.2	23.6	6.27	−0.4
Matubase	40.6	39.0	75.3	7.6	4.6	40.8	6.32	1.3
Matuai	36.3	37.8	68.1	1.1	8.6	35.4	3.51	−2.4
Aizu	25.7	30.7	61.0	0.4	15.0	15.0	−0.48	0.9
Middle Area								
Hitoyosi	45.8	12.5	29.6	−6.9	−29.8	5.0	−6.59	−0.3
Sasiki	30.8	18.2	42.3	−3.2	−4.2	0.0	−2.35	−0.8
Rankuti	21.4	20.7	66.5	16.6	10.0	−4.0	16.57	0.0
Hondo	11.5	29.9	56.8	−5.2	30.2	−5.4	−4.29	−0.9
Tomioka	2.0	31.5	63.3	−2.1	46.2	−4.8	−4.12	2.0
Southern Area								
Kukino	31.7	10.3	20.1	−16.2	−14.4	−10.6	−14.00	−2.2
Yunoko	25.2	14.0	48.6	7.0	−1.8	−11.0	9.85	−2.9
Akune*	11.9	1.0	47.5	18.6	1.0	−42.0	17.52	1.1
Nagasima	10.8	11.6	40.2	−1.0	14.2	−27.4	−3.38	2.4
Usibuka	1.7	11.6	32.9	−9.8	25.4	−35.2	−8.38	−1.4
Kamenoura	2.0	16.3	42.4	−9.6	30.2	−28.0	−8.61	−1.0
Takahama	0.1	22.3	49.3	−4.5	39.0	−20.4	−8.51	4.0

*Kagosima Prefecture

Fig. 3 shows the results of observation and calculation.

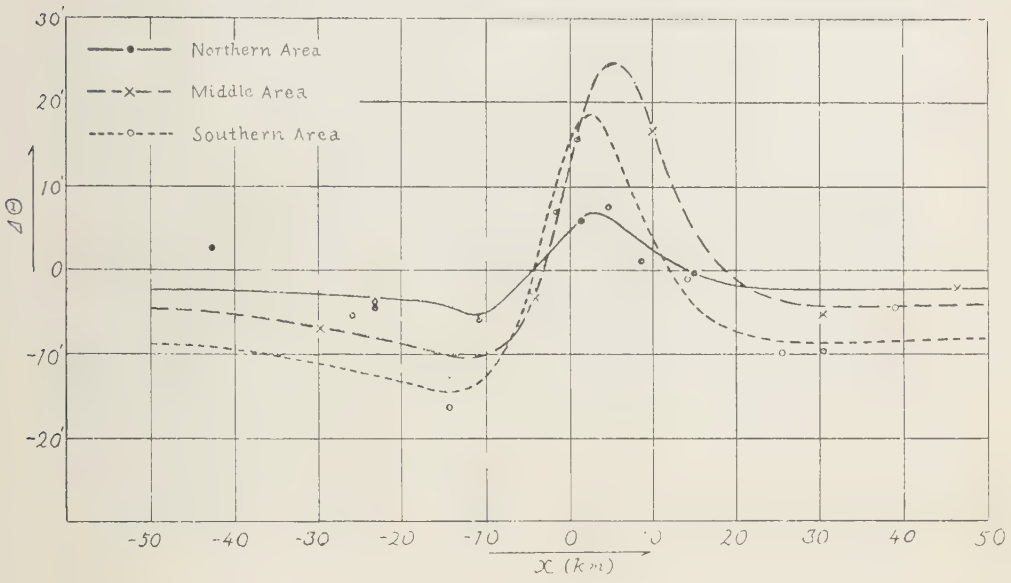

8. Seismic zone

On the northern extension of this disturbed line, a strong earthquake occurred near the city of Kumamoto in 1889 and of its southern extension earthquakes are occasionary observed near the isles of Kosiki. In the bay of Yatusiro small earthquakes are also observed. The existence of fault line along the east coast of the bay is also proved geologically and geographically, though it is not yet known it is active of not. The magnetic disturbance observed may be attributed to the seismic zone runs along this fault line, and from this evidence the fault there exists may be an active one. Activity may be possiblly detected, if the magnetic observations are repeated in short interval of time, say 5 of 6 times every year at a few stations distributed along the coast.

In conclusion the authors must express their courteous thanks to shin Nippon Chisso Hiryo K.K. who helps us during the cource of the observation in various ways.
This work is a part of the research financially supported by the Scientific Research Expenditure of the Ministry of Education.

SOME STUDIES ON VOLCANO ASO AND KUJIU (PART 7)
ON ANNUAL AND SECULAR VARIATIONS OF THE HYDROSTATIC HEAD OF HOT SPRING

Tosisato MUROTA

(Received September 1, 1953)

Abstract

The writer examined quantitatively the effects of precipitation and atmospheric pressure upon the annual and secular variations of the hydrostatic head of hot spring at the Uchinomaki Volcano and Hot-Spring Laboratory in Aso crater atrio (about 11 km distant from the present crater of Nakadake), and ascertained the tendency of natural fall of the hydrostatic head of hot spring. Moreover the writer studied on the correlation between the variations of hydrostatic head of hot spring and of volcanic activity, and found a key to the problem of forecasting the volcanic activity.

1. Introduction

As it is impossible to research freely after a hot spring which belongs to a private person, Dr. Nomitsu and Dr. Namba planned to bore a hot spring for research-worker's special

Fig. 1 A, Vertical conduit through which hot water ascends ; B, Beckmann's thermometer; C, Sale aud Glass tube which may be connected with A by a indiarubber tube for the measurement of head

use at Uchinomaki. They started their work in March 1941 and ejection of hot water began on lst July. The depth of the boring is 153 m [1]. The gap between the vertical conduit through which hot water ascends and the lowest impermeable stratum througugh which the conduit passes, was cemented to prevent the leakage of hot water. Therefore if one closes pipe through which hot water streams to bath, one can measure the height of hydrostatic head (see Fig. 1).

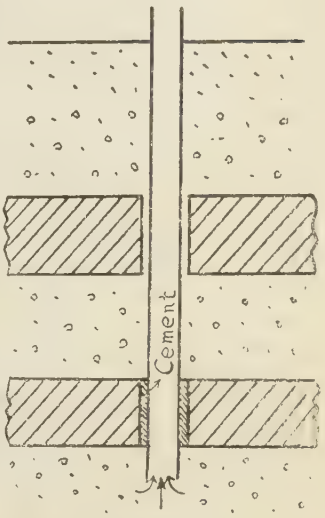

Fig. 2

The value of hydrostatic head of the above described hot spring which was obsreved once every day at 10 a.m. from April 1942 to December 1949 and daily amount of precipitation during the same time at Uchinomaki are given in Table 1. Using this data and comparing the variation of hydrostatic head with precipitation and variations in atmospheric pressure and volcanic activity, the witer discussed (1) the tendency of natural fall of the hydrostatic head (2) the effects of precipitation and variation in atmospheric pressure upon the hydrostatic head (3) the correlation between the variation of hydrostatic head and that in volcanic activity and (4) a key to the problem of forecasting volcanic activity. He will discuss the variation of hydrostatic head of short period in the following paper.

2. Natural Fall of the Hydrostatic Head

The monthly mean values of hydrostatic head and atmospheric pressure and the monthly precipitation are as given in Table 2 and graphically represented in Fig. 3 (monthly precipitation is reduced as days in a month to bo 30, and as data of atmospheric pressure in 1949 is not satisfactory it is excluded. Moreover precipitation of each 10 days is shown in Fig. 3).

As a matter of course, Fig. 3 shows that, under the influences of precipitation and change in atmospheric pressure, the hydrostatic head of hot spring is high in warm season and low in cold season. An examination in the diagram of hydrostatic head in Fig. 3 shows that there exists a tendency of natural fall of the hydrostatic head in exponential fashion, as secular trend.

Let H be annual mean of head, λ decay constant, t year, then the secular trend may be writton

Table 1.

Observed Data of the Hydrostatic Head of Hot Spring at Uchinomaki Observatory (+1500mm), and the Precipitation (from April 1942 to December 1949)

1942

Month / Observation Day	Apr.		May		June		July		Aug.		Sep.		Oct.		Nov.		Dec.	
	Head (mm)	Pre. (mm)	Head (mm)	Pre. (mm)	Head (mm)	Pre. (mm)	Head (mm)	Pre. (mm)	Head (mm)	Pre. (mm)	Head (mm)	Pre. (mm)	Head (mm)	Pre. (mm)	Head (mm)	Pre. (mm)	Head (mm)	Pre. (mm)
1	2519		2628		2591		3050	52.5	2723		2624		2692	3.3	2567		2456	
2	2536		2627	51.6	2587		3067	35.7	2714		2625		—		2558		2439	
3	2540		2669	2.7	2589	29.7	3050	58.5	2653		—	23.4	2682		—		—	1.2
4	2549	60.0	2638		2615	12.3	3101	10.9	2677		—	3.4	2676		2548	1.2	2435	
5	2609	10.0	2636		2602		3109	2.3	2663	0.7	—	5.6	2661	86.0	2544	0.3	2434	3.2
6	2578		2638	19.5	2591	67.5	3147	12.3	2715	23.5	—		2688	0.1	2538	0.8	2434	
7	2584		2649	2.6	—	61.5	3145	2.9	2721	0.2	—	8.8	2662		2538		2422	0.1
8	2584		2631		2617		3152		2696	83.7	2657	14.7	2658	9.2	2532		2421	0.5
9	2598	3.5	2624		2649		3146		2674		2655	9.1	2663	21.8	2527		2417	
10	2618	0.3	2620		2687		3142		2658	1.0	2655		2671		2515		2410	13.3
11	2617		2618	7.2	2710		3127		2691		2646		2647		2515		2415	
12	2627	11.4	2621	6.7	2727	3.7	3110		2681	22.6	2635	1.1	2657	1.0	2502		2416	
13	2636	0.3	2626		2750	186.4	—		2682		2635	0.8	2652		2507	0.7	2409	
14	2635	2.8	2619		2829	142.2	—		2723	6.2	2630	37.0	—		2507	2.2	2402	
15	2637	10.5	—		2847		—		2717	30.4	—	25.5	2656		2499		2405	
16	2649	30.8	2617		2954	1.5	—		2619	73.2	2637	7.1	2674	11.8	2496		2402	0.7
17	2648		2611	0.9	3023	67.6	—		2645	1.9	2629	17.3	2653		2489	0.1	2402	1.9
18	2638		—	63.0	3097	108.5	—		2614		2632	46.3	2645		2478		2412	0.1
19	2638	34.3	2632	0.5	3122	16.4	—	13.0	2608		2640	12.8	2637		2477		2400	
20	2667	12.2	2607		3151	1.4	3027		2608		2638	30.8	2635		2465	1.9	2396	
21	2651		2597		3182	2.3	3029		2607		2656	8.8	2627		2476	0.1	—	
22	2636		2597		3195	13.0	3007		2603		2652	1.0	2630		2475		2395	1.8
23	2619		2590		3216	14.9	2982		2615	6.6	2652		2617		2471		2391	6.2
24	2617		2587	21.7	3187	28.5	2964	16.5	2616	23.2	2657		2617		2462		2390	
25	2620		2669		—	17.8	2943	23.2	2617	0.2	2673		2614		2456		2378	1.3
26	2625		2588	30.2	3142		2839		2614	30.1	—		2613		2450	9.3	2379	
27	2626	19.3	2611		3107		2821		2637	80.1	2675		2602		2457	1.5	2376	
28	2634	5.9	2599		3110		2822		2636	11.0	2678		2599		2456		2373	
29	2635		2597		3079	82.5	2810	4.7	2621	0.6	2681	19.2	2597		2447		2375	2.6
30	2630		2591		3082	5.6	2800	0.6	2630		2695	4.5	—		2444	14.1	2370	2.2
31			2592				—		2607	0.5			2575				2375	
Mean	2613		2618		2894				2655				2642		2496		2402	
Total		201.4		206.6		863.3	3016	233.1		395.7	2652	277.2		133.2		32.2		35.1

Month / Hourly Days	Jan.		Feb.		Mar.		Apr.		May		June		July		Aug.		Sep.		Oct.		Nov.		Dec.	
	Head	Pre.	Head	Pre.	Head	Pre.	Head	Pre.	Head	Pre.	Head	Pre.	Head	Pre.	Head	Pre.	Head	Pre.	Head	Pre.	Head	Pre.	Head	Pre.
	mm	mm	mm	mm	mm	mm	mm	mm	mm	mm	mm	mm	mm	mm	mm	mm	mm	mm	mm	mm	mm	mm	mm	mm
1	2376		—	1.7	2316		2264		2288		2656		2823	85.5	3090		2623		2712		2466		2423	
2	2375		2919	36.4	2309		2253		2294		2678	7.3	2830	46.3	3050		2618		2778	2.2	2518		2423	
3	2376		2355		2302		2260	33.5	2303		2704	68.5	2796	4.6	3060		2608		2813		2523		2430	
4	2376		2330		2297		2300	29.3	2303	2.6	2758	0.4	2824	1.7	3033	5.0	2568		2811		2518		2413	
5	2364		2319		2297	7.2	2280		2309	17.0	2712	43.5	2866	3.2	3042		2586	4.2	2745		2506	3.8	—	
6	2357		2325	17.2	2304		2280	18.6	2318		2760	49.6	2890	38.8	3025	5.5	2608	9.5	2759		2506		2403	7.0
7	2356	0.7	2337		2300		2301	11.6	2308		2774	29.5	2917	0.5	2955		2578	5.7	2754		2493	10.0	2408	
8	2357		2332	0.3	2299	0.1	2310	1.2	2303		2810	12.0	2963	1.0	2945		2574		2756		2497	34.2	2405	
9	2382	0.1	2328	4.0	2298		2299	2.4	2310		2845	9.5	2944		2968		2566		2713	19.9	2528	38.4	2395	
10	2385	12.0	2319	2.0	2294		2288	1.2	2305		2890	20.0	2943		2935		2553	33.8	2725		2508		2397	
11	2398		2317	0.9	2290		2297	22.8	2303		2931		2945	0.5	2920	20.1	2600	8.7	2693		2502		2386	
12	2394		2317		2287	0.5	2303		2299		2945	2.8	2943	2.5	2905	2.1	2602	33.9	2749		2492		2395	
13	2395	1.0	2317		2279		2303		2299	11.7	2974	39.0	2945		2885	2.2	2608	0.6	2670		2483		2382	
14	2389		2319		2282		2300	0.9	2307		2986		2928		2870	0.7	2600		2705	0.2	2477	0.7	2384	2.4
15	2388	0.4	2319		2310		2300		2304	86.6	2995		2935	23.1	2843		2582	10.0	2662	10.2	2487	24.5	—	25.9
16	2386		2316		2286		—		2375	27.6	2984		2925	1.8	2827	1.5	2578		2665		—	2.0	2421	5.6
17	2392		2317	22.0	2278		2296		2331		2975	37.8	2905	0.2	2813		2579	10.0	2653	0.5	2487		2392	
18	2382		2330	2.0	2276	4.8	2300	21.0	2323		—	7.5	2855		2798		2570	45.6	2653		2482		2355	
19	2382	1.8	2320		—	12.7	2318		2313		2962		2874	1.5	2783	10.0	2593	240.8	2644		2472		2343	
20	2378		2319		2289		2308		2308		9296		2858	2.5	2783	10.1	2780	19.7	2630	0.7	2479	10.9	2338	
21	2375	6.3	2315		2272	8.5	2301		2297		2937		2846	117.5	2758		2600		2625		2465		2344	
22	2378	1.2	2316		2261	11.2	2305		2303		2922		2961	65.8	—	0.7	2641		2698		2467		2337	
23	2377		2315		2281	2.0	2217		2302	125.0	2905		2868	82.5	2722		2681		2598	0.5	2456		2325	4.0
24	2376		2310		2281	1.2	2295		2447	38.0	2895		2898	5.5	2703		2720	3.2	2588	17.2	2459		2341	
25	2379		2313		2282		2297		2253	1.0	2878		2883		2687	2.4	2743	20.9	2601	12.2	2453		2332	
26	2375		2309		2270		2298	4.0	2383	14.0	2811	5.2	2930	107.8	2674	15.7	2768	7.3	2589		2453		2322	
27	2367	0.4	2300		2269	10.5	2303		2427	88.6	2856	20.2	2989	22.4	2669		2788	3.0	2577		2443		2323	
28	2368		2300	21.6	2289	0.8	2298	2.2	2478		2856		3035	6.2	2688	0.2	2790	0.5	2569	0.5	2473	0.9	2315	
29	2367				2273	11.3	2313		2503		2831	6.7	3073	1.5	2641		2788		2569	0.8	2495		2283	
30	2359				2273	2.9	2300		2557	9.3	2825	25.0	3082		2633	45.8	2780		2551		2436		2293	9.0
31	2351	0.2			2241				2614	0.9			3075		2648				2537				2300	
Mean	3742		2320		2287		2293		2351		2865		2920	622.9	2849		2642		2668		2481		2360	
Total		24.1		108.1		73.7		148.7		414.3		384.5				122.0		457.4		64.9		125.4		59.3

1941

Month / Date	Jan.		Feb.		Mar.		Apr.		May		June		July		Aug.		Sep.		Oct.		Nov.		Dec.	
	Head (mm)	Pre. (mm)	Head (mm)	Pre. (mm)	Head (mm)	Pre. (mm)	Head (mm)	Pre. (mm)	Head (mm)	Pre. (mm)	Head (mm)	Pre. (mm)	Head (mm)	Pre. (mm)	Head (mm)	Pre. (mm)	Head (mm)	Pre. (mm)	Head (mm)	Pre. (mm)	Head (mm)	Pre. (mm)	Head (mm)	Pre. (mm)
1	2290		2145		2088			16.0	2072		2261		2065	5.1	2060		1940		1870		1735		1749	2.0
2	2280			20.7	2075			1.2					2033	6.2	2033		1935		1858		1755	42.7	1736	
3	2287		2143	8.4		1.8	2057		2072			76.5	2055	11.4	2054		1923		1853	8.7	1795		1735	
4	2249	5.3	2153	2.0		16.2	2047		2085	33.0	2376	31.0	2065	23.9	2059		1920		1848		1787		1720	
5	2259	1.4	2152		2084		2048		2103		2273		2068	18.2	2056		1912		1855		1777		1720	4.6
6	2234	3.3	2113		2090		2033	10.2	2093		2234		2075	0.7			1933	33.5	1848		1773		1715	3.5
7	2230		2117	1.8	2073	9.0	2062	70.2	2080		2209					6.4	1920		1857	3.8	1738	38.5	1705	
8	2225		2104		2083	0.4	2092		2082		2213		2068	2.0	2050	71.9	1915		1831		1807	28.1	1655	
9	2220	17.2	2109		2075	0.5	2078		2089	192.0	2190		2067		2055	0.6	2000		1812		1885		1670	
10	2235		2113	0.2	2072	2.8	2082		2261	79.5	2176				2060		1880		1818		1812		1665	
11	2220		2091		2067	1.2	2075		2250	0.2	2177				2059	1.2	1888	22.0	1814		1812		1670	0.7
12	2205		2106	55.3	2083		2079	3.7	2237		2175				2047		1899		1803		1803		1685	12.5
13	2209	2.6	2140		2087	0.4	2095	5.7	2292		2183	2.7	2057		2037		1887		1802		1780		1625	
14	2205		2108		2107		2093		2297		2170		2052		2088	0.7	1873		1770		1814		1675	
15	2207		2099		2090	1.2	2092		2323		2151		2055		2085				1767		1781	11.5	1675	
16	2191		2109		2090		2092		2340	6.6		7.4	2047		2068		1870		1770	2.9	1785		1670	
17	2185		2114		2100	11.0	2093	0.9	2351	22.2	2138				2067			99.5		15.3	1775		1685	
18	2182		2122		2090	4.0	2104	15.5	2382				2048		2052	0.3	1935	21.0	1783		1774		1665	
19	2170		2124		2083		2120	2.0	2353		2150		2053		2050	8.0	1925		1782	2.0	1750		1667	
20	2170		2130	0.9	2072		2115		2352	6.0	2130		2063	6.2	2040		1920		1785		1751	2.9	1650	
21	2171	4.6	2122	0.2	2075		2113		2348		2085	1.7	2101	26.3	2030		1910		1797		1758	1.2	1655	
22	2170	3.8	2110		2035		2117	1.0	2332		2105		2164	111.4	2033	7.8	1895		1779		1744		1655	
23	2177		2098	21.5	2035	0.5	2084		2338		2085		2071	2.0	2030		1875	0.7	1781		1740		1657	
24	2175		2141	3.2	2030		2085	8.4	2320		2064		1951		2012		1875		1774		1739		1660	0.2
25	2175		2111		2052		2100	3.5	2313	9.7	2059	28.2	2047		1998		1865	16.6	1764		1740	18.2	1650	
26	2176		2107		2045	7.5	2090		2318	6.2	2070	48.1	2045	8.0	1990		1880		1763	8.5	1713		1642	
27	2153		2092	1.7	2059	56.0	2092	19.9	2318		2084	18.5	2055	3.8	1985		1875		1775	6.8	1708	28.0	1640	
28	2143		2107		2090	2.0	2111		2304		2075	26.4	2050	9.2	1985		1855		1761		1732	2.2	1645	
29	2118	1.0	2090		2078	3.4	2110		2294		2095	0.1	2035		1970		1847	4.3	1757	3.0	1723	12.2	1635	
30	2149				2075		2087		2288				2065		1955		1853	37.1	1751		1727	6.2	1635	
31	2140				2065				2257				2065		1950				1755				1635	
Mean	2201		2113		2077		2087		2246		2157		2061		2037		1901		1800		1767		1672	
Toatl		39.2		115.9		117.9		158.2		355.4		240.6		237.4		96.9		234.7		51.0		191.7		23.5

Month, Calendar Day	Jan.		Feb.		Mar.		Apr.		May		June		July		Aug.		Sep.		Oct.		Nov.		Dec.	
	Head (mm)	Pre. (mm)	Head (mm)	Pre. (mm)	Head (mm)	Pre. (mm)	Head (mm)	Pre. (mm)	Head (mm)	Pre. (mm)	Head (mm)	Pre. (mm)	Head (mm)	Pre. (mm)	Head (mm)	Pre. (mm)	Head (mm)	Pre. (mm)	Head (mm)	Pre. (mm)	Head (mm)	Pre. (mm)	Head (mm)	Pre (mm)
1	1635		1575	14.2	1555	11.2	1580		1575	15.2	1610	14.1	2085	6.0	2395	14.0	1975	64.2	2330	5.0	2145		1860	
2	1630		1576		1570	22.4	1580		1575		1630	1.9	2080		2380	23.0	2140	14.9	2335	28.5	2125		1860	
3	1620	8.4	1572		1485		1580	10.0	1570		1635		2075		2385	1.8	2115	112.5	2345	7.0	2105		1845	1.6
4	1628		1578		1575		1570		1585		1635		2065		2320	9.0	2240	26.4	2325		2085		1850	2.8
5	1628		1575		1580	32.4	1580		1575	4.5	1635		2085		2300	46.6	2235		2215		2085		1840	
6	1613		1565		1610		1580		1570		1630	11.0	2095	28.9	2315		2305	15.0	2282		2070		1830	5.6
7	1615		1570	10.7	1580		1580	7.0	1565		1625	0.2	2125		2265		2330		2260	18.1	2030		1840	
8	1607	4.9	1555		1587		1587	2.0	1570	4.3	1620		2120		2225		2365	12.5	2280	92.0	2040		1835	
9	1612		1555	5.0	1585	3.5	1575	18.5	1575		1605		2110		2205		2365		2405	49.8	2025		1815	2.5
10	1605		1545		1575		1600	9.7	1575	6.0	1610		2100		2185		2365	1.2	2420	35.7	2015		1810	0.8
11	1615		1530		1570		1610		1590	12.8	1630	25.5	2120	61.3	2155		2325	17.2	2430	2.0	2020		1800	
12	1600		1585		1575		1608		1600		1655	127.1	2180	116.0	2155		2330	1.3	2405		2000		1795	
13	1599		1530		1580	3.5	1580		1585	4.0	1805	99.5	2330	13.8	2155		2325	9.8	2410		1985	3.5	1804	9.0
14	1600		1560		1580	27.0	1583		1590	7.0	1865	1.5	2285	115.0	2135	6.7	2360	3.8	3415		1985	10.0	1800	
15	1602		1585		1610		1587		1590		1815	69.0	2405		2125		2310		2420		2000		1788	
16	1595		1549		1585		1590		1600		1925	23.5	2420	57.0	2120		2275	54.1	2395		1985	3.5	1778	45.2
17	1595		1551		1585		1570		1605		1935	20.4	2500	65.1	2075		2420	62.2	2280	7.5	1960		1850	2.4
18	1585		1552		1585		1585	10.5	1600		1980	20.0	2510		2060		2320		2380	32.5	1955		1820	0.3
19		0.5	1550		1570	3.5	1585	4.0	1585	13.5	1995		2535	1.9	2045		2365		2404	0.5	1925		1795	
20	1585		1530		1560	1.2	1592		1600	13.9	2005		2555	59.0	2020		2360		2400	5.0	1930		1800	
21	1590		1530	16.5	1575		1580		1620	68.5	2030		2660	1.7	2015		2360	40.9	2345	1.5	1930	22.5	1782	14.0
22	1585		1545		1570	34.2	1575		1675	2.7	2040		2565		2000		2410	7.5	2345	7.5	1940		1820	40.4
23	1575		1530		1615		1585		1650		2055	31.6	2525		1980		2400		2310		1920		1855	
24	1580		1545	22.6	1625		1590		1645		2085	3.2	2510		1975		2395		2290		1915		1825	
25	1580		1550		1595		1580		1630		2060		2485		1960		2395		2255		1915		1880	
26	1570		1555		1590		1575		1630		2055	0.5	2460		1945	100.6	2350	4.3	2245		1900	8.5	1800	
27			1540		1590		1575		1635	2.0	2040	27.0	2435		2160	14.2	2350	46.2	2225		1905		1800	
28	1575		1550		1600		1570		1620		2075	10.5	2400		2030	5.2	2405		2200		1900		1810	
29	1565				1595		1530		1620		2045	50.0	2470		1990	12.7	2365	1.9	2185	10.0	1875		1790	
30	1575				1615		1555	2.6	1620		2115	19.0	2460		1975	16.0	2345	7.6	2195	1.3	1870		1793	4.7
31	1570				1585				1620				2420		1965	34.6			2165				1790	
Mean	1598		1555		1582		1581		1600		1848		2327		2129		2321		2319		1985		1815	
Toatl		13.8		69.0		189.9		64.3		154.4		555.5		525.7		284.4		503.5		303.9		48.0		129.3

Month / Observation Day	Jan.		Feb.		Mar.		Apr.		May		June		July		Aug.		Sep.		Oct.		Nov.		Dec.	
	Head (mm)	Pre. (mm)	Head (mm)	Pre. (mm)	Head (mm)	Pre. (mm)	Head (mm)	Pre. (mm)	Head (mm)	Pre. (mm)	Head (mm)	Pre. (mm)	Head (mm)	Pre. (mm)	Head (mm)	Pre. (mm)	Head (mm)	Pre. (mm)	Head (mm)	Pre. (mm)	Head (mm)	Pre. (mm)	Head (mm)	Pre. (mm)
1	1779		1722		1715	8.4	1918		2178	134.0	2100	1.0	—	1.0	2071		1804		1772		—		1560	27.0
2	1772	7.1	1715		1716	26.9	1915		2415	7.4	2017	2.8	2383	9.5	2058		1790	1.8	1775		—		1600	4.2
3	1775	9.0	1702		1759		1910	49.0	2343		2103	17.2	2375	23.4	2039		1775	49.0	1775	9.7	1645	5.5	1605	
4	1785		1685		1740		2010		2365	7.3	2090		2375		2030	7.2	—		1777		1635	4.5	1565	
5	1770		1697	32.6	1750	16.4	1975	60.3	2405		2063		2387		2040		1801		1773		1630	4.7	1560	3.4
6	1765	0.3	1743		1770		2048		2380		2034		2299	1.4	2015		1783		1765	24.3	1635		1560	
7	1770		1723		1759		2010		2382	32.8	2018	1.3	2261	67.6	2006		1760		1790		—		1555	8.5
8	1761		1725		1785		2005		2405		2013	20.6	2352	77.4	1893	8.5	1750		1780		1630		1570	8.4
9	1763		1714		1735	7.0	2020		2385		2031	21.7	2321	5.9	1971		1740		1775		1620		1570	2.5
10	1746		1702		1755	27.0	2015	8.5	2362		2063	31.8	2288		1963	9.0	1732		1775	24.0	1615		1560	
11	1735		1695		1755	2.0	2035	5.8	2320	6.4	2055		2256		1965		1722		1798		1610		1560	
12	1745		1702		1760	18.0	2041		2319	148.2	2022		2261		1930		1713	11.7	1797		1600		1560	
13	1739	0.3	1700		1763		2027		2575		2009		2234		1912		1721	27.8	1780		1605		1555	
14	1745	3.5	1699		1773	11.5	2025		2484		2003		2249		1899		1736		1778		1595		1550	7.3
15	1740		1695		1785		2017		2440		1990	220.0	2237		1880		1720		1760		1595		1555	
16	1727	0.9	1699		1785	13.0	1990	45.5	2420		2589	37.5	2218		1880		1710		1757		1590		1545	
17	1730		1675	1.7	1800	24.8	2049	7.0	2397	13.0	2289		2208		1880		1710	18.0	1745		1600		1545	
18	1721		1688		1860	45.6	2030		2405		2238	0.6	2200		1850		1723		1738		1585		1535	
19	1720	0.2	1684		1900		1995		2375		2299	33.9	2193		1860	4.9	1695		1730		—		1523	
20	1727	17.8	1689		1860		1984	20.5	2348	3.9	2345	17.9	2181		1842	2.6	1685		1715		—		1519	
21	1744	3.5	1677		1845		2000		2329		2347	103.3	2169		1845		1682		1722		—		1545	
22	1727		1670		1862	21.8	1983	3.0	2295		2589	17.2	2149	6.5	1840	32.2	1665	1.8	1715		—		1505	1.2
23	1717		1658		1903	8.6	1970	54.2	2261		2452	0.4	2131		1844	25.3	1670	0.4	1710		1570		1550	
24	1723		1667	41.0	1897		2025	91.8	2245	20.2	2473		2130		1861	11.0	1662	23.0	1707		1565		1592	9.2
25	1723	0.7	1714		1890		2143		2260	2.6	2483	7.6	—		1855	4.8	1675	50.4	1685		1570		1601	
26	1720	15.9	1689	6.0	1900		2100		2240		2481	1.2	2108		1854	32.3	1745	15.2	1675		1560	33.5	1590	77.9
27	1733	9.0	1695	8.6	1903	4.5	2095		2192		2460	0.6	2090		1851	6.0	1753	63.0	1677		1625	6.6	1780	1.2
28	1726	13.5	1695	22.2	1910	32.2	2100	34.2	2180		2467		2080	28.4	1823		1825	2.8	1666		—		1700	1.7
29	1735	1.8			1940		2168		2145		2453		2068	26.8	1802		1807		1663		—		1685	
30	1724				1935		2145	23.6	2130		2428		2125	4.0	—		1790		—		1560		1670	
31	1720	4.2			1935				2120				2080		1797	17.4			—		—		1665	18.0
Mean	1742		1697		1819		2025		2326		2236		2220		1912		1736		1744		1602		1581	
Total		87.7		115.1		267.7		403.4		375.8		536.6		251.9		161.5		264.9		58.0		54.8		169.6

Month / Observation Day	Jan.		Feb.		Mar.		Apr.		May		June		July		Aug.		Sep.		Oct.		Nov.		Dec.	
	Head (mm)	Pre. (mm)	Head (mm)	Pre. (mm)	Head (mm)	Pre. (mm)	Head (mm)	Pre. (mm)	Head (mm)	Pre. (mm)	Head (mm)	Pre. (mm)	Head (mm)	Pre. (mm)	Head (mm)	Pre. (mm)	Head (mm)	Pre. (mm)	Head (mm)	Pre. (mm)	Head (mm)	Pre. (mm)	Head (mm)	Pre. (mm)
1	1685		1620	2.8	1430	1.6	1415	36.0	1395	5.0	1575	5.1	2245		1925	15.5	1585	1.4	1655		1315		1180	30.8
2	1660		1625		1535		1520		1375	49.0	1575		2185	1.7	1905		1535	16.0	1650	3.4	1295		1025	
3	1645		1654		1525		1475		1485	0.1	1520		2155		1875		1575		1610		1285		1125	
4	1620	26.1	1575		1505		1495		1435	1.0	1505		2155	0.5	1875		1555		1595		1285		1125	
5	1665		1555		1515	0.8	1475		1435		1525		1930	2.0	1855		1525		1550	0.5	1270		1190	
6	1655	2.8	1555		1510		1475		1435	37.4	1490	11.5	1940		1935		1590		1555		1270		1180	
7	1645		1555		1505		1445	0.2	1520	63.5	1535		1960		1825	5.0	1500		1560		1280		1185	9.1
8	1660		1565		1505		1445	0.4	1630		1545		1975	24.5	1825	72.2	1500	20.5	1555	0.5	1275		1195	0.4
9	1620		1550		1480		1445		1585		1525	32.9	2085	22.6	1945	1.3	1515	0.6	1555	10.0	1290		1200	26.5
10	1605	58.5	1545		1465	0.6	1435		1575	41.8	1515	4.0	1860	0.5	1905		1505	0.2	1565		1270		1235	1.0
11	1740		1540	1.2	1470		1435		1555	0.7	1550	2.5	2085		1825		1500	33.0	1555		1255		1235	
12	1715		1530		1470		1415		1735		1520		2025	0.4	1800		1555	2.5	1535		1225		1215	
13	1695		1525	19.1	1470		1415		1635		1465		2005	3.8	1770		1525	0.8	1520		1225		1215	
14	1690		1555	13.7	1470	0.6	1415		1610		1545	31.2	1995	1.2	1750		1585		1515	0.5	1225		1200	
15	1665		1555		1470	9.3	1405		1595		1630	5.0	1935	14.0	1725	5.0	1575		1500	4.1	1225		1205	0.4
16	1645		1560		1465		1405		1580	2.0	1590		1945	22.6	1735	0.5	1575		1500	1.8	1225		1200	21.2
17	1665	17.8	1540		1455		1385		1595	23.7	1570		1965		1715		1560		1500		1225		1220	9.0
18	1655		1525		1455		1380		1575		1565		1925	85.7	1695	18.4	1550		1485	3.4	1225	1.4	1225	
19	1630		1510		1455	2.5	1375	6.2	1585		1585		1995	19.9	1715	8.6	1535		1485	8.6	1215	0.4	1215	
20	1640		1520		1430	32.3	1395	13.0	1565		1540	2.6	1995	21.3	1700		1480	1.4	1465		1215		1215	
21	1625		1505		1485		1415		1585		1540	48.2	1985	60.5	1655		1615		1475		1205	0.2	1215	0.4
22	1615	6.0	1450		1455		1405		1620		1655	31.5	2085	19.6	1635		1645		1485		1195	0.6	1220	
23	1620	13.0	1445		1435		1385		1575		1655	148.5	2010		1620		1560		1385		1195		1210	
24	1620	5.9	1440		1445	5.0	1380		1570	45.5	2040	63.5	1965		1610	21.4	1550		1355	1.0	1195		1215	
25	1615	2.0	1485	1.0	1445		1380		1635	11.5	2000	1.0	2005		1630		1555		1355	6.0	925		1205	
26	1615		1485		1425		1375		1670		1985	38.8	2015	1.3	1615		1650		1355	2.0	880		1200	
27	1605	0.5	1475		1415		1375	32.0	1625		2034	40.3	1995	4.0	1590	30.0	1700	2.1	1340	12.7	1165		1200	64.0
28	1610		1475		1405	21.5	1425		1580		2119	34.5	1985		1575	2.5	1665	32.2	1325		1160	2.5	1280	
29	1610				1435	0.6	1400		1590		2125	19.0	1985		1555		1655		1320		1175	27.5	1285	
30	1605				1435		1395		1595	5.9	2115	61.7	1950	0.6	1555	21.4	1655		1320		1175		1250	
31	1620				1435				1570				1935		1500				1320	0.2			1255	13.0
Mean	1644		1532		1466		1420		1568		1670		2011		1737		1567		1482		1212		1204	
Toatl		132.6		37.8		74.8		87.8		287.1		576.8		306.7		201.8		110.7		48.7		38.6		175.8

Month and day	Jan.		Feb.		Mar.		Apr.		May		June		July		Aug.		Sep.		Oct.		Nov.		Dec.	
	Head mm	Pre. mm	Head mm	Pre. mm	Head mm	Pre. mm	Head mm	Pre. mm	Head mm	Pre. mm	Head mm	Pre. mm	Head mm	Pre. mm	Head mm	Pre. mm	Head mm	Pre. mm	Head mm	Pre. mm	Head mm	Pre. mm	Head mm	Pre. mm
1	1260	0.8	1225	13.6	1180		1270	12.6	1245		1595	9.2	1735	49.2	1885		1545	16.0	1520		1400		1290	
2	1255	1.4	1230		1180		1280	1.2	1260	67.4	1565		1725	53.6	1865	17.0	1540	0.2	1510		1325		1300	0.7
3	1245		1215		1180		1270	2.1	1370	49.6	1520		1735	86.6	1820		1530		1510	1.0	1335	12.5	1295	
4	1230		1205		1175		1270		1460		1485		1985		1820	6.7	1520		1505		1400		1290	
5	1235	7.1	1205		1180		1265		1450		1455		1900	56.3	1800	20.5	1515	0.2	1505	21.4	1400	4.2	1285	12.6
6	1235		1180		1175	25.3	1245		1430	10.1	1435		2055	2.9	1810	5.2	1520	7.1	1515		1390		1310	31.0
7	1235		1185		1280		1245		1425	0.7	1415		1995	48.9	1780		1525	2.3	1505		1390		1340	
8	1220	9.1	1180		1175		1240		1420	25.1	1405		2080	76.3	1755		1535	6.3	1495		1375		1330	
9	1245		1180		1175		1235		1420		1400		2195	21.2	1785		1545		1485	26.5	1365	0.4	1325	5.0
10	1230		1180	4.1	1175	28.5	1230	19.1	1360	61.0	1395		2165	11.3	1710		1545	28.2	1525		1365		1325	
11	1225		1190		1225		1230		1525		1385		2170	37.5	1685		1560	21.6	1495		1360		1310	
12	1225		1170		1205	9.0	1230	3.1	1470		1360		2225	37.4	1630		1620	22.9	1495		1360		1315	
13	1225	25.8	1170	49.0	1205	56.7	1225		1445		1365	63.6	2210	39.0	1650		1635		1485		1345		1315	0.5
14	1250	2.0	1225		1215	17.5	1285	43.0	1425		1455	45.9	2250	28.0	1625		1625		1495	0.5	1345		1315	7.7
15	1250		1230	7.5	1285	5.2	1285	2.2	1405		1485		2250	1.9	1605	0.9	1625		1475		1335	2.6	1315	
16	1250	10.6	1250		1340	13.5	1285		1420		1465		2250	20.1	1585	2.6	1615		1475		1305	0.3	1200	
17	1235		1230		1345	1.6	1270		1415		1450		2220	1.0	1565		1585		1465		1325		1325	
18	1230		1225	0.6	1335		1245		1415		1425		2105	4.8	1550		1550		1445		1325	4.4	1290	2.1
19	1235		1225		1295	6.6	1245	2.5	1405		1425	1.0	2185	33.7	1530		1530		1435		1340		1300	
20	1235		1215	21.5	1340	22.6	1240	6.8	1400		1420		2185	4.6	1520		1555	18.9	1422	5.4	1300		1290	47.3
21	1230		1250	1.0	1565	1.6	1245	13.0	1405	1.0	1400		2145	15.3	1585		1555	0.8	1435		1305		1385	2.3
22	1220		1230		1555	0.7	1250	0.4	1400	0.2	1415		2135	34.1	1508	1.9	1485	14.1	1425		1305		1360	10.6
23	1225	7.3	1215		1345		1260		1400		1405		2165	3.8	1485		1545	27.7	1425		1320	8.0	1355	6.5
24	1235		1215		1325		1260		1390	6.1	1405		2115	0.4	1475		1585		1415	1.1	1315	17.8	1360	30.8
25	1225		1210		1325		1240	8.8	1390		1405	63.0	2005		1455	64.9	1535	7.0	1410		1325		1400	21.4
26	1215		1205		1320		1250	27.9	1375		1538	48.2	2015		1535	20.7	1535	19.0	1405		1315	2.4	1445	8.2
27	1205		1200	8.2	1300		1290	0.2	1365		1585	13.7	2005		1530	88.9	1575		1385		1310		1480	0.8
28	1205	0.2	1200	0.2	1300		1275		1360		1550		1955		1685	5.9	1555		1380	5.0	1300		1430	
29	1200		1200		1310		1250		1360		1525		1925		1650		1535		1385	34.2	1295		1410	
30	1205				1280		1250		1340		1520	93.2	1895		1625				1435		1295		1395	6.8
31	1195	14.5			1270				1335	109.4			1885		1575				1410				1400	42.0
Mean	1229		1209		1277		1254		1396		1455		2060		1651		1559		1430		1340		1338	
Total		78.8		105.7		188.8		142.9		330.6		340.9		667.9		236.1		202.8		95.1		52.6		236.0

Month / Observation day	Jan.		Feb.		Mar.		Apr.		May		June		July		Aug.		Sep.		Oct.		Nov.		Dec.	
	Head	Pre.	Head	Pre.	Head	Pre.	Head	Pre.	Head	Pre.	Head	Pre.	Head	Pre.	Head	Pre.	Head	Pre.	Head	Pre.	Head	Pre.	Head	Pre.
	mm	mm	mm	mm	mm	mm	mm	mm	mm	mm	mm	mm	mm	mm	mm	mm	(mm)	mm	(mm)	(mm)	(mm)	(mm)	mm	(mm)
1	1530	32.0	1350	21.0	1385	2.8	1490		1493	0.1	1795	5.1	2395	38.6	2135	40.8	2045		1828	7.3	1515		1435	0.1
2	1495	7.2	1385	0.3	1370		1475	1.4	1490	1.0	1795	3.9	2405	80.9	2155	0.5	2030		1765	0.8	1510		1425	20.6
3	1460	21.2	1375	4.2	1360		1480	9.4	1445		1780	1.0	2429	0.4	2120	0.5	2005		1715	16.8	1494	19.6	1450	0.1
4	1500		1370		1360	39.6	1480		1410		1770		2342	112.7	2105	3.9	2030	4.9	1710	56.0	1513	48.7	1430	
5	1485		1360		1425	1.1	1465	6.0	1415	19.7	1745		2637	161.5	2075		1984		1810	57.6	1585		1419	
6	1485		1365	0.6	1400	1.0	1455	0.3	1445		1720	39.6	2851	1.3	2055	0.8	1930		1905	0.1	1570		1495	
7	1470		1350		1395		1460		1425		1790	31.0	2655	7.5	2030		1940		1850		1540	2.2	1405	
8	1465		1345		1380	8.3	1435		1440		1805	4.2	2309	0.2	2015		1927		1770	1.0	1535	37.6	1400	
9	1455		1340		1385	0.8	1425		1405		1770		2534	17.8	1995		1905	3.0	1830	1.8	1585	0.7	1393	
10	1445		1335		1385	66.7	1425	10.0	1395		1740		2487	98.1	1895		1905	4.8	1825		1545		1395	17.0
11	1445		1330	28.8	1405		1430		1390	5.4	1735		2656	5.2	1965		1907	0.3	1795		1545	21.3	1408	
12	1445	0.8	1380	5.3	1475		1400		1405	31.3	1700		2524		1940	31.6	1873		1795	0.1	1570	1.5	1400	
13	1445		1370	6.8	1465	34.3	1400	0.4	1445	9.8	1695		2430		1970	40.8	1855		1785	0.4	1570	6.6	1395	3.6
14	1440	3.5	1380	5.2	1520	38.7	1390		1440		1690		2429		2010	6.9	1828	0.2	1770		1535		1388	
15	1440		1375	4.3	1575	2.6	1385	1.2	1425		1680	69.7	2874	0.1	1998	45.1	1819	27.2	1760	0.4	1515		1389	
16	1430		1360		1555		1380		1405		1835	1.2	2324	2.3	2162	117.6	1829		1740		1505	1.3	1383	0.2
17	1430		1360	1.8	1550	14.8	1370	0.5	1405	6.1	1735	3.8	2356	45.1	2247	68.7	1800		1730		1480		1380	
18	1425	5.4	1360		1570		1370	15.2	1415		1705	149.8	2421	83.2	2253	10.9	1790	2.5	1720	3.3	1475		1370	
19	1415	2.2	1335	2.0	1555		1385	0.1	1410	127.6	2115	8.8	2481		2168	0.2	1779	18.4	1715		1460		1365	4.8
20	1405		1345	2.1	1565	11.9	1375		1730		2015	58.7	2416	1.6	2100		1800	12.6	1705		1450		1375	47.0
21	1400		1345	3.9	1580		1365		1600		2195	20.9	2385		2080	31.1	1795	3.7	1680	0.3	1360	6.8	1460	
22	1395		1340	34.1	1460		1350	15.4	1585	114.2	2140	9.0	2369		2114	26.7	1665	2.8	1665	4.5	1451	15.5	1429	0.2
23	1385		1395		1570		1350	6.8	1840	12.0	2080		2346		2125	5.7	1841	1.3	1655		1469	0.5	1410	24.1
24	1370		1370	22.5	1570		1365		1785	8.5	2040		2314	1.1	2180		1638		1640		1435		1464	
25	1370		1425	0.9	1550	2.5	1360	1.4	1750		2035		2288	3.1	2087	32.4	1620		1695		1430	0.7	1415	
26	1385		1410		1540	7.0	1360	81.1	1735		2005	16.0	2275	0.5	2149	19.4	1630	2.6	1625	14.8	1419	0.5	1405	23.2
27	1395	0.2	1410	0.2	1540	0.2	1510	0.3	1750	16.9	2060	7.3	2265		2115	19.6	1614	0.3	1630		1425	1.0	1459	0.8
28	1355		1385		1525		1460		1935	1.4	2035	64.3	2237		2125	0.1	1590		1601	0.9	1415		1442	0.5
29	1345	23.2			1520		1440		1830	4.8	2105	104.7	2205		2105		1585	2.3	1595	0.2	1410		1420	0.5
30	1380				1510		1425	36.6	1820		2335	41.9	2185	11.9	2074	0.4	1575	120.2	1570	0.1	1410	16.0	1415	19.1
31	1365	3.2			1500	0.9			1810	0.4			2185	2.5	2067	1.5			1550				1440	34.8
Mean	1426		1366		1482		1415		1559		1889		2413		2082		1811		1722		1491		1412	
Total		98.9		144.0		233.2		186.1		389.2		639.2		676.6		496.2		207.1		166.4		180.5		196.6

Table 2 Monthly Value

Hydrostatic Head (mm)

year / Month	1942	1943	1944	1945	1946	1947	1948	1949	Mean (1943—1949)
1	—	2374	2201	1598	1742	1644	1229	1426	1745
2	—	2320	2113	1555	1697	1532	1209	1366	1685
3	—	2287	2077	1552	1819	1466	1277	1482	1713
4	2613	2293	2087	1581	2025	1420	1254	1415	1725
5	2618	2351	2246	1800	2326	1568	1396	1559	1864
6	2894	2865	2157	1848	2236	1670	1455	1889	2017
7	3016	2920	2061	2327	2220	2011	2060	2413	2287
8	2655	2849	2037	2129	1912	1737	1651	2082	2057
9	2652	2642	1901	2321	1736	1567	1559	1811	1934
10	2642	2668	1800	2319	1744	1482	1460	1722	1885
11	2496	2481	1767	1985	1602	1212	1340	1491	1697
12	2402	2366	1672	1815	1581	1204	1338	1412	1627
Mean	2665	2535	2010	1888	1887	1543	1436	1672	1853

Atmospheric Pressure (+700mm)

year / Month	1942	1943	1944	1945	1946	1947	1948	Mean (1943—1948)
1	18.94	20.07	21.09	18.44	19.96	19.04	19.45	19.68
2	18.90	19.65	18.67	18.35	19.01	17.93	18.66	18.71
3	18.94	16.13	16.55	19.90	19.02	18.80	18.86	18.18
4	18.17	17.75	15.90	16.81	17.14	16.44	16.80	16.81
5	14.25	15.32	15.27	18.26	14.79	15.05	15.72	14.90
6	12.79	13.08	13.35	13.05	14.25	13.18	12.50	13.24
7	14.53	12.94	15.03	12.67	12.26	14.64	14.50	13.67
8	12.67	14.29	15.21	15.31	12.80	17.13	13.28	14.69
9	15.51	15.87	15.28	18.14	15.61	15.30	16.52	16.12
10	18.46	18.16	18.52	17.96	19.39	19.09	19.11	18.71
11	19.86	20.35	18.25	19.48	19.25	20.97	21.74	20.01
12	19.08	22.02	19.76	18.63	18.82	20.83	20.47	20.09
Mean	16.84	17.14	16.91	16.83	16.86	17.35	17.31	17.07

Precipitation (mm)

year / Month	1942	1943	1944	1945	1946	1947	1948	1949	Mean (1943—1949)
1	81.2	23.3	37.9	13.4	84.9	128.3	76.3	95.7	65.7
2	84.2	115.8	119.9	73.9	123.3	40.5	109.3	154.3	105.3
3	247.0	71.3	114.1	135.4	259.1	72.4	182.7	225.7	151.5
4	201.4	148.7	158.2	64.3	403.4	87.8	142.9	186.1	170.2
5	199.9	400.9	343.9	149.4	363.7	277.8	319.9	376.6	318.9
6	863.3	384.5	240.6	555.5	536.6	576.8	340.9	639.2	467.7
7	225.6	602.8	229.7	508.6	243.8	296.8	645.4	654.8	454.7
8	382.9	118.1	93.7	275.2	156.3	195.3	228.5	480.2	221.0
9	277.2	457.4	234.7	503.5	264.9	110.7	202.3	207.1	282.9
10	128.9	62.8	49.4	294.1	56.1	47.1	92.0	161.0	108.9
11	32.2	125.4	191.7	48.0	54.8	38.6	52.6	180.5	98.8
12	34.0	57.4	22.7	125.1	164.1	170.1	229.0	190.3	137.0
Total	2757.8	2568.4	1836.5	2746.4	2711.0	2042.2	2622.8	3551.5	2582.6
Mean	229.8	214.0	153.0	228.9	225.9	170.2	218.6	296.0	215.2

$$H = H_0 e^{-\lambda t}$$

Using the observed data, the writer determined the value of constants H_0 and λ, and got

$$H = 2335\, e^{-0.0823t} \quad \cdots\cdots (1)$$

provided that $t = 0$ is the year of 1943.

From (1) the value of H is calculated and represented by the broken line in Fig. 3. It may be said that the diagram of calculated H illustrates the natural fall of hydrostatic head in case when both precipitation and atmospheric pressure are uniform throughout the years. Main causes of variation of hydrostattic head are as follows;

〔I〕 internal causes

(1) variation in pressure which acts on the virgin water of hot spring

(2) decrepitude of installation, etc.

〔II〕 external causes

(1) amount of precipitation

(2) variation in atmospheric pressure.

Internal causes except the variation in volcanic activity and accidental events (earthquake, etc.) should have influence on the hydrostatic head as natural fall, therefore the natural fall above doscribed may be calculated by using the equation (1). The natural fall of head per month (mm/month) in each year is calculalated and given in Table 3.

Table 3 Natural Fall of Hydrostatic Head

year	1942	1943	1944	1945	1946	1947	1948	1949	Mean (1943–1949)
Fall $\left(\frac{\text{mm}}{\text{Month}}\right)$	17	16	15	14	13	12	11	10	13

In general the hot water from a hot spring originates part in virgin water and part in precipitaation. In a case when assumed that atmospheric presessure does not change, the writer will temporally call the part of hydrostatic head due to internal causes except variation in volcanic activity and accidental events the "virgin water head". In the present case, the virgin water head will go down in the rate which the equation (1) shows, namely in the rate Table 3 shows.

3. Effects of Atmospheric Pressure and Precipitation on the Hydrostatic Head

It may be determined, the effect of change in atmospheric pessure upon the hydrostatic head, from the relation between the variation of head and the change in atmospheric pressure in no-precipitation day. Fig. 4 is the diagram of observed result on 1st-2nd May 1942

at Uchinomaki. Using several odserved results analogous to the above descrived one, the writer calculated the effect of change in atmospheric pressure on the variation of hydrostatic head. The result is

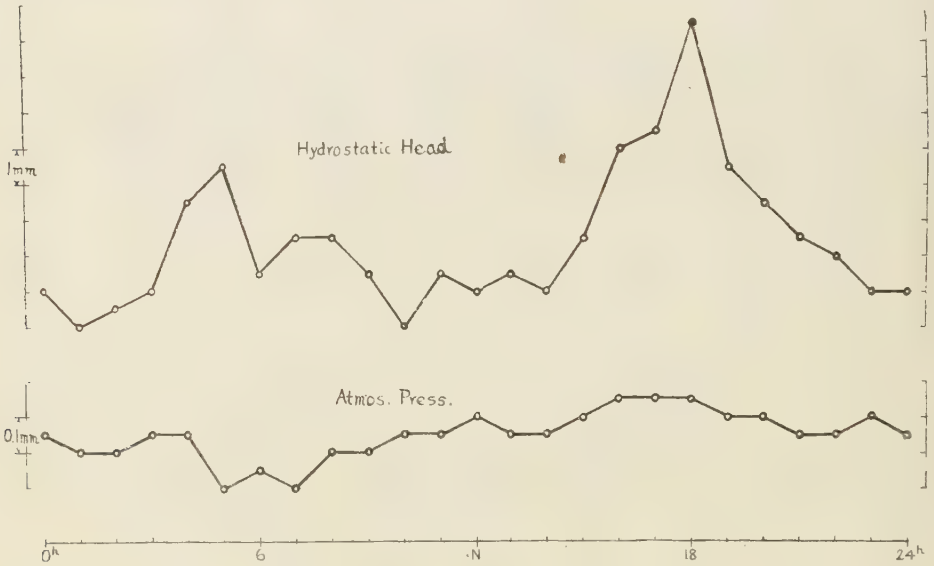

Fig. 4 Variation of the Hydrostatic Head and Atmospheric Pressure (May 1~2, 1942)

$$\frac{\partial H}{\partial p} = -14\left(\frac{mm}{mm}\right)$$

the writer will call it the "coefficient of effect of atmospheric pressure".

Next, to estimate the effect of precipitation on the hydrostatic head, the writer picked up such cases when the monthly precipitation and the monthly mean head have a regular tendency in variation from the Table 2, and calculated the effect of precipitation. The results are tabulated in Table 4, the mean valuee 0.7 is the approximate value of the coefficient of effect of precipitation.

Let H be the head in a month, H′ ditto in the nextmonth, then we get approximately

$$H = V + N - 14 \cdot \Delta p \quad \cdots\cdots (2)$$

$$H' = V' + Ne^{-\mu} - 14 \cdot \Delta p' + 0.7W'$$

where N = effect of precipitaion untill the month above described

V = virgin water head in the month above described

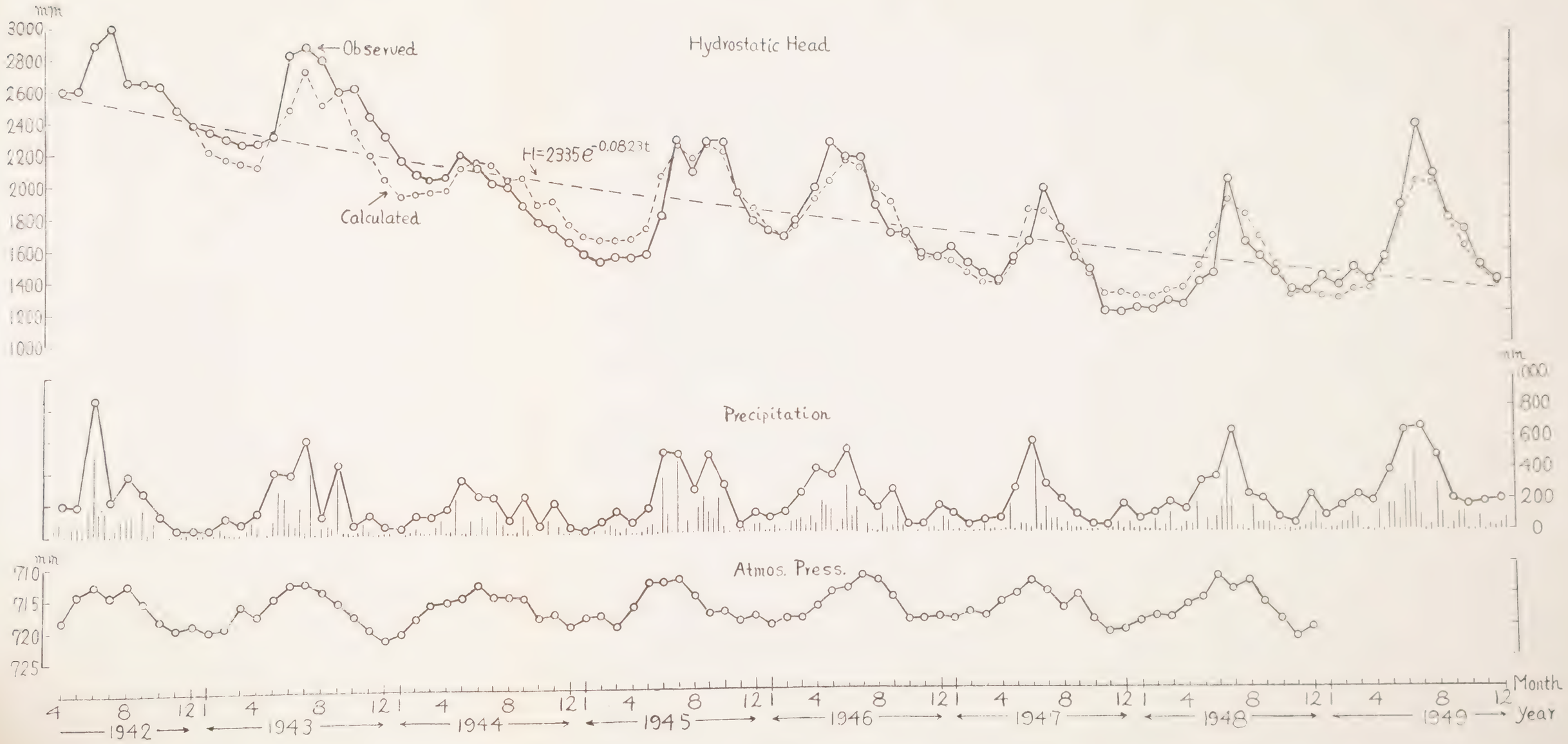
m/m
3000
2800
2600
2400
2200
2000
1800
1600
1400
1200
1000
Observed
Hydrostatic Head
H=2335e^-0.0823t
Calculated
m/m
1000
800
600
400
200
0
Precipitation
m/m
710
715
720
725
Atmos. Press.
Month
4 8 12 1 4 8 12 1 4 8 12 1 4 8 12 1 4 8 12 1 4 8 12 1 4 8 12
1942
1943
1944
1945
1946
1947
1948
1949
Year

Fig. 3

Table 4

year	Month	Head (Hmm)	ΔH	Precipitation (Wmm)	ΔW	$\frac{\Delta H}{\Delta W}$ (month^{-1})
1942	5	2618	276	199.9	663.4	0.42
	6	2894		863.3		
1944	4	2087	159	158.2	185.7	0.86
	5	2246		343.9		
1945	5	1600	248	149.4	406.1	0.61
	6	1848		555.5		
1947	4	1420	148	87.8	190.0	0.78
	5	1568		277.8		
					Mean	0.67 ~ 0.7

V' = ditto in the next month

Δp = deviation of atmospheric pressure in the month above described

$\Delta p'$ = ditto in the next month

W' = amount of precipitation in the next month

μ = decay constant of effect of precipitation (per month)

from (2) and (3) we obtain

$$\frac{H - V + 14\cdot\Delta p}{H' - V' + 14\cdot\Delta p' - 0.7W'} = e^{\mu} \quad \cdots\cdots (4)$$

If we have twe equations similar to (4), we can determine the value V and μ, using the observed values H, H, W, Δp. and $\Delta p'$. In order to make the error which results from the use of approximate value 0.7, small as possible, it is reasonable to make use of the case in which precipitation W' is comparatively small. So the writer used the data shown in Tabl 5 and got

V = 1524 mm (Nov. 1944)

μ = 0.34 (ppr moth).

Table 5

year	Month	Observed Head (Hmm)	Virgin Water Head (mm)	Precipitation (Wmm)	Deviation of Atm. Press. (Δp mm)
1944	11	1767	V		1.18
	12	1672	V−15	22.7	2.69
1947	1	1644	V−351		1.97
	2	1532	V−363	40.5	0.86

(Values of vergin water head are calculated, using Tble 3, assuming that the value in November 1944 is Vmm.)

4. Annual Variation of the Hydrostatic Head (1943-1949)

Making use of the virgin water head $V = 1524$ mm (Nov. 1944) and decay constant of effect of precipitation $\mu = 0.34$, the writer will study on the effects of the mean monthly precipitation and deviation of atmospheric pressure upon the mean monthly heads from 1943 to 1949. The effect of deviation of atmospheric pressure is as given in Table 6 (as stated before, the data of atmospheric pressure in 1949 are excluded, therefore the adopted value is the mean from 1943 to 1948).

Table 6

Month	1	2	3	4	5	6	7	8	9	10	11	12
Deviation of Atm. Press. (Δp mm)	2.61	1.64	1.11	−0.26	−2.17	−3.83	−3.40	−2.38	−0.95	1.64	2.94	3.02
Effect of Δp ($-14 \cdot \Delta p$ mm)	−37	−23	−16	4	30	54	48	33	13	−23	−41	−42

The mean monthly head may be written as follows:

the head in January

$$H_1 = V_1 + N_1 - 37$$

ditto in February

$$H_2 = V_2 + N_1 e^{-0.34} - 23 + \alpha W_2$$

ditto in March

$$H_3 = V_3 + N_1 e^{-0.34\times 2} - 16 + \alpha (W_3 + W_2 e^{-0.34}) \qquad \cdots\cdots (5)$$

ditto in the month of t

$$H_t = V_t + N_1 e^{-0.34(t-1)} - 14 \cdot \Delta p_t + \alpha \sum_{n=2}^{t} W_n e^{-0.34(t-n)}$$

where N_1 = effect of precipitation including that in January

V_t = virgin water head in the month of t

W_t = precipitation in the month of t

Δp_t = deviation of atmospheric pressure in the month of t

α = coefficient of effect of precipitation

Using Table 3, the writer obtained

$V_1 = 1352$ mm, $N_1 = 430$ mm.

The mean monthly values of observed head, virgin water head and precioitation from 1943 to 1949, and assumed head in case of no-precipitation from February onwards, effect of pre-

cipitation (H−assumed head) and calculated value of

$$\sum_{n=2}^{t} W_n e^{-0.34(t-n)}$$

are given in Table 7.

Table 7

t (Month)	1	2	3	4	5	6	7	8	9	10	11	12	
H (Observed)	1745	1685	1713	1725	1864	2017	2287	2057	1934	1885	1697	1627	
V_t	1352	1339	1326	1313	1300	1287	1274	1261	1248	1235	1222	1209	
$-14\Delta p_t$	−37	−23	−16	4	30	54	48	33	13	−23	−41	−42	
$N_1 e^{-0.34(t-1)}$	430	306	218	155	111	79	56	40	28	20	14	10	
Assumed Head $(V_t-\Delta p_t+N_1 e^{-0.34(t-1)})$	1745	1622	1528	1472	1441	1420	1378	1334	1289	1232	1195	1177	
Effect of Precipitation from Feb. onwards (H−Assumed Head)		63	185	253	423	597	909	723	645	653	502	450	Total 5403
W_t		105.3	151.5	170.2	318.9	467.7	454.7	221.0	282.9	108.9	98.8	137.0	
$\sum_{n=2}^{t} W_n e^{-0.34(t-n)}$		105.3	226.5	331.5	554.9	862.9	1069.0	982.0	982.2	808.1	674.2	616.9	7213.5
Celcnlated Head	1745	1701	1698	1720	1857	2066	2179	2070	2025	1887	1700	1639	

Effect of precipitation in the month of t must be equal to

$$\alpha \sum_{n=2}^{t} W_n e^{-0.34(t-n)}$$

therefore we get

$$\alpha = \frac{5403}{7213.5} = 0.749$$

This result shows it is proper that the writer has used the approximate value $\alpha = 0.7$ in article 3. Using, $\alpha = 0.749$, the values $H_1, H_2, \cdots H_t \cdots$ are calculated from equation (5) and shown in the last row in Table 7.

The calculated head and the observed head are shown in Fig. 5. It will be seen from the Table and Figure that the calculated value approximately agrees with the observed value. Comparatively large difference which appears in July may be partly attributed to the fact that precipitation was much at the end in June and at the beginning in July (see Table 8). Not only in Jnly but also in other months there appear some differences. These

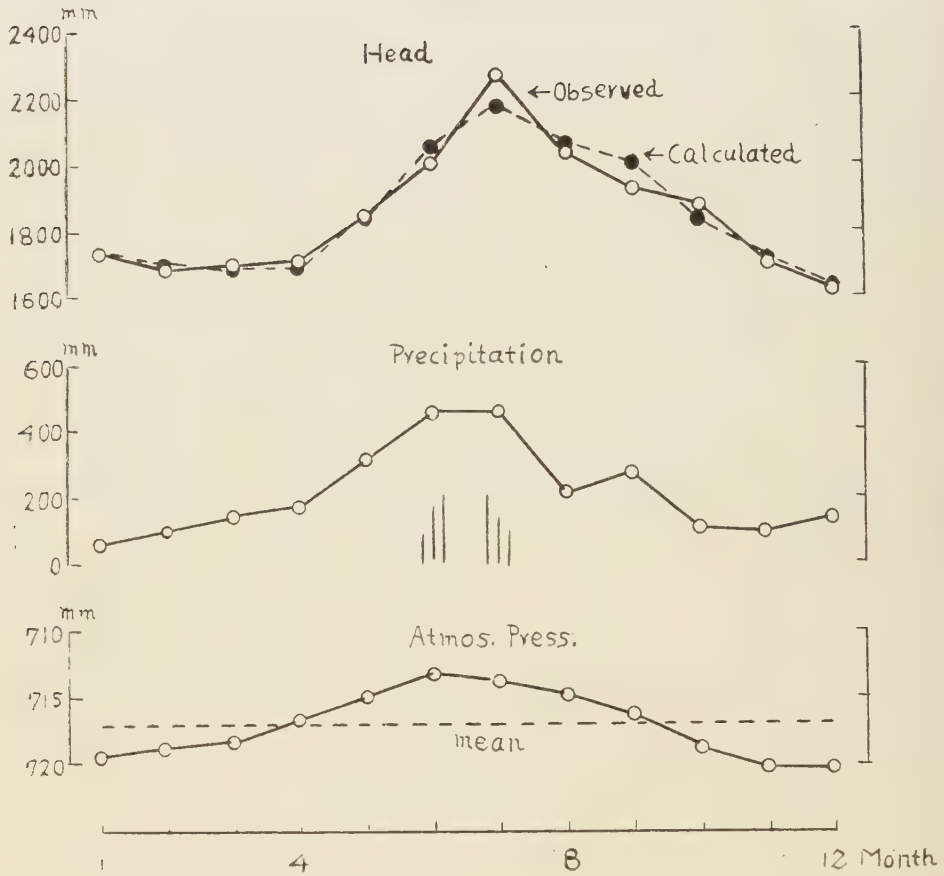

Fig. 5

differences may be related to the variation in the activity of Volcano Aso, which the writer left out of account. On that point he will study afterwards

Table 8 Mean Value of Amount of 10 Days Precipitatation

(1943-1949)

Month	June			July		
Term	1—10	11—20	21—30	1—10	11—20	21—30
Mean Precip. (mm)	88.1	176.8	202.8	207.2	149.0	113.6

5. Monthly Mean Values of Observed Head and Calculated Head (from January 1943 to December 1949)

Making use of $V = 1524$ mm (Nov. 1944), $\mu = 0.34$, $\alpha = 0.749$ and assuming that the observed head just agrees with the calculated head in December 1942, the writer calculated the values of head for every month from January 1943 to December 1949 (he used, in place of monthly value of atmospheric pressure in 1949, the mean monthly value from 1943 to 1948) and shows it in Table 9 and represents by the broken line in Fig. 3. The calculated head is in good accordance with the observed head. As similar to the preceeding article, the difference between the observed value and the calculated value may be attributed partly to the fact that precipitation was much at the beginning or the end in month, and partly to the variation in volcanic activity.

Table 9 Calculated Values of Hydrostatic Head (mm)

(1943-1949)

Month / year	1	2	3	4	5	6	7	8	9	10	11	12	Mean
1943	2231	2190	2168	2149	2368	2515	2759	2544	2632	2378	2231	2070	2353
1944	1966	1975	1977	1996	2146	2193	2171	2062	2087	1918	1953	1793	2018
1945	1715	1688	1689	1692	1771	2096	2292	2211	2307	2245	1990	1886	1965
1946	1756	1713	1772	1944	2048	2230	2161	2014	1954	1726	1598	1590	1876
1947	1547	1466	1407	1411	1550	1881	1866	1754	1600	1469	1334	1355	1558
1948	1315	1306	1339	1362	1501	1648	1918	1829	1688	1496	1318	1362	1507
1949	1291	1287	1332	1346	1508	1822	2032	2037	1824	1613	1482	1405	1582

6. True Virgin Water Head and Volcanic Activity

For every month from January 1943 to December 1949, the values

observed head − (*effect of precipitation* + *effect of atmospheric pressure*) ..... (6)

are calculated and given in Table 10.

Table 10 True Virgin Water Head (mm) and its Percentage (%)

Month / year	1	2	3	4	5	6	7	8	9	10	11	12	Mean (%)
1943	2008	1979	1952	1961	1784	2135	1930	2058	1747	2011	1955	1985	
	84.6	85.3	85.4	85.5	75.9	74.5	66.1	72.2	66.1	75.4	78.8	83.9	77.8
1944	1909	1797	1744	1720	1714	1563	1474	1544	1388	1421	1356	1388	
	86.7	85.0	84.0	82.4	76.3	72.5	71.5	75.8	72.0	78.9	76.7	83.0	78.7
1945	1378	1348	1360	1342	1268	1177	4146	1315	1397	1443	1350	1270	
	86.2	86.7	86.0	84.9	79.3	63.7	62.1	61.8	60.2	62.2	68.0	70.0	72.6
1946	1314	1299	1349	1370	1554	1269	1309	1135	1006	1229	1202	1176	
	75.4	76.5	74.2	67.7	66.8	56.8	59.0	59.4	57.9	70.5	75.0	74.4	67.8
1947	1270	1227	1208	1146	1143	902	1246	1072	984	1078	931	890	
	77.3	80.1	82.4	80.7	72.9	54.1	62.0	61.7	62.8	72.7	46.8	73.9	71.5
1948	944	922	946	889	881	782	1106	775	813	891	942	885	
	76.8	76.3	74.1	70.9	63.1	53.7	58.7	46.9	52.1	61.0	70.3	66.1	63.8
1949	1034	968	1029	93.8	910	916	1220	874	806	918	808	796	
	72.5	70.9	69.4	66.3	58.4	48.5	50.6	42.0	44.5	53.3	54.2	56.4	57.3

Mean 69.9 .70

The value defined by the expression (6) may be regarded as head due to internal causes which include the variation in volcanic activity, etc. In order to distinguish it from the virgin water head which the writer temporally has called so in article 2, he will call it the "true virgin water head". The rate of the true virgin water head to the observed head and its yearly mean are as given in Table 10, in percentage. The yearly mean and numbers of explosion in Volcano Aso are shown in Fig. 6 [2]. From Fig. 6, it may be seen that if thers is a year in which the percentage of true virgin water head is smaller than 75%, the volcanic activity increases in the following year. In other words, if there is a year in which the rate of the true virgin water head to the observed head is less than 3/4, Volcano Aso has a tendency to explode within one year. The writer already reported that volcanic activity depends upon the variation in atmospheric pressure and the precipitation [3]. Furthermore, it may be said that the variation of the hydrostatic head of hot spring offers a key to the problem of forecasting the volcanic activity. The procedure is as follows: in case of Uchinomaki Laboratory hot spring, first substituting the observed value and constants which the writer has determined in the expression (6), calculate the true virgin water head, next calculate the rate of it to the observed head, and then one may forecast the tendency of activity of Volcano Aso.

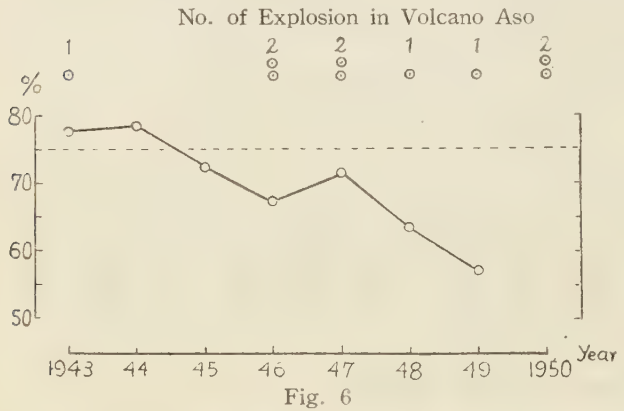

Fig. 6

7. Conclusion

The main points of the presnt studies are summarised as follows:

(1) The hydrostatic head of hot spring at Uchinomaki Laboratory, under the influences of precipitation and change in atmospheric pressure, is high in warm season and low in cold season. And as secular trend the head goes down in exponential fashion which may be written

$$H = H_0 e^{-\lambda t}$$ (t shows year)

(2) (a) 1 mm deviation of atmospheric pressure causes the fall of hydrostatic head about 14 mm. (b) W mm precipitation per month causes the rise of monthly mean hydrostatic head about 0.75W mm. (c) The effect of precipitation upon the head is not only seen

in the preseut month, but it remains in future. This after-effect decreases in exponenfial fashion, it may be written as follows

$$\alpha W e^{-\mu t}$$

where W = monthly precipitation, $\alpha = 0.749$, $\mu = 0.34$ and

t = months after the precipitation Wmm.

(3) The rate of the head due to virgin water which the writer has called the "true virgin water head" to the observed head is about 7/10 on an average.

(4) If there is a year in which the rate of the true virgin water head to the obscrved hesd is smaller than 3/4, Volcano Aso has a tendency to explode within a year. This tendency offers a key to the problem of forecasting the velcanic activity.

A part of the cost of this research was defrayed from the Scientific Reserch Expenditure of the Department of Education. In concluding this paper the writer wishes to exprss his hearty thanks to Dr. Namba for his kind advices and encouragement.

References

1. Nomitsu: Geophysics Vol. VI, No. 1 (1942) **1**
2. Kumamoto Weather Station: Disasters Occured in Kumamoto Prefecture, Oct. (1952) **166** And etc. (unpublished)
3. Namba and Murota: Kumamoto J. of Science Vol. 1, No. 1 (1952) **58**

DISTRIBUTION OF RADON IN CENTRAL KYUSHU (Part I)

Koichi KAKU

Introduction

In connection with the special characteristics of hot springs in this country, investigations on radon content have been carried on since the latter part of Meiji Era, and although more and more studies are being made recently many problem still remain unsolved. I have focused my studies on:

1. To study the relation of the iso-radon curve (so-called by the author) to the geological structure and to infer from this the spouting mechanism of hot springs.

2. To examine the equilibrium of radon in gas and liquid statistically.

And added to the above.

3. To make abundant the data (on distribution of radon in Central Kyushu) now existing only in fragmentary studies.

As considerable data has been obtained I submit the present report with the above three objectives in view.

Section I. Relation Between Radon Distribution and Geology.

1. Method of Measurement.

Measurements were made on the radon content of some 47 hot springs in Central Kyushu, using the I. M. Fontactoscope. The constant of Fontactoscope was 2.82×10^{-10} Currie radons/degree/minute. Moreover, the Fontactoscope was rather old, being of 1937 make. Properly speaking the sub-standard had to be certified again, but fortunately on comparison it coincided exactly with the new apparatus at the Kumamoto Prefectural Health Laboratory, so I decided to use it as it was.

Furthermore, radon is gas and easily escapable in a open vessel, but completely sealed in some bottle, it must be ascertained what amount of radon changes during the time the water is taken until the time of measurement as Rn results due to distintegration of Ra in the hot spring water. According to Prof. Iwasaki and Ishimori the radon disintegration constant is 0.0075 and they calculated the change of amount of radon after disposing a sample one or two hours, in which originally N atoms of radon coexisting of 0, 0.01, 0.1, 1, 10, 100 times the equilibrium amounts of radium. Calculations of radon after one or two hours the results are shown in Table 1-1. Thus no great mistakes occur when disposing within two hours' time the matter to be examined, wherein an equilibrium amount of not

Table 1-1 Time Changes in Radon coexisting with Radium

Radium coexisting with Radon	Radon after one hour	Radon after two hours
	Initial quantity of Radon	Initial quantity of Radon
0.00×equilibrium quan.	0. 9 9	0. 9 8
0.01 〃	0. 9 9	0. 9 9
0.10 〃	0. 9 9	0. 9 9
1.00 〃	1. 0 0	1. 0 0
10.00 〃	1. 0 7	1. 1 5
100.00 〃	1. 7 4	2. 3 7

more than tenfold radium coexists. To be strictly exact the quantity of radium should be determined and corrected, but it is clear from Table 1-1 that we may consider this to be within the range of error in I. M. Fontactoscope.

Since practically no differences could be observed in between the values obtained on the spot and that in the laboratory, I decided to measure the hot spring water in the laboratory, bringing back the water in a small necked one-litre bottle. An apparatus of Ishimori style[2] was used in getting the water, taking care to get the water as soon as possible after spouting. Care was taken that no air remained in the bottle and sealed immediately. Minute care was also taken in placing the sample in the ionisation chamber by using a funnel and a rubber tube so as not to cause unnecessary agitation. The following is a comparison between the resuits obtained in this manner and the results obtained on the spot:

a. At spot (well in the campus) 2.02 mache strong
   After 3 hours portage on bus 2.02 mache weak
b. At spot (Ueki Primary School) 0.33 mache
   After bringing it back on bus 0.32 mache
   (About one hour after taking)

Measurements coincide within the range of error if taken immediately on return followig a few hours portage.

PH on Table 1-2 and Table 1-3 are measurement values on Toyo pH test paper made by Toyo Roshi. Considerable errors cannot be avoided in comparing with the real pH at the hot springs where the buffer action is small, but pH is given here as a means to show the change in the nature of the hot springs,

2. Results of the Measurements and Consideration.

Measurement results are shown in Table 1-2 and Table 1-3. For purposes of reference the results obtained by Dr. Ishizu and Prof. Iwasaki are shown in Table 1-4. Dr. Ishizu's data was obtained in 1913 and 1914, some forty years ago, but Funakoya, Hinagu, Hitoyoshi and others practically coincide, except Musashi which is about 3 to 4 times greater. On

Fig, 1-1. Location of Hot Springs.

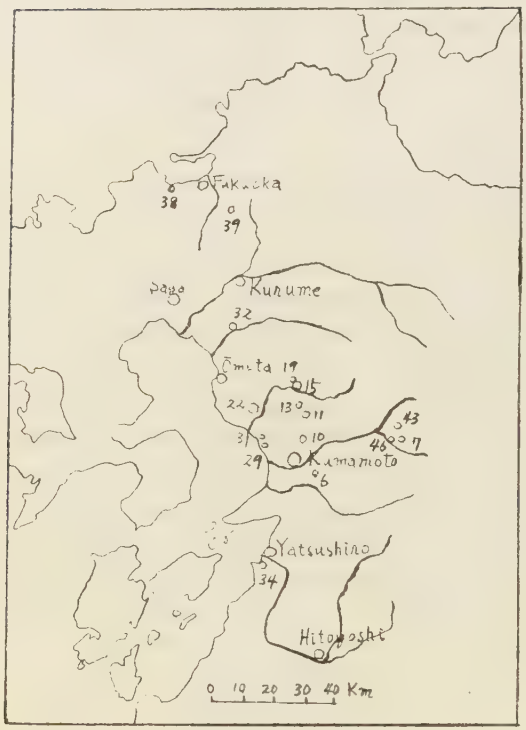

examination, also, of Taiko water which spouts in the foothills of Mt. Nagatare, well known to have pegmatite vein producing beside Lepidolite and other minerals containing radio-active elments, the results coincide with the results of measurements made by Prof. Iwasaki about 10 years ago in December 1941. Musashi shows slightly smaller results but the place of measurement is different and comparison cannot be made. The results, however, generally coincide. Funakoya almost coincides also. The greatest measurement value was 12. 1 mache for Yakushi-no-yu of the Musashi Hot Springs, the smallest 0.11 mache for Tamago Jigoku of the Aso Jigoku Hot Springs. Various distributions are manifested starting with such small values, but it would seem that the hot springs come within a definite range for the group such as about

Table 1-2 Radon Content in Spring Water

No	Location	Spring	Date	D	T_A	T_s	pH	E_w	Note
1	Botanical garden, Kumamoto University	well	showa 26. 5.24		26°C	17.7°C	7.0	2.07	Alluvium
2	Suizenji Park	well No. I	〃 5.27		26	18	7.0	2.03	〃
3	Hakenomiya	well	〃 5.28		25	19	7.2	1.38	Aso lava
4	Faculty of Science, Kumamoto University	well	〃 6.6		25	17	6.8	0.85	
5	Suizenji Park	well No. 2	〃 6.24		25	18.5	6.8	2.09	
6	Kamimasikigun Rokka-mura	well	〃 6.27		17.5	19.3	6.8	2.03	
7	Aso Jigoku-onsen	Tamogo-jigoku A	〃 8.4		—	83	5.4	0.32	Andesite
8	〃	〃 B	〃		—	95	〃	0.11	
9	〃	〃 C	〃		—	38	〃	1.30	

Tble 1-2 continuation

10	Ueki	well, Primary school	〃 8.27		30	16.7	6.6	0.33	
11	Hirasima	Irohakan-no-yu A	〃 10.19	35ken	29	32.5	7.6	1.16	Diluvium
12	〃	〃 B	〃	50	〃	37.5	7.8	1.50	
13	Miyanohara	Chōmeikn-no-yu	〃 10.22		23	19.5	6.8	1.98	
14	〃	well	〃		〃	22.5	6.6	1.89	
15	Yamaga	Tsujiso-no-yu	〃 10.26	75	21	43	8.8	1.60	Volcanic Debris
16	〃	well, Tsujisō	〃	20	〃	25	6.8	0.58	
17	〃	Matsu-no-yu	〃		〃	42	8.8	1.80	
18	〃	Sakura-yu	〃	0	〃	41.5	8.8	1.82	
19	Kumairi	Furu-yu	〃 10.29	63	25.5	39	8.6	1.21	
20	〃	well	〃		〃	19	6.8	0.95	
21	〃	Gofukuonsen-no-yu	〃	98	〃	38	8.8	1.18	
22	Ryūganji	Hikinosō-no-yu	〃 11.6	16	24.5	48.5	7.0	6.43	Crant e
23	〃	well, Hiki-nosō	〃 11.6	3	24.5	23.5	6.4	2.46	
24	〃	Ryūzenin-no-yu	〃 11.10	12.5	〃	45	6.8	6.27	
25	〃	Gyokueikan-no-yu	〃	58	19	47.5	6.4	6.11	
26	Ryūganji	Fujikan-no-yu	11.10	6	19	45.5	7.0	6.64	
27	〃	well, Fujikan	〃	3.5	〃	20	6.4	1.41	
28	〃	Tokaerikan-no-yu	〃	42	〃	46	7.0	7.43	
29	Kawachi	Kyōdo-yu A	26.11.16	37	20	33	6.6	1.22	Andesite
30	〃	〃 B	〃	28	〃	30	6.6	0.92	
31	Oama	Mumei-yu	〃		〃	35	6.6	0.89	
32	Funakoya	well No. III	〃 11.19	4	18	19	5.8	1.06	Diluvium
33	〃	〃 No. I	〃	〃	〃	20	5.6	0.37	
34	Hinagu	Nisi-yu	〃 11.25	30	13.5	45	7.2	0.91	Paleoxoic Sediments
35	〃	Kinparo-no-yu	〃	〃	〃	〃	7.2	0.46	
36	〃	Gozen-yu	〃	〃	〃	48	7.4	2.86	
37	〃	Otyugi-yu	〃		〃	〃	〃	3.45	
38	Mt. Nagatare, Fukuoka-city	Taikosui	〃 12. 4		10.5	16	6.4	6.75	Pegmatite
39	Futsukaichi	Yakusi-yu	〃		13	38.5	6.4	12.11	Granite
40	〃	Gozen-yu	〃		13	44	6.8	12.0	
41	Hayashi, Hitoyoshi-city	Suiranrō-no-yu	〃 12. 9	63	8.7	48	7.8	1.07	Alluvium
42	〃	Furō-onsen-no-yu	〃	87	〃	47.5	7.8	1.43	
43	Aso Yunotani	Bozujigoku A	27.10.26		23	37.3	3.9	1.15	Andesite
44	〃	〃 B	〃		22	50.3	2.8	3.32	
45	〃	〃 C	〃		17.8	63.5	3.9	1.28	
46	Tochinoki	Tadeyu	27. 6.18		27	46	7.6	0.17	
47	〃	Oyamakan-no-yu	〃		〃	39	7.6	0.47	

Note

D; Depth

T_A; Atmospheric temperture in °C

T_S; Temperature of Spring in °C
Ew; Emanion per litre of water in Mache's units
Showa 27; 1952

Table 1—3 Radon Content in Gas

No.	Location	Spring	Date	T_A	T_S	pH	E_g	Note
			Showa					
1	Aso Jigoku-onsen	Tamago-jigoku A	26. 8. 4		83	5.4	7.88	
2	〃	〃 B	〃		95	〃	8.87	
3	〃	〃 C	〃		38	〃	24.1	
4	Aso Yuotani	Bozu-jigoku A	27.10.26	23	37.3	3.9	15.6	
5	〃	〃 B	〃	22	50.3	2.8	23.7	
6	〃	〃 C	〃	17.8	63.5	3.9	12.4	

Note
Eg; Emanation per litre of gas in Mache's units

Tabie 1—4 Data of Reference

Loction	Spring	Date	T_S	Ew	literature
Musashi	Yakusi-no-yu No. 1	1914. 7.30	41.0	2.00	R. Isizu; The mineral springs of Japan
〃	〃 No. 2	〃 7.29	44.0	4.07	〃
〃	Enju-no-yu	〃 7.31	46.0	3.70	〃
〃	Osakya-no-yu	〃 7.30	44.5	3.21	〃
Funagoya	Kyōdō-yu	〃 8. 2	17.5	0.94	〃
〃	Nomi-yu	〃	21.0	0.40	〃
Hinag	Otsugi-yu		48.5	3.80	〃
〃	Gata-yu		45.2	0.88	〃
〃	Kinparo-no-yu		46.5	0.58	〃
Hayasi	Motoyu		50.0	1.27	〃
〃	Suiranrō-no-yu I		48.4	1.16	〃
〃	〃 II		48.8	0.88	〃
Aso Tarutama	Jigoku	1913. 3.14	75	0.10	〃
〃	Kamino-yu	〃	57	1.05	〃
		Shōwa			
Mt. Nagatare Musashi	Taikosui	16.12. 7	15.5	7.0	Iwasaki; J. Chem. Soc. Japan **64**, 941
	Daimaru-no-yu	16. 5. 5	46.5	16.8	〃 ibid.: **63**, 20
Funagoya	Well No. I	16. 8.30	20.0	0.59	〃
〃	Well No. II	〃	20.9	0.34	〃
Aso Yunotani	Hōkōjigoku	17. 8. 7	68.0	0.95	〃 ibid,: **64**, 941
〃	Siraikejigoku	17. 5.25	62.0	0.33	〃
〃	gas	17. 5.27	74.80	24.0	〃
〃	〃	17. 8.11	68.3	61.6	〃

12 mache for Musashi, about 7 mache for Mt. Nagatare, about 6-7.5 mache for Ryuganji, about 2 mache for Miyahara, 1.6-1.8 for Yamaga. The spouting structure in the various hot spring groups is about the same according to the group, and it can be considered that the radon content is determind by the spouting route taken by the hot springs. Assuming this to be so, the geology of each district would be as shown in Table 1-2. Minerals, containing radioactive substances, would generally be found in plutonic rocks such as granite, orthocloase, piorite or produced as specil substance of pegmatite penetrating through metamorphic rocks like gneiss or schist and is realy found in stratified rocks and practically does not exist in volcanic rock. It is clear from Table 1-2 that radon content is great in grannite districts and small in volcanic rock districts. In Central Kyushu even in the granite districts the content is not great and hot spring contents generally fall within the following range.

Granite	6-12 mache
Andesite	0.1-1.0 mache
Alluvium, Diluvium	1.0-2.0 mache

Of course, even in granite district, it is natural that changes occur according to structure of spouting. The radon content of vadose (superficial) water circulating in the alluvium can be thought to be small, but results of measurment at Ryuganji Hot Springs was 6-7.5 mache for hot spring water and approximately 1.5 mache for well water. Perhaps the difference of radon content of Ryuganji and Musashi hot springs is due to the difference of the quality of the granite.

What about the volcanic rock districts ? Aso Tochinoki Hot Springs is 0.47 mache, Aso Uchinomaki Hot Springs 0.2-1.5 mache (reference Section 4). Kawachi Hot Springs and Oama Hot Springs, which belong to Mt. Kinbo range, that is another volcanic range to Aso volcano and lying west of Kumamoto City and facing Shimabara Bay, are approximately 0.9-1.2 mache and almost coincide.

Then what of those in the same hot spring group? We can say that there is not much change in the same hot spa group, taking for instance Ryuganji 6-8 mache, Musashi about 12mache and Yamaga 2 mache. But in Hinagu Hot Springs there is such a big difference 3.5 mache for Otsugi-yu, whereas 0.46 mache for Kinparo-no-yu, separated only by some dozen meters. What is the reason for this? Most likely this is due to the difference in the structure of earth crust but the subject demands close investigation. This matter will be taken up in Section 2 and subsequently.

Yunotani Hot Springs and Jigoku Hot Springs in Aso are absolutely different from the forementioned hot springs and are situated on the old crater. According to Prof. Iwasaki, as shown in Table 1-4, inspite of 0.3-1.0 mache for the hot springs, the radon in hot spring

gas is 24.0-61.6 mache and an amazing value of 208 mache is recorded for geyser during the lull in eruption.

In measuring Bōzu Jigoku, a little further hinterland from the Hōkō Jigoku, I get values that almost coincide with the results of Prof. Iwasaki. Again at Tamago Jigoku of the Jigoku Hot SpringS, three kilometers due south of Yunotani, there were not much differences in the low temperature ones as compared to Yunotani, but in the high temperature springs the radon content in the erupted gas was low. In considering the quantity of eruption, the high temperature is 1.7 litres per minute, low temperature 0.5 litres per minute. Thus smaller the gas eruption the greater the radon content. This coincides with Mr. kamata's observation[3] on the hot spring gas in the Kirishima volcanic area. According to Mr. Kamata,[1] he found some hot spring gas in Ibusuki district in which the radon content in the hot spring gas (closely related to fumarole gas) was as high as 291 mache and toron 4300 mache. Gas with such large radon content are as yet unknown in the Aso district. Attempts were made to measure the toron in Bōzu Jigoku but measurements were difficult due to small rate of toron against radon.

The relations among pH, the temperature of spring and the radon content are not clear. Granite district, where radon content is great, however, is either slightly acidic or neutral.

Section 2. Radon Distribution at Ryuganji Hot Springs.

1. Method of Measurement.

Aluminium leaf was used. Measurements were made with I. M. Fontactoscope. The constant of Fontactoscope, K, was 3.58×10^{-10} Currie radon/degree. The amber of this Fontactscope went out of order during radon distribution measurements at Ryuganji and became impossible to use. Therefore an amber offered by Prof. Namba was used, shaped on a lathe and thoroughly polished. This is working well at present. The N. L. is below 0.05 and ordinarily used at 0.1; the amber is repolished when N. L. rises above this.

2. Results of Measurements and Consideration of Results.

Ryuganji Hot Springs at Takase Machi, Kumamoto Prefecture, spout from a shallow valley on the south foothills of Mt. Shodai, located north northwest of Kumamoto City and near the Fukuoka prefectural border. This belongs to a simple type hot springs and spouts in 14 places. The temperature is 41-48° C. and measurements at Gyokuei Hotel in October 1926 was 7.93 mache[5]. Thus at the begining of Showa Era Ryuganji was publicized for a while as radium hot springs. There are a large number of mottled teeth patients and fluorine content is quite large (maximum around 9.5 ppm[6]). Wells are few in this hot spring area and it is to be assumed from the temperature of the water that there is a mixing with hot spring water, so I decided to take up first the wells in Takase Machi. The results of the

Table 2—1 Radon Content of Ryuganji

No.	Location	Date	D	T_w	pH	E_w
		Showa				
1	Well, Konkō-kyōkai	27. 8. 4		19.5	6.6	1.01
2	Well in the neighborhood of Nisikibridge	27. 8. 7		24	6.6	1.34
3	Takemoto-onsen-no-yu	〃		24	6.6	1.65
4	Public well	27. 8. 5		19	6.6	1.54
5	Well, Gangyoji	〃		19	6.6	1.27
6	Well, Joanji	〃		18	6.6	0.62
7	Yayoikan-no-yu	27. 8. 8	195	36	6.6	6.78
			ken			
8	Miharasi-onsen-no-yu	27. 8. 7	67	46.5	6.8	0.25
9	〃	26.11. 7		46.0	6.6	0.20
10	Shōsenkaku-no-yu	27. 8. 9	50	47.0	6.6	9.07
11	〃	26.11. 6		46.5	6.6	9.32

measurements are shown in Table 2-1. The wells were numbered in order from the south according to location and the water temprature and radon content examined as shown in Fig. 2—1. The water temperature and radon content is greatest at Takemoto Mineral Spring. This would indicate that there must be something out of ordinary in the structure of the earth crust near the Takemoto Mineral Spring. Next as shown in Table 1-2 of Ssction 1 the radon content of the hot springs in tde Ryuganji is practically the same at 6-7.5 mache. A part of granite is exposed and Biotite-granite was obtained from boring. Shosen Kaku, however, on the right hand side of the entrance to the hot springs is 9 mache while the town operated bath, 30 meters away on a little hill across the road, has a very small 0.25 mache. The temperature and the depth of boring were 47° C. and 50 ken (90 metre) for the former and 46.5° C. and 67 ken (112 m.) for the latter. It should be noted that radon content for the latter is very small inspite of greater depth of boring. Iso-radon curve is given herein. Of caurse, there is room for argument as to whether radon content curve has physical reality or not but here the curve is drawn merely mechanically from points taken mechanically. Line A cutting across the high point may be interpreted as showing the crack.

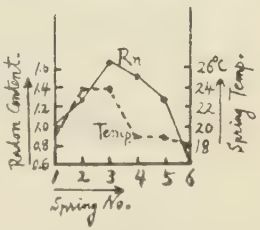

Fig2-1

Ryuganji Hot Springs are located in the shallow valley running along the road leading northwest from Shosen Kaku and according to Mr. Imanishi[7] it may be safely surmised that geologically the crack runs in the direction of the road, which lise just on the A line given above, although conclusions cannot be confirmed directly on account of the surface coverage of alluvium. In other words, there seems to exist some relation between the iso-radon curve and the structure of the earth crust. On examination, other chemical composition, the

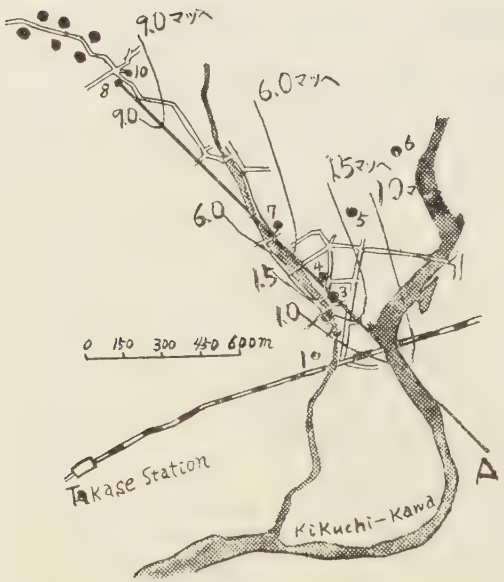

Fig 2-2 Iso-radon Curves.
Note: マッヘ=Mache

distribution of fluorine for instance, seems to be the greatest on this A line.[8] It is considerably interesting problem whether the distributions of other chemical components show the extremum on the A line or not. Furtherermore, by closely examing the relation of radon and other disintegration products the spouting mechanism of the springs of these location will become clear.

Section 3. Radon Distribution in the Kumamoto Plains.

1. Method of Measurement.

Same as Sections 1 and 2.

2. Seasonal Change.

In order to draw iso-radon curves, measurements should be taken at identical times, but as this is impossible measurements should be taken with mature consideration to the time changes. In comparing the data obtained, as mentioned in Section 1, by Dr. Ishizu about 40 years ago, data by Prof. Iwasaki about 10 years ago and the data given in Table 1-2 of Secotion 1, Musashi Hot Spring has changed considerably but the others are about the same. In studyng the Kumamoto plains, water from tha wells in the University campus, with comparatively large radon content for alluvium and conveniently located,

Talbe 3—1 Seasonal Changes of Radon Content in the Well-Water

No.	Location	Date	T_s	pH	E_w	Note	
1	Well, Botanical Garden,	Showa 26. 5.24	17.7	7.0	2.07		
2	Kumamoto University	7.23	17	6.8	2.30	depth of water,	2m 80cm
3		8.20	〃	〃	1.98	〃	1m 90cm
4		10.15	〃	〃	1.95	〃	1m 70cm
5		27. 4.23	〃	6.6	2.15		
6		7.14	17.5	6.8	2.20	〃	2m 40cm
7	Well, Faculty of Science,	26. 6. 6	17	6.8	0.85	〃	1m 20cm
8	Kumamoto University	〃 7.22	〃	〃	1.12		3m
9		〃 8.21	〃	〃	0.88		1m 70cm
10		27. 5. 7	16	〃	0.90		

was measured from time to time. The results are shown in Table 3-1. Aside from a slight increase of radon content when the water increased after a rain there were hardly any changes. Of course, each well probably has its own characteristics but from the above-mentioned fact we need not consider the time change. (The degree of rough measurements does not present any problem and there is no harm in assuming there are no changes.) Therefore, taking it for granted that there are no changes, the results of two years of measurements were all treated alike witout considering the date of measurement.

3. Aso Lava and Radon Distribution.

The results of measurements are shown on Table 3-2.

Suizenji and Rokka are famous from olden days for the abundant clear spring water, running under the Aso lava and welling up to the surface of the earth at the end of the

Table 3—2 Radon Content of Well-and River-water in the Kumamoto Plains

No.	Location	Date	D	T_S	pH	F_W	Note
		Showa					
1	Suizenji Park	27. 5. 2		18.3	6.6	2.17	
2	Rokka	27. 5. 1		19.2	〃	2.14	
3	Nakanose	27. 7.16		18	6.6	1.59	
4	Osakamura	〃	22ken	18	〃	1.14	
5	Tatsutaguchi	〃 5.12	3	19	6.4	1.08	
6	Sanrigi-Kaitakudan	〃 11. 8	28	17	〃	0.61	
7	Sakaenomatsu	〃	25	〃	〃	0.25	
8	〃	〃 5.18	〃	18	〃	0.29	
9	Haramizu-station	〃 6.13	18	〃	〃	0.41	
10	Sakura public well, Ōtsu-machi	〃 5.17		〃	〃	2.84	
11	Seta Fukita	〃		17	〃	0.93	
12	River-water of Sirakawa in the neighbourhood Tochinoki	〃 6.18		24	7.2	trace	
13	River-water of Kurokawa in the neighbourhood of Tosita	〃 6.19		21	6.4	0.14	
14	Tosima	〃 7.15	5	17.5	6.6	1.74	
15	Kiyama	〃	3	17.5	6.6	2.11	
16	Hiratamachi, Kumoto-city	〃 7.17	2	19	〃	1.43	
17	Kawajiri	〃	1	21	〃	0.51	
18	Uto-staton	〃 7.18	2	20	〃	1.60	
19	Matsubase	〃	1	20	〃	2.81	
20	Amitsu A	〃 8.11		19	〃	1.66	
21	〃 B	〃		18	〃	0.94	
22	Sumiyosi	〃		21	〃	0.40	
23	Hakenomiya	〃 5. 8		19	〃	1.58	

24	Tsujikubo	〃 5.10	4	15	6.4	0.98
25	Kikuchi	〃	10	17	〃	1.47
26	Hirose	〃 5. 9	2	16	〃	2.67
27	Kikuchi-shrine	〃		16	〃	1.25
28	Ueki station	〃 7.21	5	19	〃	0.56
29	Konohastation	〃	3	18.8	〃	0.69
30	Ikura station	〃 7.19	4	20	6.8	0.52
31	Eta	〃 8. 4		18	6.6	2.73
32	Sakasita	〃 8.12		18.5	6.4	0.10
33	Nankan I	〃 8.13	4	17.5	6.6	0.42
34	〃 II	〃		16	6.8	1.51
35	Keifuen I	〃 7.17	50	17	6.6	0.21
36	〃 II	〃	42	〃	〃	0.24
37	Miyoshi	〃 11. 9		〃	〃	1.59
38	Ichihongi	〃		21	6.6	1.54

Fig3-1 Outline of Aso Lava Distribution

lava (so it is said). The water from the wells in the University campus, Suizenji, Kiyama, Rokka and others show very similar radon content. Prof. Matsumoto has made a very detailed study of Aso lava distribution and outline of his results are shown in Figure 3-1. From this diagram it can be seen that the University, Suizenji, Kiyama and Rokka are located at the end of the lava. The lava of this vicinity is so-called mud lava of volcanic ash nature, but the radon content at Tochinoki Hot Springs, spouting from andesite of the Aso somma rings, is of small value 0. 17-0. 47 mache. The maximum radon content at Uchinomaki Hot Springs located on the volcanic ash soils is 1.5 mache (see Section 4). The Kuro-kawa flowing through Aso Valley where Uchinomaki is located contains a large quantity of volcanic ash and the radon content of the river water is 0.14 mache; while in Shira-kawa, flowing through Tochinoki and having no volcanic ash content, it is impossible to detect any radon content by I. M. Fontactoscope. It can be surmised from this that Aso volcanic ash, or volcanic ash nature, contains more radioactive substance as compared with other andesite. Radon content has been observed to increase as the place of measurement becomes lower as in the cases of Masutomi and Mt. Nagatare.[3] Thinking that the radon content of water from Aso flowig underneath the lava might gradually increase, efforts were made to observe the process of increase enroute but as the underground water beneath the lava flows at a depth of about 55 ken (100 meters) below the surface there were only three wells penetrating the lava, namely; two wells at Keifuen and one at Sanrigi Land Reclamation Colony. As water in the wells at Keifuen is brought to the surface by air blown into the well it would seem that considerable radon escapes but the results of measurements were small, 0.21 and 0.24 mache. Sanrigi Land Reclamation Colony uses several flights of pumps and the quantity of radon escape when compared with that of Ryuganji or Yamaga is of lesser percentage, but the results of measurements was 0.61 mache. The water from Suzume-no-Jigoku (No. 1 well) of Funakoya Mineral Springs was agitaited by spouting of carbonic acid gas and its radon content was 0. 57 mache but the water from the nearby No. 3 well, where there was no spouting of carbonic acide gas, was 1.96 mache. If we are to believe the values obtained at the reclamation colony, the well at Haramizu where the lava has come off is 0.41 mache, the deep well above the lava at Sanrigi Sakaenomatsu is 0. 3 mache while the well at the reclamation colony is about the same though slightly more.

This water has its origin near the Futae-no-Toge of the Aso Somma rings and is generally throught to come to the surface at Ippongi. in the proximity of Hakenomiya. The radon content in the proximity of Hakenomiya is approximately 1. 6 mache and compared to this the radon at the colony is too small.

The sudden increase might be considered to be due to difference in the nature of

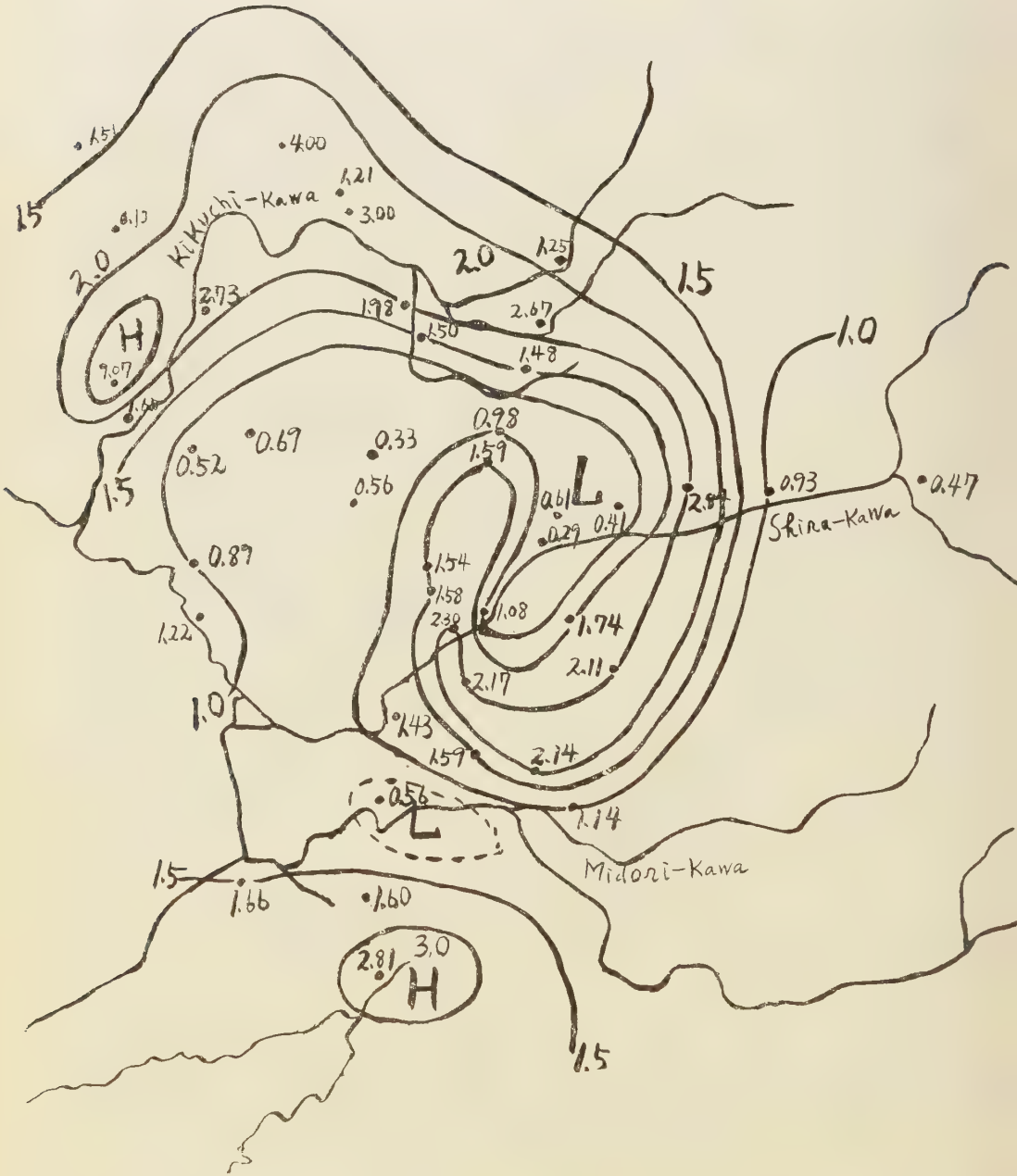

Fig 3-2. Iso-radon Curves

lava at the end. It cannot be throught so, however, because the lava end near Hakenomiya and that at the University, Suizenji and Kiyama are all lava ends made so by peeling off by the river lava that widely covers the Kumamoto plains.

We may, therefore, consider for the present that radon content has no connection with Aso lava though it may seem a little hasty conclusion in view of the fact that it was possible to measure only one well.

4. Iso-radon Curve for Kumamoto Plains.

Whenever there were many measurement values for the same area, the data obtained up to the present was put in order and the highest value taken as the value for that area. Iso-radon curve was drawn as shown in Figure 3-2. The curve will probably change as further studies are conducted since only about 40 spots were measured in the entire Kumamoto Plains and many important spots overlooked such as Ryumon and Tatekado of the Kikuchi-kawa head arear, the mountainous area from Ōyanohara to Kōsa, Mt. Kinbo vicinity and other places where inconveniences in transportation made measrements difficult. On comparing Figure3-1 and 3-2, one immediately notices that distributions of lava and radon do not coincide. The radon content is great also in the area linking the University, Suizenji, Kiyama and Rokka and the radon content decreases with separation from the region. The general trend is to extend northeast and the fact that the geological structure of this district runs practically east northeast is a matter of deep interest, too. The places marked H are the places of a large quantity of radon content. Ryuganji on the north is a hot spring area, but low temperature hot springs are also found near Matsubase on the south. The base rock at Ryuganji is granite; while in the proximity of Matsubase it is granite-gneiss.

The places of a small quantity of radon content are indicated by L. According to the measurement of terrestrial (or earth) magnetism by Prof. S. T. Nakamura,[1] the earth magnetism shows high value in places where radon content is L. Tochinoki where the radon content is small has on the contrary very high earth magnetism. Judging from what has been mentioned above, the radon distribution in Kumamoto plains seems to have no relation with Aso lava but is related to rock structure underneath the lava. This is a matter of deep interest and I hope to carry on further detailed studies in the future.

Section 4. Radon Distribution at Aso Uchinomaki Hot Springs.

1. General Facts on Uchinomaki Hot Springs and Results of Measurements.

Uchinomaki Hot Springs (Aso-gun, Kumamoto Prefecture), as shown in Figure 4-1,[2] is located at the crossing point of a line radiating from Aso Nakadake and passing through the Motozuka Hot Spring spouting in the oldest small volcano, Motozuka, and the arc connecting Yuyama, Uchinomaki, Orito, Matoishi, Kurumagaeri and Tocinoki hot springs.

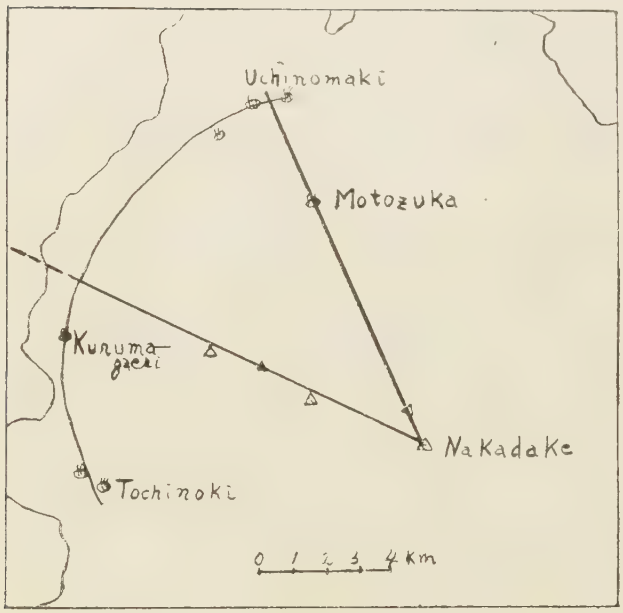

Fig 4-1 Location of Aso Uchinomaki Hot Springs.

Uchinomaki is one of the most popular hot spring districts in the narrow ribbon-like area of the Aso volcanic range stretching more than two kirometers from Yuyama on the east to Orito on the west. About 70 hot springs are found here.

The radon distribution for Uchinomaki Hot Springs was measured at the spot during the period of August 19 to September 5, 1952 using I. M. Fontactoscope. Aluminium leafe was used on the I. M. Fontactoscope. The constant of this was 3.5×10^{-10} Currie radon/degree/minute. PH was measured by Toyo pH test paper for the purpose of giving a rough value. The results of measurement are shown in Table 4-1. The sites of hot springs measured are shown in Figure 4-2.

Table 4-1 Radon Content of Uchinomaki Hot Springs

No.	Spring	D	T_S	pH	E_w	NH_4^+	Note
		ken				mg/l	
1	Orito	0	34	7.0	1.06	1.76	Collourless
2	Public Bath (Orito)	26	40.5	7.0	0.42	7.30	〃
3	Ist well in the neighbourhood of San-ōkaku	40	40	6.8	0.19	4.58	
4	Hokensho	85	43.7	7.1	1.06	6.80	Collourless
5	IInd well in the neighbourhood of San-ōkaku	70	40.8	6.8	0.82	24.69	
6	Public Bath (Simo-ozato)	45	39.4	6.8	1.40	30.0	light yellow colour
7	Primary school	85	42.7	7.2	0.60	8.48	〃
8	Komeya	85	46·5	7.3	0.66	2.04	Collourless
9	Yachiyo	90	48.0	7.1	1.16	3.94	〃

10	Takedaya.	74	46.8	7.2	0.42	2.65	〃
11	Private Bath (K. Uchino)	89	47.8	7.2	0.28	3.27	〃
12	〃 (M. Nagata)	84	48.7	7.2	0.25	2.47	〃
13	〃 (H. Higashi)	83	47.5	7.2	0.20	1.87	〃
14	〃 (Institute of volcano)	83	47.8	7.2	0.44	3.40	〃
15	Public Bath B (Kami-ozato)	42	39.6	7.0	1.39	23.03	light yellow colour
16	Well (Kami-Ozato)	42	39.6	6.8	1.51	20.86	〃
17	Private Bath (U. Adachi)	83	45	7.3	0.27	0.93	
18	〃 (K. Sugihaara)	70	39.7	7.2	0.12	3.14	Collourless
19	Yuyama	0	21.5	6.8	1.26	0.35	〃
20	Public Bath (Tamachi)	94	47.7	7.2	0.44	2.8*	〃
21	Tomosita	40	42	7.2	0.54	4.1*	〃
22	Public Bath (miyanohara)	40	41.8	7.0	0.37	1.9*	〃
23	Well (S. Yamasita)	40	40.3	7.0	0.32	5.4*	〃
24	Well (M. Ōkura)	37	37	7.0	1.50	30.5*	Yellow
25	Well (S. Murakami)	37	35	7.2	1.29	33.4*	〃
26	Private Bath (S. Matsuoka)	75	42	7.2	0.13		Collourless
27	Kadoman	85	45	7.2	0.43		〃
28	Private Bath (M. Kai)	65	41.6	7.2	1.16		〃
29	〃 (K. Sugita)	90	45	7.2	0.20		light yellow
30	Sintsutaya	65	41	7.2	1.40		Collourless
31	Kakihara	80	35.8	7.0	0.62		〃
32	MantoKuji	78	35.8	7.0	0.55		〃
33	Private Bath (T. Kojima)	80	28	7.0	0.59		〃
34	Obiya	80	34.8	7.2	0.82		light yellow

NH_4^+; Shinomiya, Kokubu, Nanba, Naitō; J. Chem. Soc. Japan **72**. 846 (1951)

* ; unpublished data

2. Iso-radon Curve.

From Table 4-1 it can be seen that the depth of the hot springs belong in general to three groups, namely; about 40 ken (named the 40 ken layer) about 60 ken (60 ken layer) and about 80 ken (80 ken layer), and as there were only two examples, in the Table, of the 60 ken layer, the 60 ken layer has been omitted and study conducted on the 40 ken and 80 ken layers. The iso-radon curves of these two are shown in Figures 4-3 and 4-4. As mentioned in Setion 2 the sharp points of the iso-radon curve coincide with the crack line. Figure 4-3 shows the crossing of the two crack lines and indicates the two crack lines shown in Figure 4-1. Of course, Figure 4-1 is supposed to be a model indication and undoubtedly there are many cracks running parallel to this. The dotted line shows the crack direction of the results of Prof. Namba's measurements of electric resistance. Figure 4-4 is the iso-radon curve for 40 ken layer; the curve is concentric arc and the crack line in the figure concentrates at one point. The maximum value of radon content for each layer

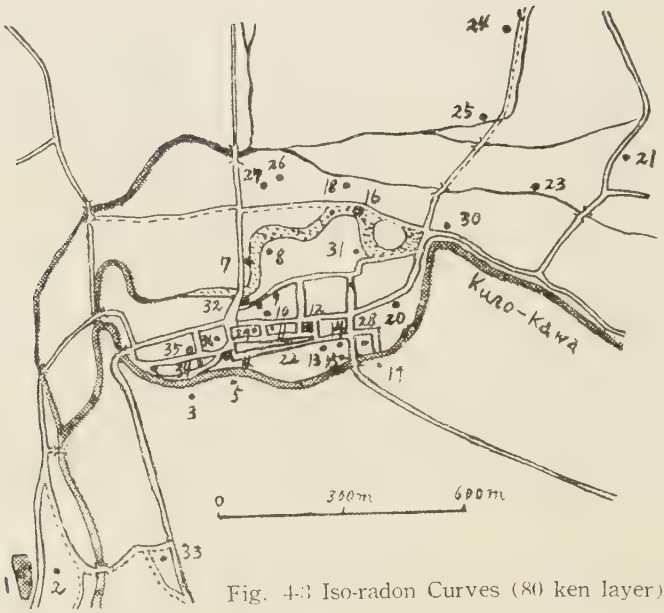

Fig. 4-3 Iso-radon Curves (80 ken layer)

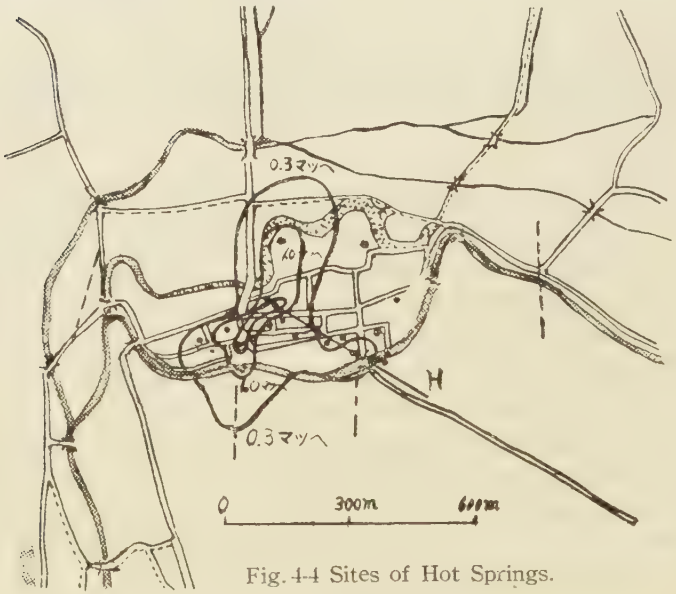

Fig. 4-4 Sites of Hot Springs.

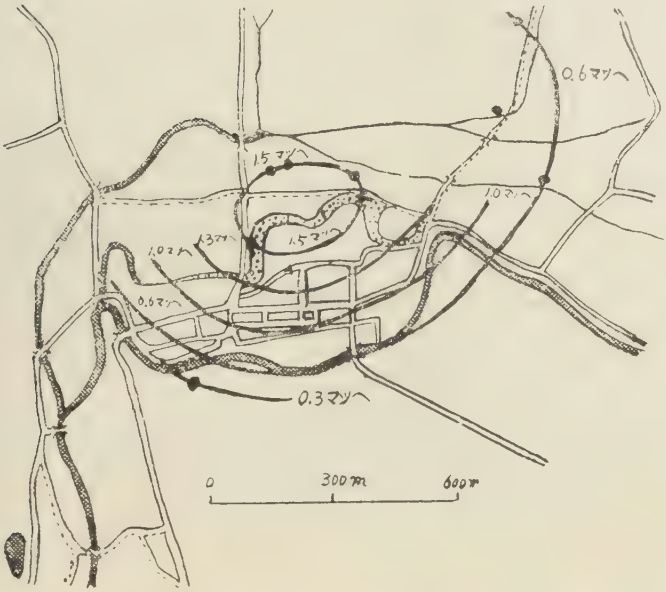

Fig 4-4 Iso-radon Curves (40 ken layer)

was: 1.16 mache 48°C for 80 ken layer 1.51 mache 39.6°C for 40 ken layer; average value of 80 ken layer is 0.58 mache 43.7°C, and of 40 ken layer is 0.95 mache 39.4°C. Then, radon content is greater in shallow than in deep place and in low temperature than in high temperature places and on scrutinizing each layer the greatest radon content is at Yachiyo Hotel but the highest temperatuure is in the 80 ken layer. Uchinomaki Hot Springs contain gas, though of very small quantity, and bubbles rise to the surface sometimes. Measurements were not made for difficulty in obtaining the gas in most cases but judging from similar cases in southern Kyushu[5] we may safely consider that it is near equilibrium. Then as the temperature fall sit dissolves into the liquid causing greater radon content in the 40 ken layer. The radon content, however, increases too much in the average value, an increase of 1.6 times for a mere 43°C drop in temperture. This may be due to passage through some 50 meters' thickness of clayish volcanic ash which does not permit penetration of water. The layer penetrable by water is composed of gravel or sand of Aso lava, but it was not possible to measure the radio activity of thd sand obtained from boring at the 40 ken layer with Lauritsen electroscope, but it was possible to measure the clay obtained from undeaneath that, though weak. At Toshita, the confluence point of the Kuro-kawa

Shira-kawa, the water of Kuro-kawa, containing a great deal of lava ash, was 0.14 mache; while the water of Shira-kawa, with no lava content, could not be measured with I.M. Fontactoscope. Hot springs at Tochinoki spout directly from a crack in pyroxene-andesite forming the Aso somma rings and showed radon content of 0.17-0.47 mache, temperature 46-39°C.

The line H of Figure 4-3 is the line of spouting of high temperature springs and Yachiyo Hotel situated at the end shows the highest temperature and higest radon content for the 80 ken layer. Assuming that the hot springs spout in the center of the concentric arc of the 40 ken layer running along to the cave-in surface of the caldera, cra crack parallel to the cave-in surface from this 80 ken layer position, the slant of the cave-in surface is calculated to be around 17°30′ and well coincides with the somma ring slant of 16° 23′ in the proximity of Uchinomaki.

3. Radon Distribution and Ammonium content of water.

Prof. Shinomiya and Naito[13] of the Engineering Department have made studies on the distribution and monthly changes of ammonium and the data offered by them are shown together in Table 4-1. In the 80 ken layer, as pointed out by Prof. Shinomiya and Naito,[14] the greast is near the crack lines, but as the spots of mesurement were not equally

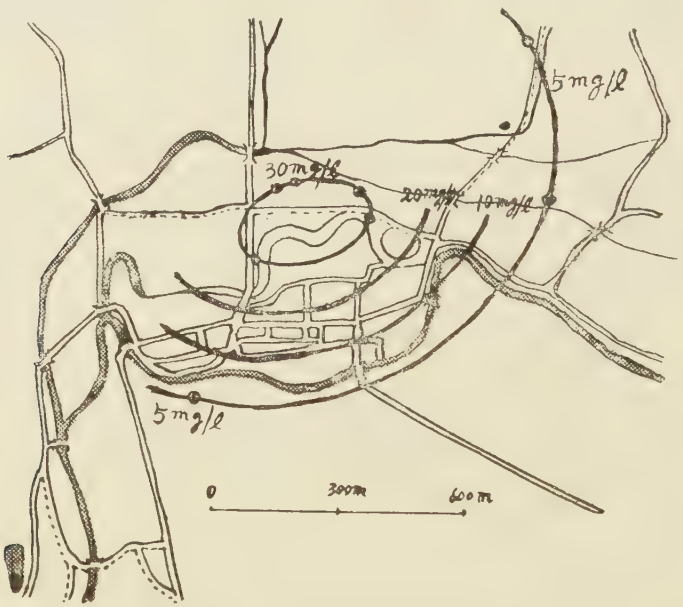

Fig 4-5 Iso-ammonium Curves (40 ken layer)

distributed it was not possible to draw the iso-ammonium curve. In the 40 ken layer a curve very similar to radon was obtained. The average for each layer is 80 ken layer 3.6 mg/l, 40 ken layer 17.2 mg/l, natural spouting 1.05 mg/l. It can be seen that natural spouting springs spout directly from the crack in the rock at base, and if we consider this value to be the value of ammonium content of hot springs spouting from the rock at base about 200 ken below the accumulate layer near Uchinomaki, the ammonium content in hot springs increase approximately 3.6 mg/l till the hot water reaches the 80 ken layer. Considering the value to be zero at first there is only an increase of 3.6 mg/l. Between the 80 and 40 ken layers, difference in depth of 40 ken. there is an increase of about 13.6 mg/l. Sudden increase occurs as it nears the surface. At the time of lava ash eruption during July 16 to 18 in 1928 Mr. Kiyota [15] has obtained a value of NH_4^+ in the lava ash. If the ammonium ion has its origin in lava ash there should be a change in ammonium content at the time of eruptions rather than the tendency for increase according to depth. Again if there is not much difference in ammonium content at the time of eruptions we must look for ammonium origin in other causes than lava ash. At present there is not much difference in the composition of lava according to the time of its eruption. The fact that a large quantity of ammonium is distributed in the vicinity of the river-bed of the old Kuro-kawa, that water of hot springs tinted yellow, always contain considerable quantities of ammonium-ion and that the coloring is due to some organic substance and not inorganic substance such as iron, behooves us to search for the origin in something eles than lava ash.

Section 5. Distribution of Radon at Yamaga Hot Springs.

1. General Facts on Yamaga Hot Springs and Results of Measurements.

Yamaga Hot Springs, as shown in Figure 5-1, is located about 28 kilometers north of Kumamoto City along the Kikuchi-kawa and comprises of a group of about 30 spouting springs. The characteristics of this hot spring group are:

1. Presence of mottled teeth patients.
2. Sweet taste of tea made with hot spring water.
3. Slimy feeling at bathing.
4. Soap lathers freely. The people there utlise hot springs for their washing.

We can assume the presence of fluorine from the cases of mottled teeth[16] and the sweetness of tea.[17] According to Prof. Ohara[18] considerable quantity of fluorine exists. Hot spring water, with the exception of the town operated Sakura Baths, is obtained by boring. As the volume of spouting hot water is small, the hot water is pumped with motors in all instances. All shallow hot springs such as Sakura-yu, Tatsunoyu, Kyoei Hotel, Yoshida Footwear store, Hayashida and Hayami lie in the shallow valley. Radon distribution was

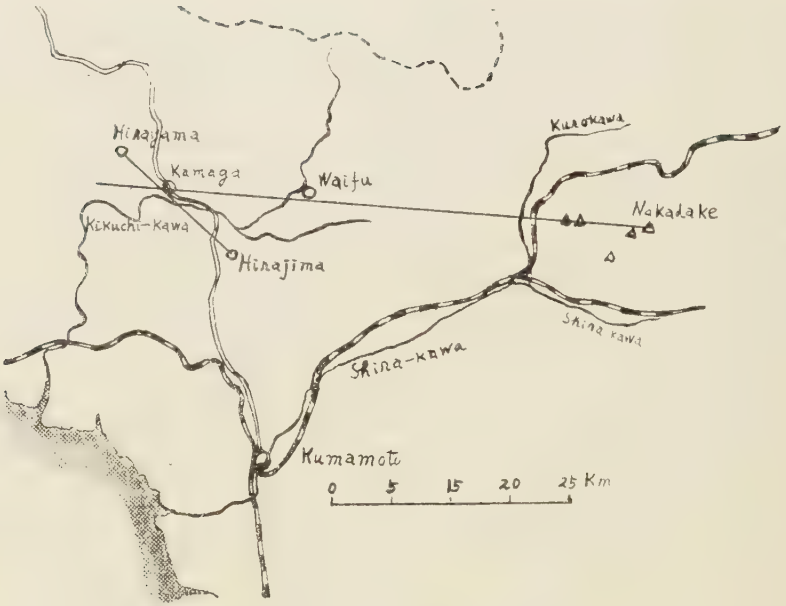

Fig 5-1. Location of Yamaga Hot Springs

measured but as it was impossible to take measurements simultaneously, the same place was measured once each week with mature consideration to the time change. The largest difference in values between the maximum and minimum during the period of measurement was at Egami. 0.4 mache, and about 0.3 mache at the town operated Shinyu. The general tendency of iso-radon curve, however, does not seem to be affected.

The measurement results are shown in Table 5-1 and the location of the hot springs

Table 5-1 Radon Content of Yamaga Hot Springs

No.	Spring	Date	D	T_s	pH	E_w
		Showa	ken			
1	Tsujisō	27. 12. 29	116	43. 0	9. 43*	1. 68
2	Private Bath (Egami)	28. 1. 8	96	43. 2	9. 71*	2. 98
3	Sin-yu, Public Bath	27. 12. 13	121	43. 2	9. 60*	2. 43
4	Takenouchi	28. 2. 5	100	39. 5	8. 3	2. 73
5	Suehiro-nosen	27. 12. 28	120	39. 0	8. 7	2. 21
6	Yakushido-on-yu	28. 1. 7	110	41. 0	9. 5	2. 07
7	Sakura-yu	〃	0	40. 5	9. 3	2. 24
8	Tatsu-no-yu	〃 1. 8	16	41. 2	9. 58*	2. 41

9	Hoyōsho	〃 1.17	70	38.5	7.4	1.03
10	Private Bath (Sakanashi)	27.12.29	74	39.5	8.0	1.06
11	Kyōei	〃 12.28	16	41.8	9.5	1.30
12	Yoshida Footwear Store	〃 12.31	6	41.3	9.60*	2.31
13	Private Bath (Hayashida)	〃 12.30	8	40.3	9.2	2.52
14	〃 (Hayami)	〃	30	32.0	9.14*	1.13
15	Nakamachi washing place	〃 12.31	1	34.0	8.8	1.07
16	Munekata washing place	〃 12.27	90	37.0	9.0	1.08
17	Private Bath (Nakahara)	〃 12.30	53	27.0	7.6	0.29
18	Sinsensō	〃 12.27	60	18.0	6.8	0.33
19	Seiryusō	28. 1. 8	126	37.5	7.0	1.11
20	Yūmeionsen A	28. 1. 5	90	42.0	9.5	0.82
21	〃 B	〃	37	35.7	8.2	0.80
22	〃 C	〃	58	38.5	8.4	0.98
23	Ōtsubo onsen	28. 1. 9	75	39.6	9.2	0.97
24	Yahatamura Ishimura	〃 1.10	65	32.5	7.0	1.10
25	Kumairi Gozukuonesen	〃 1.16	98	38.0	8.6	0.99
26	Kumairi Furuyu	〃	63	35.0	8.4	0.93
27	Kumairi Kikuchiyu	28. 1.16	81	40.5	9.5	1.32
28	Midorionsen	28. 1.10	60	39.5	9.2	0.95
29	Private Bath (Miyamoto)	〃 1. 6	25	30.5	7.7	0.74
30	Kitamachi washing place	〃	20	27.8	7.4	0.53
31	Hirayama Tamanaya	〃 1.11		38.5	9.4	3.39
32	〃 Ōgiya	〃		39.0	9.0	4.20
33	〃 Public Bath	〃 1. 9		40.4	9.0	4.00

* ; Measurements with Beckman G Type pH meter.

in Figure 5-2. Mark in Table 5-1 indicates that measurements were made with Beckman G Type pH meter. The rest were measurd by Toyo pH test paper.

2, Consideration of Measurement Results.

From Table 5-1 it can be seen readily that pH is very high at Yamaga Hot Springs. Similarly, Ryuganji Hot Springs, downstream on Kikuchi-kawa, has pH of around 7.0. The rock at base at Ryuganji are Biotite-granite, at Yamaga they are Hornblende-biotite granodiorite. The radon content at Yamaga is approximately 3.0 mach, at Ryuganji approximately 9.3 mache. In other words, radon contents become less at strongly alkaline hot springs. In the Yamaga Hot Spring group, however, pH is 9.71 at Egami's, temperature 43.2°C and radon content 2.90 mache, all of which are of the highest.

Next we shall draw the iso-thermal line and iso-radon curve as shown in Figures 5-3 and 5-4. The town operated Shinyu penetrates to the base rock at 134 ken and we may consider that the 100ken layer is above the base rock. In Figure 5-3 we shall consider the

direction of long ellipse axis as a crack. In Figure 5-4 there is another ellipse protruding on the east side of the ellipse in Figure 5-3. It can be assumed that another low temperature crak cuts across here. It would seem, however, that one of these is a vein of hot spring water.

According to the geological surveying by Dr. Kobayashi,[19] there not only is a fault in the northeast direction but it coincides generally with the straight line tying Hirayama, Yamaga and Hirashima hot springs. There is no definite mention

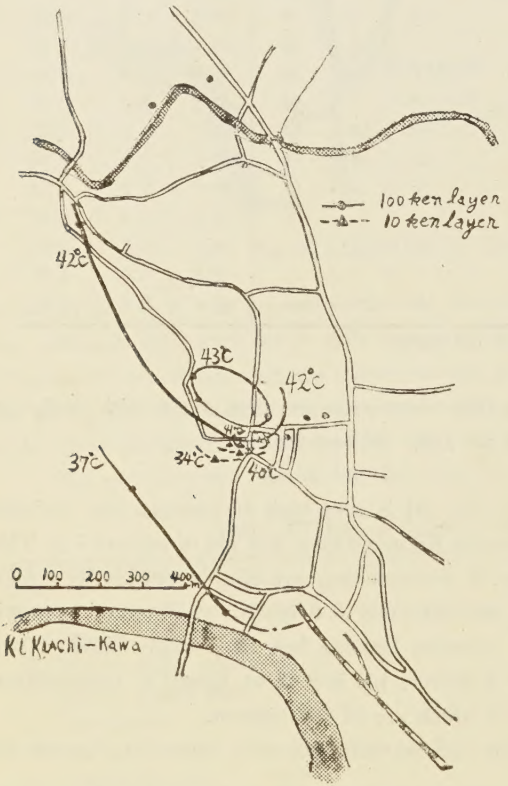

Fig 5-3 Iso-thermal Curves.

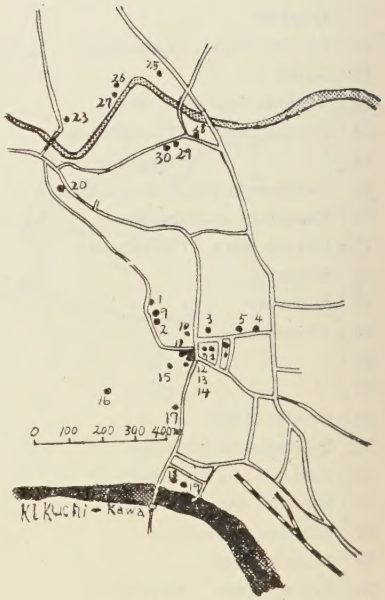

Fig 5-2 Sites of Hot Springs.

as to what the other crack is. The cracks in Aso caldera are well known from electrical resistance measurements by Prof. Nomizu[20] and others. In other words, the line binding the present active Nakadake and the old crater, Hebino-o, indicates one crack, and Narao, Kishima, Komezuka and others of the old volcano are situated on the top of this. when this is extended outside the caldera it passes south of Waifu and near the place which is now a matter of controversy in Yamaga. There is a low temperature hot spring in south of Waifu, the vicinity of this extended line. Because of this fact the outward extension seems quite reason-

able In this case Yamaga is located at the crossing point of these two cracks and one of them seems to be the hot water vein. Next the iso-thermal line and iso-radon curve for the shallow 10 ken layer are both ellips. The following is a comparison of 10 ken and 100 ken layer.

10 ken layer: temperature 39.9°C, radon content 1.98 mache, pH 9.33

100 ken layer: temperature 40.3°C, radon content 1.81 mache, pH 8.99

No great changes are noticeable in the character of both the shallow and deep places. In other words, it can be inferred from the iso-thermal line and iso-radon curve that hot spring water welling out of a crack in the base rock spouts to the surface of the earth by some convenient route in a short space of time.

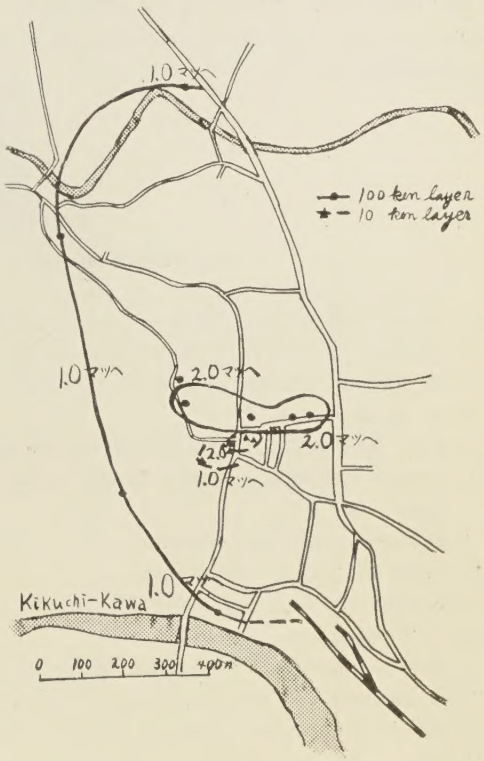

Fig 5-4. Iso-radon Curves.

Summary.

1. Radon contents of hot springs and of ground water were examined in 181 places in Central Kyusyu.

2. Ryuganji Hot Springs showed the greatest radon content, 9.31mache, in Kumamoto Prefecture. All were small and coincides with geological conditions.

3. Examination of the radon contents of groundwater gives hints on the structure of the earth crust of the region.

4. The inductions drawn from iso-radon curves regarding the structure of the earth crust at Ryugangi, Uchinomaki and Yamaga coincide well with results obtained by other means.

5. Investigations are very incomplete as to volcanic gas and the gas spouted at Jigoku. More complete study must be left for the future but to date no large values were obtained either in radon, or toron.

In conclusion I wish to express my thanks and appreciation for the valuable instruction given me by Prof. Namba with regard to geophysics and Prof. Matsumoto with regard to geology and especially Prof. Namba for his kindness in reviewing the report for me.

I also thank Prof. Shinomiya for permitting me to use his yet unpublished data on ammonium ion, and Prof. Ochiai, my beloved teacher, who encouraged and accorded me many conveniences.

References

1. Iwasaki and Ishimori; J. Chem. Soc. Japan **72**, 14 (1951)
2. Murakami and Ishimori; kagoku-no-Ryōiki **4**, 211 (1950)
3. M. Kamada, Sci. Rep. Kagoshima University **No.** 1, 1 (1952)
4. M. Kamada; ibid
5. From the Chemical composition table of the hot spring, Gyokuei Hotel.
6. Noguchi and Saijō; general discussion on geochemistry at Nagoya held by chemical society of Japan (Nov. 1952)
7. Imanishi; private communication.
8. Ōhara and Tanaka, unpublished.
9. Iwasaki; J. Cham. Soc. Japan **64**, 941 (1943)
10. S. T. Nakamura; unpublished
11. Nomitsu, Kawaguchi and Karube; Chikyu Butsuri (Kyoto) **6**, 159 (1942)
12. M. Kamada; Sci. Rep. Kagoshima University, No. 2, 101 (1953)
13. Shinomiya, Kokubu, Namba and Naitō; J. Chem. Soc. Japan **72**, 846 (1951)
14. ibid
15. K. Kiyota; J. Chem. Soc. Japan, **63**, 786 (1942)
16. Noguchi; see ref. 6.
17. Matsuura, Kokubu, Koga, Tokimasa and Wakimoto; 4th meeting of Kyushubranch of chemical socity of Japan at Kyushu University. (Nov. 1952)
18. Ōhara and Tanaka; 6th anuual meeting of chemical society of Japan (Apr. 1953)
19. Kobayashi. "Yamaga onsen Chōsahokoku" (Reportson the hot springs of Yamaga. Dec., 1949)
20. see ref 11.